1.1 Background

Over one billion people in the world have a shortage of drinkable water. In developing countries, a high percentage of people obtain water for drinking, cooking and washing from underground. The masterful technology of lifting water from underground is done by the use of a hand pump (Water Aid, 2006). Hand pump technology is capable of lifting water from underground to the surface of the ground (Reynolds, 1992).

About 884 million people in the world do not have access to improved sources of drinkable water with sub-Saharan Africa accounting for over a third of this number. The Joint Monitoring Programme defines access to drinkable water as the availability of at least 20 litres of drinking water per person per day within 1 km of that persons dwelling. Safe drinkable water can also be defined as water that meets accepted quality standards and poses no significant health risk (UNDP, Water in a Changing World, 2009).

The first international water supply and sanitation decade (IWSSD) 1982-1990, stated that all member states of the United Nations would make a considerable effort to supply safe drinkable water for all people by 1991. However, their goal was not achieved and not everyone by that time had a source of safe drinking water, because the number of the people short drinkable water increases every year.

According to the WHO/UNICEF joint monitoring programme for water supply and sanitation, worldwide nearly 780 million people use unimproved water supplies for drinking, cooking and hygiene. The lack of improved water sources in rural areas of sub-Saharan Africa has prompt governments, non-governmental agencies to invest in this sector.

In the last few decades, wells and bore holes with hand pumps were considered as the most applicable option for water supply in most of the developing countries and became the principal technology (Harvey and Reed, 2004).

RWSN had lately published statistics on the functionality of hand pumps. The statistics show that the hand pump is being used in twenty countries in sub-Saharan Africa. The data is presented in Fig.1. It is clear that across sub- Saharan Africa and most of Asia the hand pump will continue to be the main contributor to provide safe drinking water in developing countries (RWSN, 2009). Madagascar, Guinea and Uganda have the highest functionality, while DRC, Cote d'lvoire and Sierra Leone have the lowest.

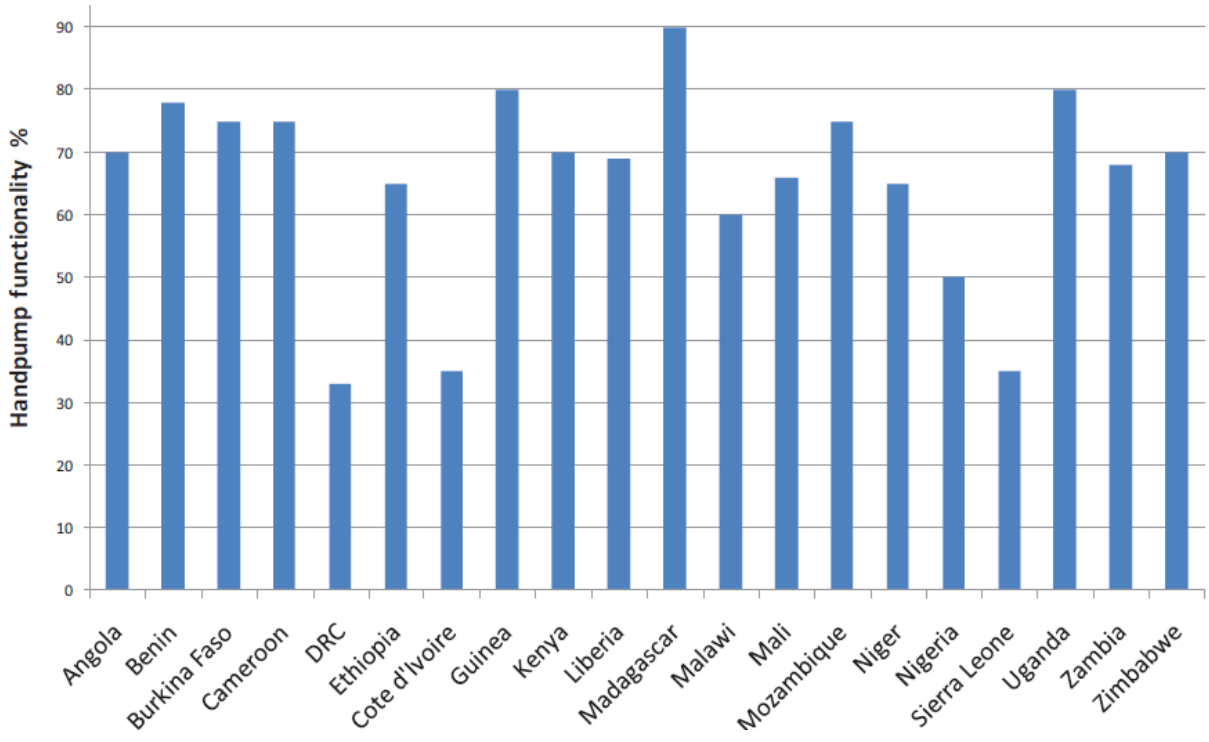

Fig.1. Functionality of hand pumps in 20 African countries [RWSN, 2009].

Research Problem and objectives of this researches:

Many hand pumps fail worldwide due to wear of the piston seals. Due to these failures of water hand pumps millions of people in developing countries cannot have safe water for drinking. This results in enormous costs for maintenance and installation of new water hand pumps. It is therefore important to analyse and find the reasons for these failures. One reason for these failures is wear of the NBR piston seal. Wear of the NBR piston seal is as a result of the influence of the contact stress generated within the pump cylinder. Distribution of the contact stress for the NBR piston seal is a very complex topic.

It is difficult to calculate and determine the contact stress and the contact area of the NBR piston seal. Therefore, an advanced numerical methods such as finite element analysis FEA will be used for analysis of wear of the NBR piston seal. There is to date no study was found related to the use of FEA to analyse the wear of NBR piston seals in water hand pump. Also there is no specific model or equation to calculate the wear rate of NBR piston seals in water hand pump.

Aim of research

This study will focus on: 1- developing a relationship for computing the friction force in NBR piston seal and for computing the wear rate of the NBR piston seal as used in the water hand pump. 2- Analysis of wear of the NBR piston seal using F.E.A method.3- analysis of the wear of NBR piston seal in wet and dry sliding conditions using experimental and FEA techniques.

Objectives

In order to increase piston seal life an understanding of the wear mechanisms and behaviour of piston seals wear is very important. To assist with this analysis a reciprocating hand pump test rigs will be developed to allow for various piston stroke lengths and different load conditions. FEA analysis will also be conducted on piston seals and a model developed to accurately analyse the complete wear mechanisms taking place.

2.1 Hand pump design, components and operation.

The system of lifting water to the surface from underground needs a source of power. While human power may be used, various other sources of power are also capable of doing the job, for example wind, which is a natural and renewable source of power.

There are also different types of pumps and choosing a pump is dependent, a mong other things, on the vertical distance between the surface of the ground and the surface of the water under the ground. The deeper the water underground is, the lesser choice of suitable hand pumps as not all types of hand pumps are capable of lifting water from long distances under the ground. These types of hand pumps are also more costly. Hence the deeper the water is, the higher the costs required for pumping [1]. Hand pumps are generally cheap and easy to operate and provide solution to millions of people around the world as a source of safe drinkable water. Hand pumps also reduce water contamination as water is easily contaminated when collected in any other ways. This is because water is completely sealed with in the pipe work when lifted. These reasons make hand pumps a very useful and suitable mechanism to supply clean water in the developing countries [2]. Hand pumps are widely used in areas where access to clean water is rare and where sources of financial investment are limited. The first generation of hand pumps were manufactured in the United Kingdom. They were released in the 1930s and were used for three decades. These pumps were made of hardened steel and cast iron and they were heavy duty pumps. However when the pumps in the colonial areas were broken, they were not repaired. The second generation of hand pumps were manufactured in India in the 1960s and was called the India “Mark II”. In 1986 the world water conference in Nairobi claimed that more than a million of these hand pumps in the subcontinent of India where not operational.

This indicated that the hand pumps were used in a large quantities and has poor maintenance [3]. Now a days, the hand pump design is no different from how it was decades ago. The basic principle of pumping water is the same. Hand pumps are simple in terms of their structure. However, high percentages (up to 68%) of the pumps break down easily [4]. The primary reason for over 25% of these failures was wear of the piston seal.Fig.1.2 show other reasons which cause break down of the hand water pumps.

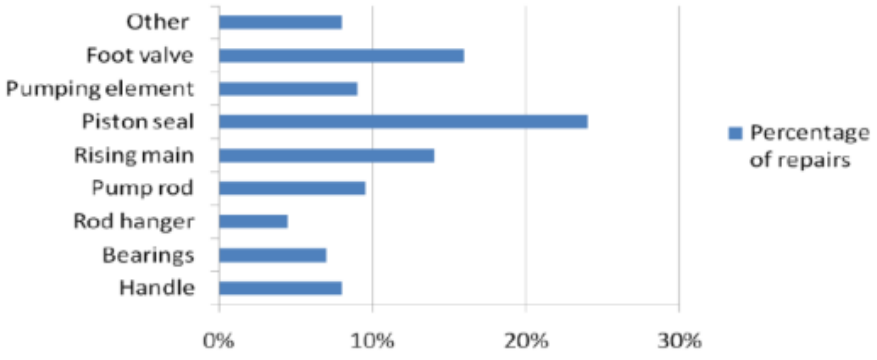

Fig. 1.2 Percentage of repairs on Hand pump components [10]

There are different types of hand water pumps, most of them are reciprocating pumps, which means positive displacement pumps [5]. Table 1 present different pumps with their lifting capabilities.

Tablle.1. Type of hand pumps and the range over which water can be lifted

Pump type	Lift (m)	Volume flow rate L/min	Location of cylinder
Suction pump	0 - 7	24-26	Above ground
Direct action pump	0 - 25	26	Under ground
Deep well pump	Up to 100	11-17	Under ground

Efforts were made over several decades on new designs. However, these new designs have to pass through VLOM (village level operation and maintenance) [6]. At the end of the first water decade, members of the community were sufficiently involved in the maintenance of the hand pump [7]. Therefore, they promoted the growth of new design of hand pumps. The design of these new pumps has to satisfy the VLOM criteria more strictly than others. As a result, markets were filled with different types of hand pumps, but with very little standardisation [8]. The reciprocating hand pump remains the most common type of hand pumps used. It works when water flows from a high pressure region to a low pressure region. An area of low pressure is created over the water; this leads the water to flow into this region. Fig.2.show a typical reciprocating hand pump, cylinder and various parts. It contains two valves: a foot valve located at the bottom of cylinder and a piston valve located in the piston. The piston valve splits the cylinder into two parts: upper and lower. The valves prevent backflow of water. When the piston moves up, the pressure of the water over the piston keeps the piston valve closed. Eventually, depending on the depth of the well and the number of strokes water then flows out of the pump. The cylinder is full of water when the piston moves down. This is due the closing of the foot valve. The piston has two seals, which have to always be sealed to prevent water leakage. These seals are called the piston seals, and play a major role in the functionality of the hand pump. They are also the main reason behind the failure of the hand pumps [9]. In Africa, new research showed that a lot of new hand pumps are broken shortly after installation. The main reason behind the hand pumps failure is wear of the piston seals. (Harvery, 2003). This leads to reduction in water flow rates. However, little research tribological wear behaviour of these piston seals [10].

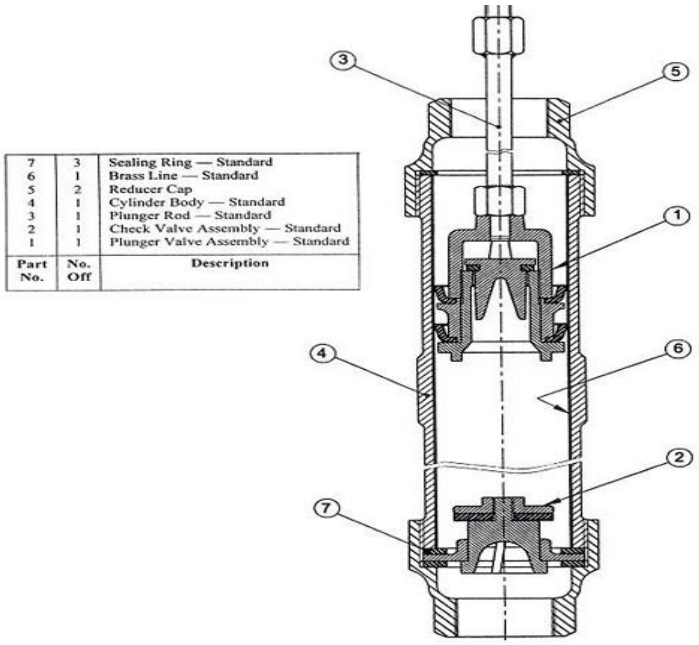

Part No.	No. Off	Description
7	3	Sealing Ring — Standard
6	1	Brass Line — Standard
5	2	Reducer Cap
4	1	Cylinder Body — Standard
3	1	Plunger Rod — Standard
2	1	Check Valve Assembly — Standard
1	1	Plunger Valve Assembly — Standard

(a) Reciprocating hand water pump parts

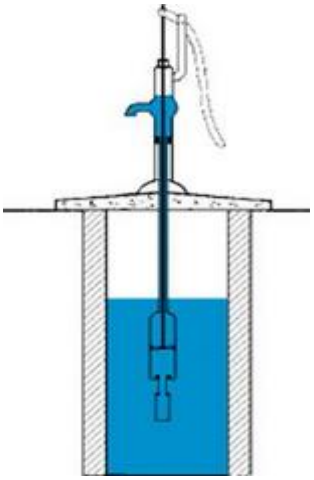

(b) Sample of reciprocating hand water pump

Fig.2. Reciprocating hands pump (a) reciprocating hand water pump parts (b) sample of reciprocating hand water pump [9].

2.2 Types of seal and seal material.

A seal is designed to control fluid leakage in pumps, for example reciprocating oscillating or rotary pumps. The most common material used for manufacturing seals is the Rubber (e.g., natural rubber, nitrile rubber, silicone and Viton).

Seals are used for sealing purpose, in order to avoid the leakage or to avoid mixing between fluids operating under different working pressures [11]. Seal elements are also used to retain fluid under specific pressure [12]. Some design, include tolerance considerations requiring a large gap between two regions (or between two surfaces) which cannot, therefore, perform the sealing function autonomously. Such gaps can be reduced to small dimensions by introducing seals as extra components [13]. The sealing effect is obtained from the seals element deformation between the movable surfaces. Considerable friction forces result in unwanted consequences on the system efficiency through considerable wear on the sealing element itself [11].

Different types of seal are used in different applications e.g., sealing in pneumatic and hydraulic equipment. Therefore, different types, shapes and designs of seals are available including O-ring, V, X, L, I and others [11, 12]. In general seals are classified as static, dynamic and rotary.

Dynamic seals are more difficult to design and more expensive than others, and have different shapes and different dimensions. There are a lot of applications for dynamic seals. Due to the relative motion between the two surfaces which cause friction and wear, the design of dynamic seals are complex, and the problems caused by using dynamic seals are

greater than the problems caused by other seals. Dynamic seals are used in hydraulic and pneumatic equipment and their shapes are different compared to a typical O-ring design with complex geometries. In general, most of the seals are made of elastomer materials (Rubber).

Dynamic seals when used with reciprocating movement are called reciprocating seals. There are two types of reciprocating seals, piston seal and rod seal. In industry, these seals are used in linear and rotational motions, for example linear hydraulic actuators and rotary actuators [14]. Fig.3. shows typical linear and rotary actuator seals .

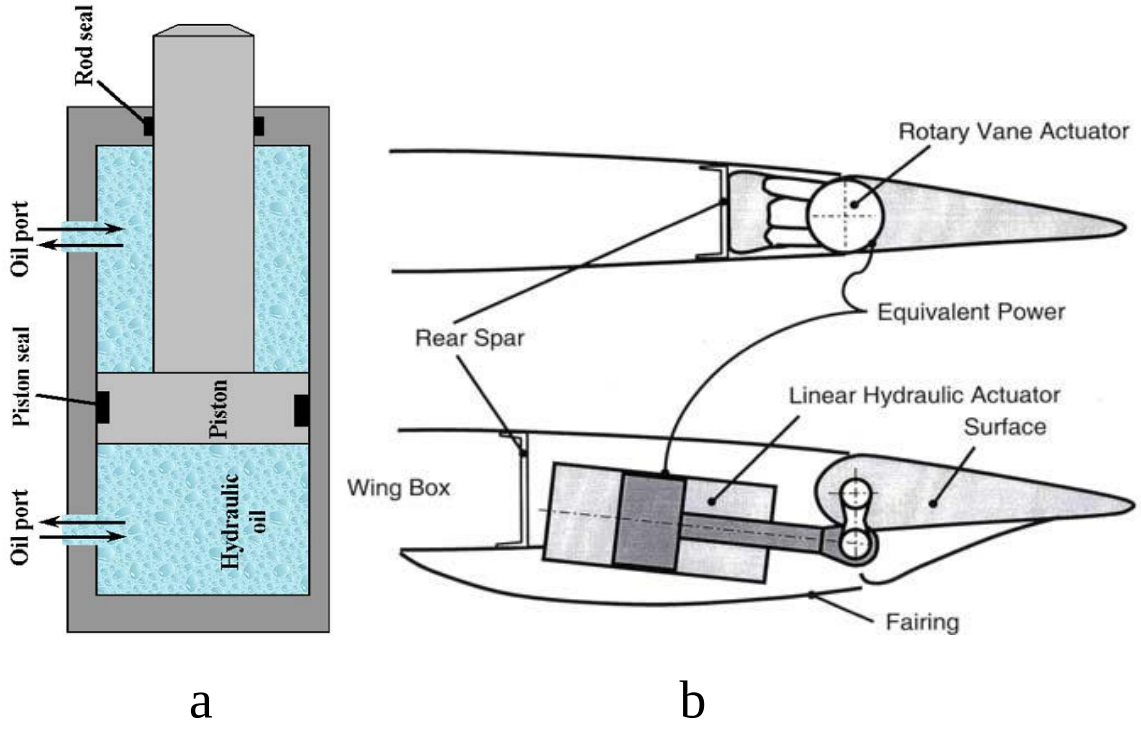

Fig.3. (a): piston seal and rod seal of linear actuator, (b): Aircraft wing control surface operated via classic linear hydraulic actuator and rotary actuator [14].

Seals are sensitive elements in all machines and equipment. Failure of the seals results in high cost which may even exceed the machine cost. The safety risk is even greater in applications, such as seals used in actuators controlling air craft landing gear and wing flaps. Although not related to reciprocating motion, the sad catastrophe of NASA shuttle challenger in 1986 was officially attributed to the failure of astatic elastomeric O-ring seals, which was used to block hot gases from leaking through a joint during the propellant burn of the right rocket motor [15].

The first well notarized systematic research program related to seal wear was connected to projects of hydraulic actuation and control, made to order by the air force in the Second World War [16]. Through the next decades, industrial growth generated, fast expansions in a lot of fields of technology, including material processing technology and hydraulics and modification of operating parameters (velocity, pressure, temperature, capacity and accuracy) were required for these machines. All these needs made higher impacts on the growth and advancement of sealing technology, in particular on reciprocating seals, piston seals and rod seals. Changes regarding design, material, form, sealing lip shape and accuracy occurred. Piston seal followed three various major lines, which began with impregnated leather (U and V rings), and then with simple rubber O-rings, and finally seal design becomes advanced [17]. Seal design was at first an experimental process through trial and error. From the 1990s onwards, design became more advanced, based on the new- computational tools such as finite element analysis (F.E.A) [18]. A lot of experiments were carried out on friction of reciprocating seals Y.Kawahra [19] and Kaneta [21] and an study by Sayles [11] concluded seal friction for reciprocating seals to be dependent on rod speed for speed less than 100 mm/s for smooth sliding.

The work of White and Danny [16] at the end of world II, which was an itemized fundamental testing work on reciprocating seals is still one of the ultimate sources of reference [19]. Most seals are made of elastomers (Rubber), because the rubber has a low modulus of elasticity, a large elongation- at break and high poisons ratio and incompressible. Rubber contains large chains of randomly oriented molecules, the chains are entangled and cross-linking, and have an impact on the viscoelastic properties, stress and relaxation. If the rubber is under the effect of stress or strain energy, internal rearrangements of rotation and extension of the polymer chain can occur. These changes are a function of the energy applied, time, rate application and temperature. Following the application of energy, rubber can become elastic (energy store) or viscous (energy dissipation). Elastic and viscous properties are very important parameters for seals.

Stresses applied to the rubber seals can induce strain which creates a sealing force. This sealing force is due to the internal friction generated internal energy which then results in a sealing force [20].

A lot of seals work in the presence of lubricants. The sealing elastomer oil interaction plays a significant role in determining the tribological performance of the elastomers. Seals may also operate under dry conditions, hence. can be affected by high friction coefficient and wear [21]. Atypical piston seal is radial in shape and has a lip. The choice of piston seal is depending on the way in which the piston operates [22]. It is very important that the piston seal and its lip design have high accuracy. Stresses applied to the piston seals result in high squeeze between the seal surface and surface of the cylinder. This generates higher friction during operation which lead to higher wear [23].

2.3 Wear of Seals

There are many descriptions used to explain what seal wear is. Wear is sometimes investigated from the view point of the types of contact interaction of the solid surfaces [24]. In general wear is the gradual removal and loss of material from contacting surfaces as a result of relative motion. Seal wear is related to frictional processes. If solid surfaces in relative motion are not separated in some way, wear can occur [25]. Fig. 4. highlights the relationship between the number of cycles and percentage of the seals worn [26].

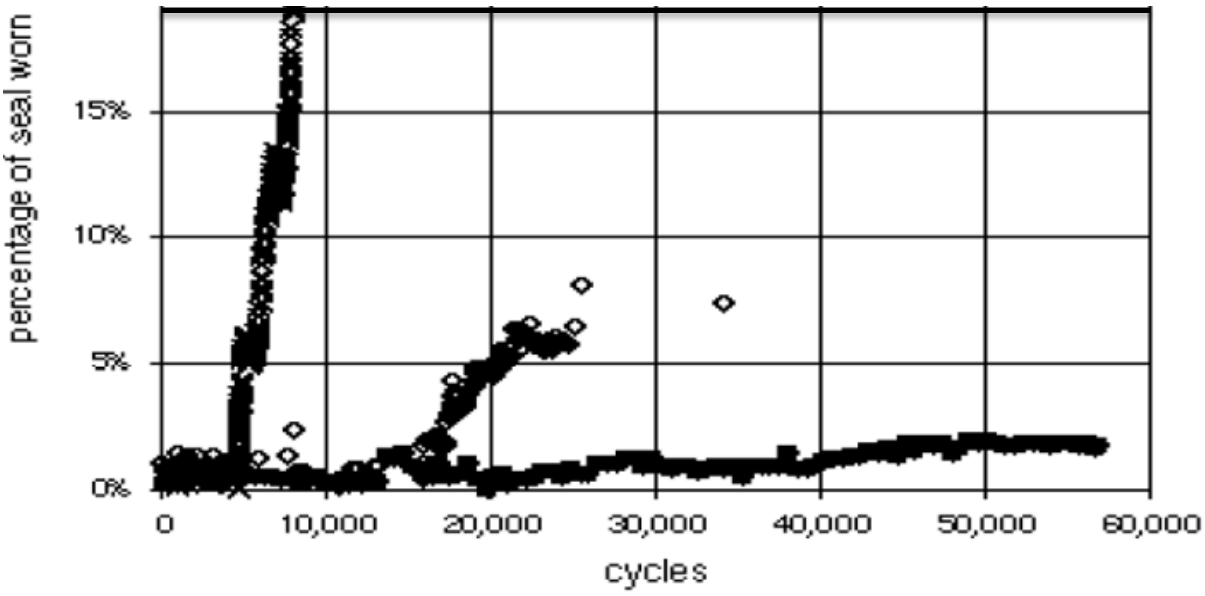

Fig.4. Piston Seal worn due to the number of cycles [26]

The first experimental investigations on wear was carried out by Hatchett [11], Experiments and observations were carried out on the various alloys and on the comparative wear of gold being the substance of report made to the Right Honourable the Lord of the Committee of Privy Council, appointed to take into consideration the state of the coins of the Kingdom.

After that experimental investigations, further experiments on wear was carried out by Rinnia [11], on the friction and abrasion of the surface of solids.

Wear can happen in different patterns and is dependent on the forms of contact and also on the way and how the materials is removed. Fig.5. highlights the descriptive keywords related to wear and their interrelations.

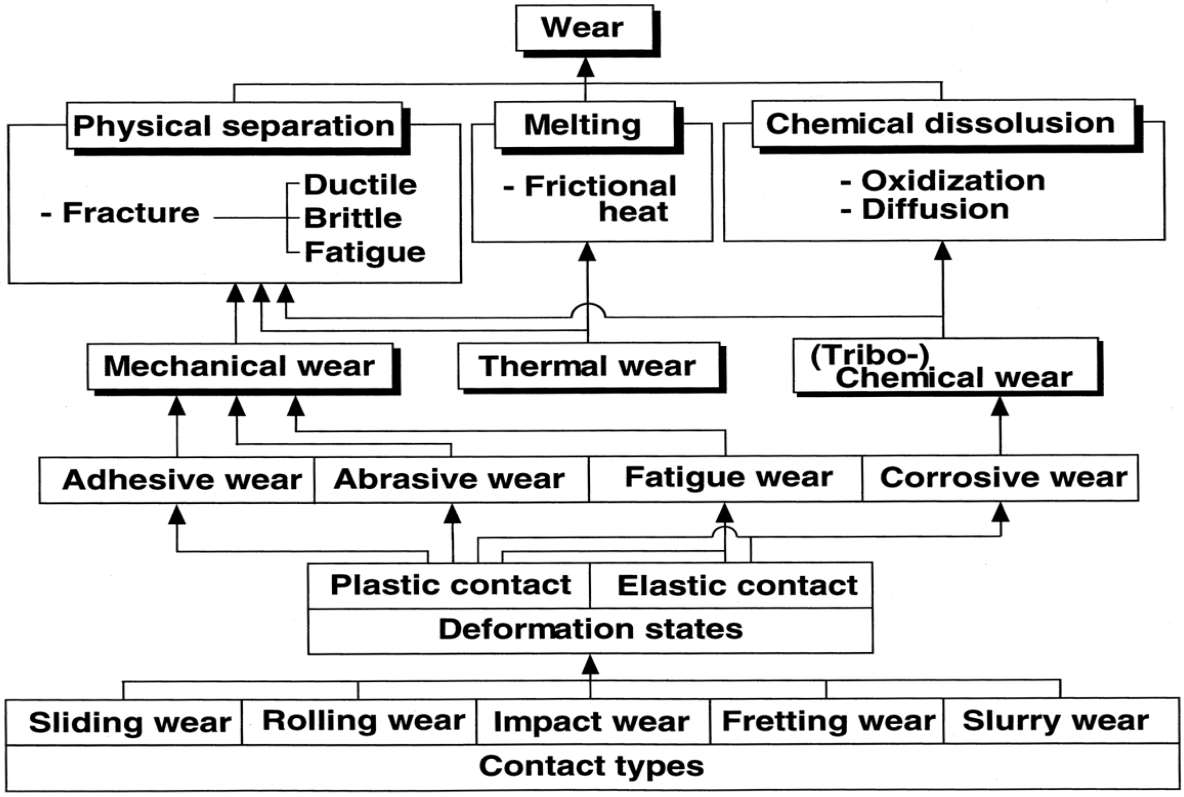

Fig.5. Keywords related to wear and their interrelations [24]

Normal compression and detachment, unidirectional sliding, unidirectional rolling, reciprocal rolling with slip, are all different contact configurations of wear, and wear in these contact types is explained as sliding wear. Rolling wear, impact wear, fretting wear, all those type of

wear are based on the contact type [24]. The main and basic wear mechanism are: adhesive wear, abrasive wear, fatigue wear, and corrosive wear Burwoll, [72]

Archard [74], proved that, whenever surfaces rub against each other, wear always occurs. One of the assumptions for wear analysis is that the contact between the surfaces occurs at asperities and that the true contact area is the sum of the individual asperity contacts. Wear is not a material property, it is a system response, and wear changes drastically even with a relatively small change in atribosystem, which is composed of dynamic parameters, environmental parameters, and material parameters [27].

The main wear pattern, adhesive wear and abrasive wear, are generated under plastic contact. If the contact is between similar materials, an adhesive wear will occur, and when the contact is between hard/sharp material and soft material an abrasive wear will occur. In the case of contact while operating, fatigue fracture is generated after repeated cycles. When the tribochemical reaction in corrosive media is brought about by material removal, the result is corrosive wear. Fatigue and corrosive wear can be generated in both plastic and elastic contacts [28]. The material removal in adhesive, abrasive, and fatigue wear in the contact region is governed by deformation and fracture, which generated by mechanically induced strain and stress. Therefore this type of wear is usually described as mechanical wear [24]. Wear also occurs when surfaces are loaded and undergo to sliding or rolling or both Archard [74]. The reciprocating movement of a piston in a hydraulic cylinder can cause wear both on the piston rings and cylinder bore. Piston ring seal, a piston seal used to prevent leakage between the upper and lower champers of the pump cylinder at different fluid pressures [29].

There are two points that make dynamic seals required in tribological science. Firstly the dynamic seals block the clean lines of the lubricant external contamination. This contributes to repressing wear by three body abrasion caused by contaminant particles. Secondly, the counter surfaces of a dynamic seal work under the same tribological laws as any sliding couples, with the requirements of low friction and low wear and a long service life. Seals for linear movement are most affected by direction of sliding, speed and lubrication [30].

Piston seals are mostly made of elastomers (Rubber). If elastomers slide against a hard substrate, there are three various mechanisms of wear that can be identified. Firstly when elastomers sliding against a hard surface with acute synthesis, abrasive wear take place as a result of rupture of the elastomers sliding surface. Another type of wear called fatigue wear occurs on the surface of an elastomer sliding against hard substrate, fatigue wear. And when a highly elastic elastomers slide against a smooth surface, roll formation occurs. In this type of wear, and a high frictional force shears a projection on the rubber surface, then rupture and the edge will roll along the direction of sliding.

If the shear stress is higher than the critical shear stress, roll formation occurs, and when the shear stress is lower than critical value, wear due to fatigue occurs [31]. The friction coefficient is one of the most important parameters governing this type of wear.

Fatigue is a result of repeated deformation cycles, which take place when rubber slides against hard and blunt projections on the hard surface at low frictional force [32]. The surface of the rubber which is worn by frictional wear or roll formation, appears as bridges perpendicular to the direction of sliding. Fatigue wear may not have any visible bridges except pitting marks [33].

At low contact pressure the loss of the mass of the elastomers is low due to lower friction [34].

A number of studies were performed on tribological performance of piston seal of nitrile rubber polyethylene and leather. These studies were performed at macro level and the state of the art at revise the time regarding piston seals was the used of leather as the material of choice. These studies found wear on the piston seals with abrasive material embedded in the seal. The wear rate in any tribological interaction varies depending on the contact conditions. The problem of the piston seals wear is compounded by the fact that the piston seal is expected to perform under dry lubrication condition. Most of the studies published on the behaviour of polymers have focused on sliding against steel under dry contact between the polymer and steel [35].

The phenomena of wear can be carried out, not only by an experimental investigations, but also by using mathematical models and by using computer simulation.

The first trials on numerical analysis of wear were given by Grib, 1982, Grib studied the Solutions of Tribological Problems with the aid of Numerical Methods. Table 2 highlights key trials conducted in simulating the wear.

.

Table.2. Trials on numerical analysis of wear

Author	Year	Study titel	Ref
Hugnell A. B. J	1996	Simulation of the mild wear in a cam-follower contact with follower rotation,	[36]
Stromberg N	1997	Thermomechanical modelling of tribological systems	[37]
Szefer G	1998	Contact problems in terms of large deformations	[38]
Agelet and Chiumenti	1999	Wear patterns and laws of wear	[39]
Franklin F. J	2001	Computer simulation of wear and rolling contact fatigue	[40]
Koetal K	2002	Classi_cation of wear mechanisms/models	[41]
Shillor M	2003	Analysis of viscoelastic contact with normal compliance, friction and wear di_usion	[42]
Mc Coll I. R	2004	Finite element simulation and experimental validation of freeting wear	[43]
Kim N. H	2005	Finite element analysis and experiments of metal/metal wear in oscillating contacts	[44]

Finite element analysis was also applied to simulate the wear caused due to pitting phenomenaunder various operating conditions [45].

From the literature it was found that a lot of previous studies were focused on reciprocating seals and some of these studies were on the piston seals of water hand pump. Some studies investigated the performance of piston seal and wear under dry sliding conditon. Few studies investigated the operation and performance of piston seals in water where water is used as a lubricant media, wear and coating of water piston seals were carried out recently by Michael Lubwama [10].

Literature also reversed that limited number of studies and trials on the wear of rubber seals were carried out using finite element analysis furthermore. There was no research using finite element methods to analysis the wear of piston seals of water hand pumps. The current research will be focused on evaluating the performance of piston seals used water hand pumps under dry and wet sliding conditions. In addition, wear models and mechanisms of the piston seals will be evaluated by wear tests in a cu stern designed test rig and by finite element analysis

2.4 Friction

2.4.1 Definition of friction.

Friction is impedance to motion and occurs whenever solid surfaces slide over each other. The resistive force, which is parallel to the direction of motion, is known as the friction force. If the solid surfaces are loaded together and a tangential force F is applied, then the tangential force that is required to initiate sliding is the Static Friction Force (SFF). This force usually requires application over a few milliseconds before sliding is initiated at the interface static force (F static). The tangential force required to preserve sliding is the Dynamic Friction Force (DFF) or kinetic friction force. The dynamic friction force is less than or equal to static friction force [46]. Fig.6. highlights the static and dynamic (kinetic) friction forces.

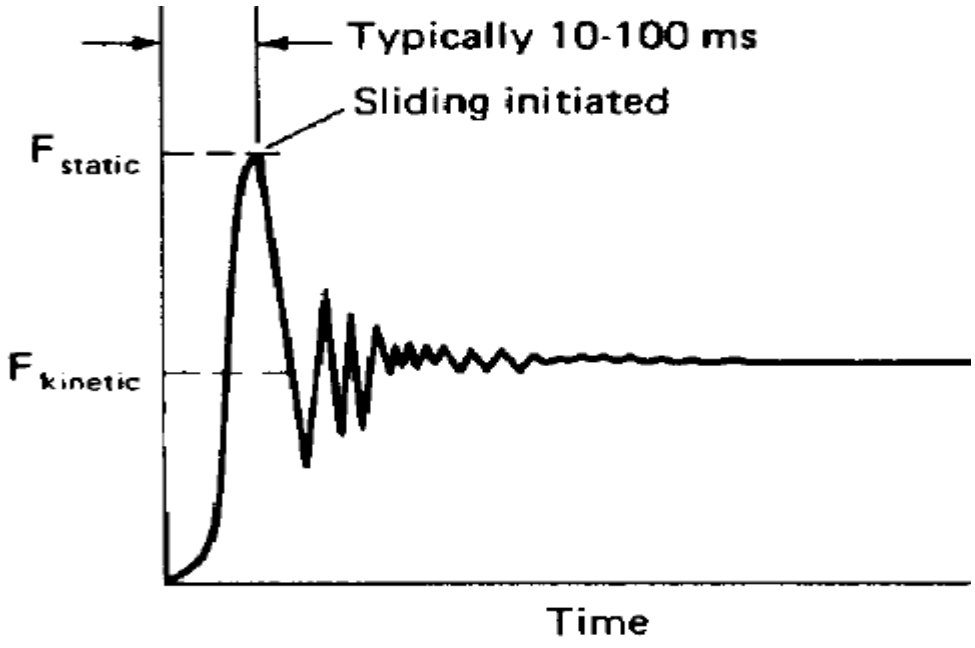

Fig.6. Static and dynamic frictions forces versus time [46]

2.4.2 Elastomers (Rubber) Friction:

Friction forces in Rubber vary in many ways from the frictional properties of most other solids. That is due to low elastic modulus, and higher internal friction exhibited by rubber. The pioneering studies of Grosch [47] show that rubber friction is caused by internal friction and his experiments of the rubber sliding against glass and silicon carbide paper surfaces give coefficient of friction values independent of force or load [47]. Fig.7. shows the graph of coefficient friction versus logarithm of sliding velocity for NBR Rubber sliding on Glass and Silicon Carbide.

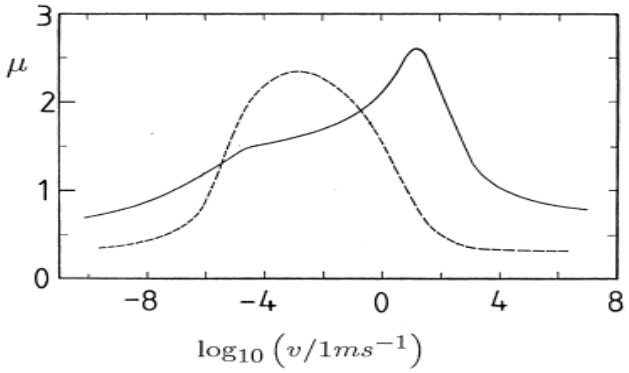

Fig.7.Coefficient of friction of NBR rubber sliding on silicon paper (solid curve), and smooth glass surface (dashed curve) due to the log of the velocity [47].

The friction force between rubber and a hard substrate is generated due to adhesion and hysteric component, respectively. The hysteric component is due to internal friction as a result of sliding, through sliding the hardness of hard substrate exert fluctuating force on the rubber surface which leads to a cyclic deformation of rubber and energy dissipation via the internal damping of the rubber. Adhesion component is occurring for very clean rubber surface [48].

Fig. 8. highlights the experimental and simulated normal and friction forces for the EPDM_30CB under 170 N with 3 rpm of the ball in Orbital-RBOP [49].

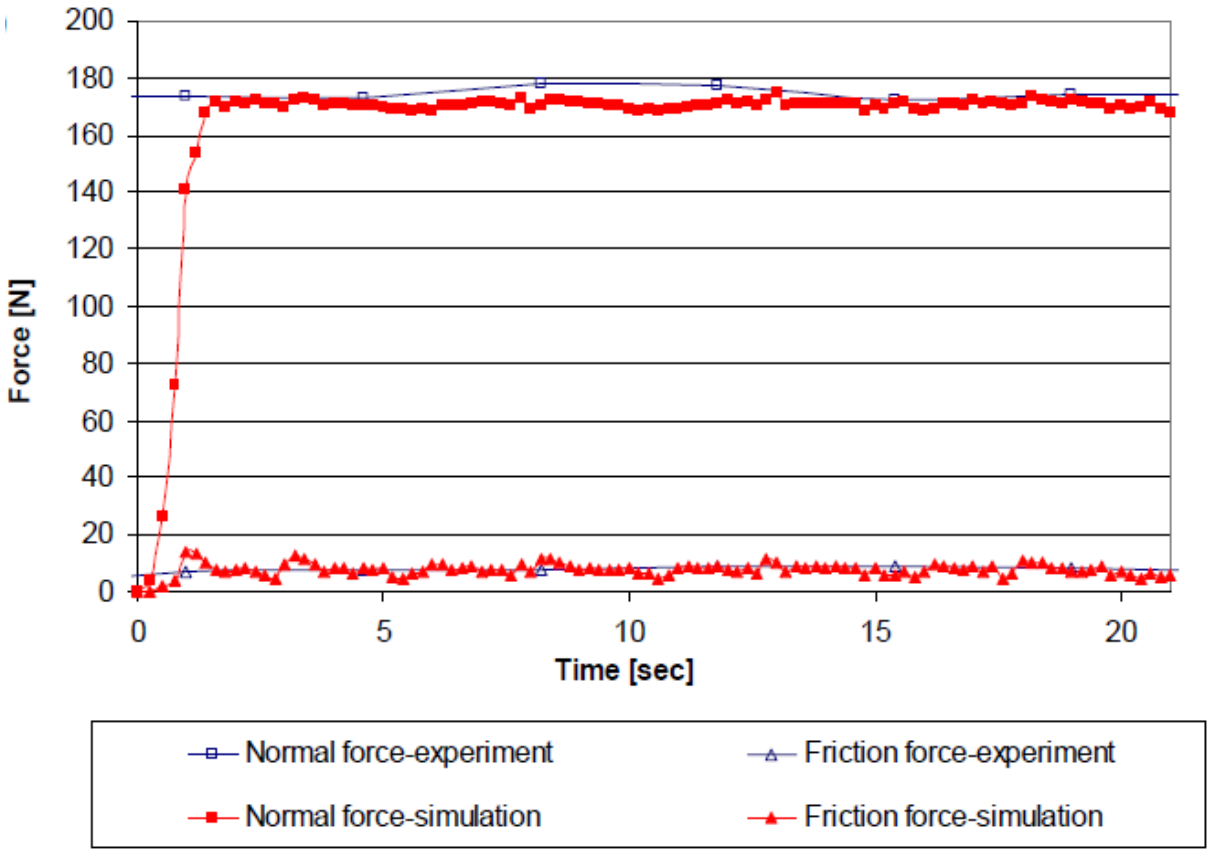

Fig. 8. Rubber friction forces during the operating time [49].

The behaviour of sliding friction of rubber substrate is very complicated due to the influence of a number of factors including contact area and contact stress. Friction coefficient of rubber sliding against a hard substrate can be expressed in terms of the contribution of adhesive and deformation (hysteric). Adhesion component of friction originates from making and breaking of junctions at a molecular level, and the hysteric friction is a consequence of energy loss associated with internal damping within the viscoelastic surface [50].

The contact area and the contact pressure play an important role in rubbers internal friction through the adhesive and hysteric components.

For elastically hard materials, adhesion does not appear itself on a macroscopic scale. The real contact area consists of randomly distributed contact areas and at higher sliding velocity, rubber become stiffer and the area of real contact is reduced, and then adhesive interaction between the substrate and rubber is also reduced [51].

As a result of the hysteresis of the deformation (by counterpart), an internal friction is generated. The hysteretic contribution which is caused by the viscoelastic properties of the materials depends on the time, temperature and frequency. Also sliding speed plays an important role for the hysteresis contribution [52]. Fig.9. Show the relationship between coefficient of friction and sliding velocity.

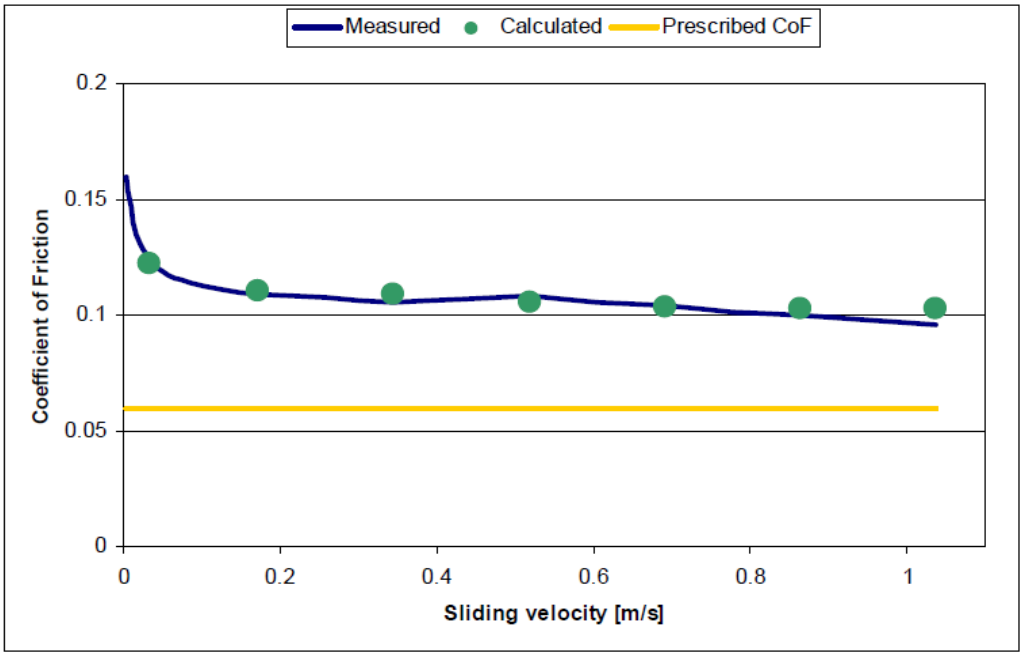

Fig.9. Relationship between coefficient of friction and the sliding speed [52].

When designing elastomers parts (Rubber) for tribological applications, explanation of friction is very important in order to determine the contact conditions. Through deformation of rubber or elastomer, and as a result of the viscoelastic material behaviour, a part of the applied strain energy is transformed to heat, caused by internal friction (hysteresis). The amount of this energy loss is the ratio of the loss and the stored moduli of the material [47]. When repeated loads are present, the hysteresis contribution to friction is more significant. In the case of sliding friction between an elastomer and rough rigid surfaces, the elastomer is subject to repeated cyclic deformation by the asperities of the rough surface. This generates heat at the surface internally and this type of internal heat generation can lead to fatigue wear [53]. Fatigue wear depended on the contact area of the elastomer with a hard surface, which decreases with an increase in sliding velocity. Fig .10. show the elastomer contact area as a function of sliding velocity.

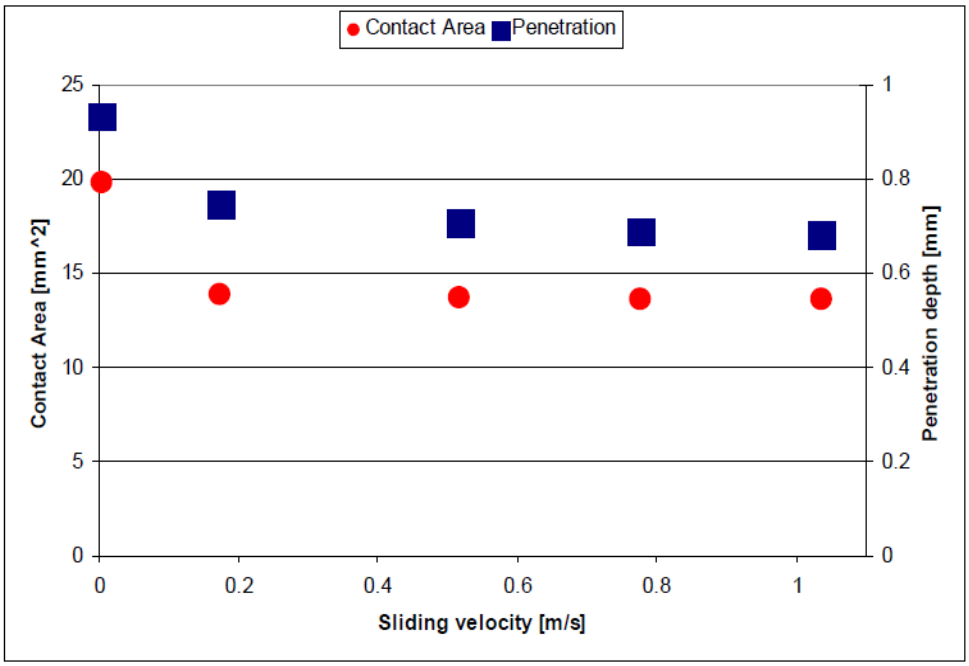

Fig.10. Rubber contact area of the counter surface as a function of sliding speed [53]

2.4.3 Rubber Friction Mechanism

The area of actual contact of the elastomers is proportional to the load. For rubber, because of the low elastic modulus and because it is relatively incompressible, it exhibits elastic instabilities during sliding. The compressed rubber surface infront of contact area is subject to bulking and output detachment waves which propagate from the front to the back end of the contact area. These wave are known as a Schallamach waves and were first discovered in 1971 [54]. When the substrate is a smooth surface the friction is due to local stick slip events at the sliding interface.

Schallamach suggested a molecular mechanism for the local stick slip, where rubber polymer chains at the interface link and attach to the moving counter face , stretches, detaches, relaxes, and reattaches to the surface to iterate the cycle, and through each cycle, the elastic energy stockpiled in the polymer chain is wasted as a heat through friction [55].

Person and Vollokitin (2006) noted that Schallamach theory of the local stick slip of rubber molecules was not completely accurate. These state that the energy bulkheads for vertical detachment are generally much higher than the energy bulkheads for lateral sliding. Therefore it is not expected that any detachment will occur. Rubber is nearly incompressible and it is not easy that a single molecule robustly confined at the interface are able to move between an elongated state and relaxed state.

In general, Schallamach waves and Stick slip waves are depended on kinetic friction coefficient μ_k and on the sliding velocity V. Schallamach waves occur when $\frac{d\mu_k}{dV} > 0$, but stick slip observed when $\frac{d\mu_k}{dV} < 0$ [56].

Schallamach waves are continuous waves over distance or time. But if the friction force or sliding velocity does not continue (with constant value) as a function of distance or time, or produce a form of fluctuation it is called a stick slip phenomena. Fig.11. Shows stick slip waves and schallamach waves. For the stick slip phenomena, through the stick stage, the friction force increases to the nominated value, and then slip occurs at the interface. Stick slip usually increases whenever the coefficient of static friction is markedly higher than the coefficient of dynamic friction, and the stick slip occurs either repetitively or in a random manner [46, 56].

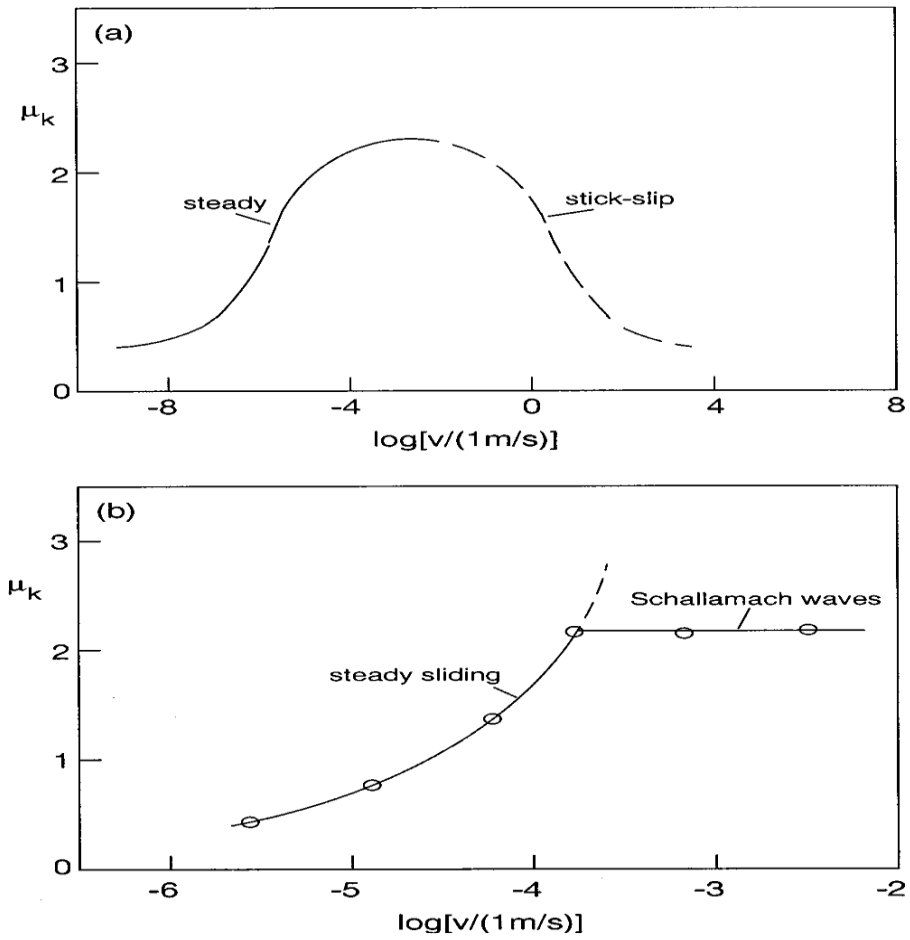

Fig.11. (a) Kinetic friction coefficient for rubber sliding on glass surface, (b) Kinetic friction coefficient for rubber sliding on Teflon surface [56].

For small tracks, during the stick the shear stress at the interface increases continuously with time up to the local shear stress (critical stress) after which a fast local slip occurs in addition during the slip the elastic deformation energy stored in the rubber during the loading stage will be dissipated partly inside the rubber and partly at the interface [57, 58, 59].

2.4.4 Friction, coefficient of friction and geometry of rubber seals.

Tribological seal friction can be assessed by analysing the friction and leakage performances, which can be obtained from endurance and friction testing related to operating parameters and conditions concerned [60]. Due to the motion, friction seals may be classified as reciprocating seals, rotary shaft seals, piston rod seals, and piston seals. The tribological behaviour of the seal, generally depends on the magnitude of losses (friction force, leakage, and wear) and on the operating parameters like contact area, contact pressure [61]. The necessity of using the sealing elements are strongly recommended, seals are exposed to higher stress through the sealing in order to avoid leakage and to prevent fluid mixing and to protect the machines. Sealing effect occurs through the deformation of the seal, and when considerable friction forces occur unwanted consequences on the system efficiency or on the sealing element itself may result [60].

Mofidi, and Prakash (2011) [62] carried out experiments to find out the influence of lubrication on two body abrasive wear of many types of sealing elastomers. Based on the experimental results they found that (1) at a normal load about 1.5 N and a speed of 10 r.p.m the friction coefficient decreased after a running-in period and the wear was insignificant (2) The longest running-in periods was observed during sliding against fine surface (3) speed dependence of friction was different for different elastomers (4) in presence of the oil, the elastomers could be in contact for longer duration.

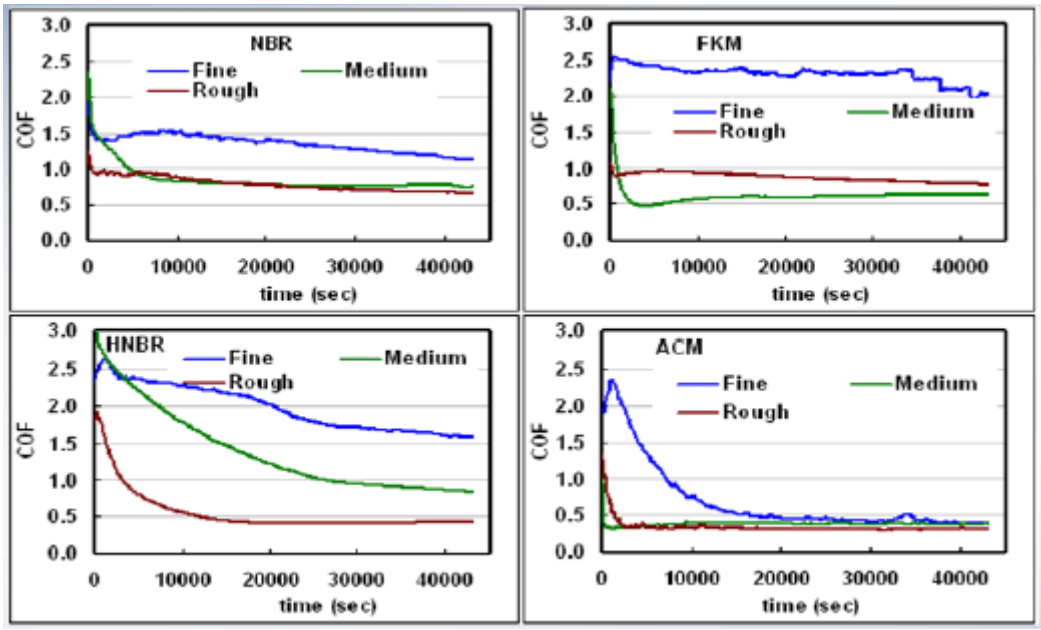

Fig. 12. (NBR, HNBR, FKM, ACM) Friction coefficients during the operating times of elastomers [62]

Many previous researchers analysed the friction of reciprocating rubber seals and they developed expressions for calculation of the seals friction force under sliding conditions, and their calculations were dependent on two factors: the seal contact surface length and the seal contact area. Determination and calculation of these two factors is key to calculation of the seal friction force.

Wendt (1971), examined stress distributions in O-rings and X-rings with emphasis of groove design. The most significant result of his work includes an expression for contact width of an unrestrained axially loaded O-ring. Molair (1973), who examined the contact surface and contact stress, lend credence to the finding of Wendt. AL-Ghathian (2005) [64], developed a relationship as practical and convenient option for computing the friction force in O-ring sealing elements as used in hydraulic and pneumatic equipment, and he developed an expression of the friction force (F_f) as:

$$F_f = 2\mu\Pi.D3rE\left(1-\frac{D3-d4}{4r}\right)\sqrt{1-\frac{(D3-d4)^2}{16r^2}} \quad (1)$$

Where μ is coefficient of fiction, D3 is the diameter of seal contact surface (mm), d4 is ram inside diameter (mm), r is O-ring radius (mm) and E is the modulus of elasticity [64]. Due to the expression above the main factor is the seal contact diameter.

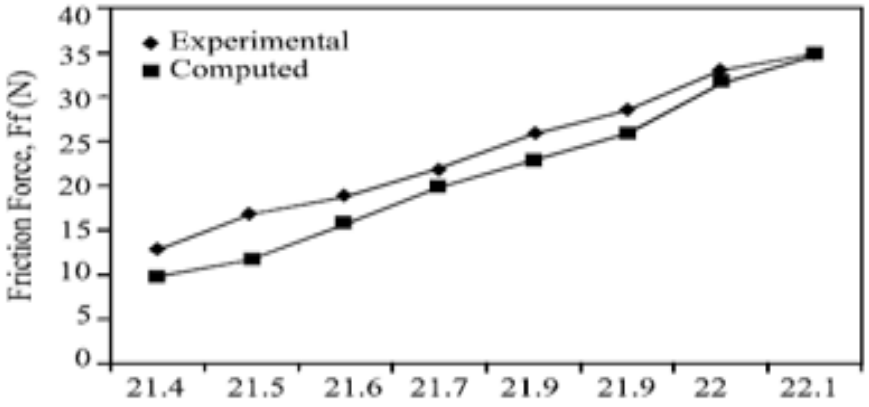

Fig.13. Relationship between friction forces and the diameter of O-ring seal [64].

Mofidi (2009) friction of sliding elastomer seals, he used a steel cylinder in contact with an NBR rubber substrate concluded that the diameter d of the contact region between the steel cylinder and the rubber substrate can be estimated using the Hertz contact theory for bodies with cylinder geometry [65].

$$d = 2\left(\frac{\mathbf{2\,Fn.D}}{\boldsymbol{\pi}\mathbf{.l.E}}\right)^{\mathbf{0.5}} \quad (2)$$

Where Fn is the load acting on the cylinder, D is cylinder diameter, E is the rubber young modulus and l is the contact length.

The average pressure in the contact region is given by.

$$P = \mathbf{0.5}\left(\frac{\boldsymbol{\pi}.\mathbf{Fn}.\mathbf{E}}{\mathbf{2}.\mathbf{L}.\mathbf{D}}\right)^{\mathbf{05}} \quad (3)$$

From these two equations the seal friction force can calculated. And also from the above expression the main contributing factor is seal contact diameter.

As a result, a lot of researches were focused on friction of elastomers seals, and few of previous researches focused on friction of the NBR piston seals used in water hand pumps.

For the piston seals used in a hand pump, seal friction force depended on the contact area, contact stress and the squeeze percentage. The lip of the piston seal limits all these factors. Diameter of the piston seal and the deflections angle of the lip are the key to calculating piston seal contact area which plays an important role of seal friction. Fig.14. displays the relationship between the number of cycles and percentage of lip worn.

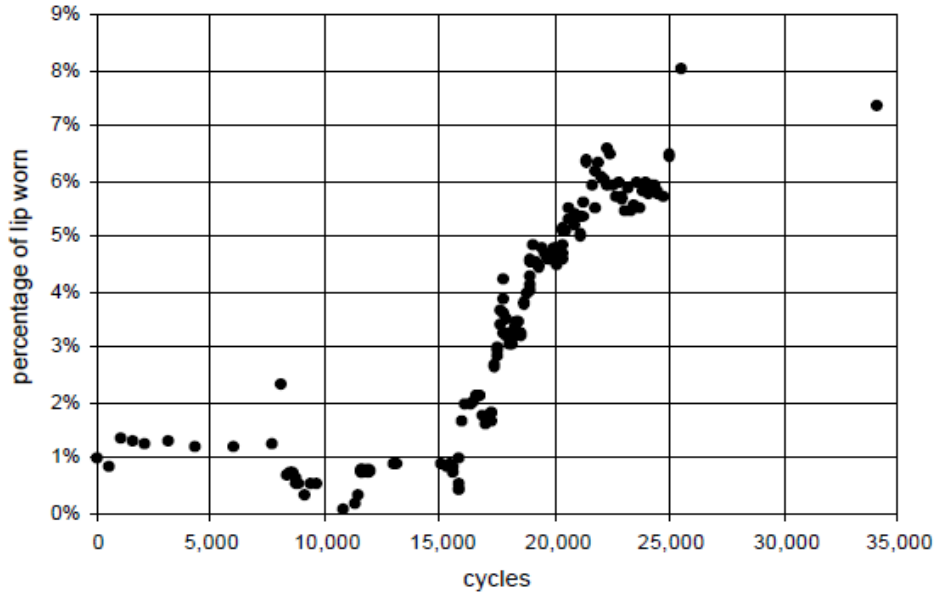

Fig.14. Wear of the lip of the seal with the number of cycles [26].

The coefficient of friction of elastomers are affected by changes in the contacting surface and contacting area. The friction coefficient decreases during running-in periods to reach steady state values.

In the dynamic seals there is a difference between the frictions at the start up and running. At the beginning of operation or beginning of movement, the start-up friction must be overcome, while the running-in friction depends on countless working factors. By calculating and determining the amount of seal squeeze and the contact pressure the performance of sealing can be predicted. When the compression of seal contact is more than the working pressure the seal will seal the joint and there is no leakage. However when the compression of seal contact area is lower than the working pressure, there is leakage, which means the contact stress is lower than the required stress. On the other hand, the increase in the amount of seal squeeze above the established limits results in higher friction and then higher removal of rubber material leading to higher seal wear. The compression is the percent decrease in diameter of the seal. Seal diameter highlights the amount of the compression and the amount of seal squeeze can be calculated by equation (iv).

$$\text{Squeeze}=\{1-\frac{\text{diameter of the seal before compression}-\text{diameter of the seal after compression}}{\text{diameter of the seal before compression}}\}\times 100\% \quad (4)$$

Fig.15 shows seals friction force due to the % of the seal compression. As a result of the seals squeeze, the contact stress will increase [64, 65].

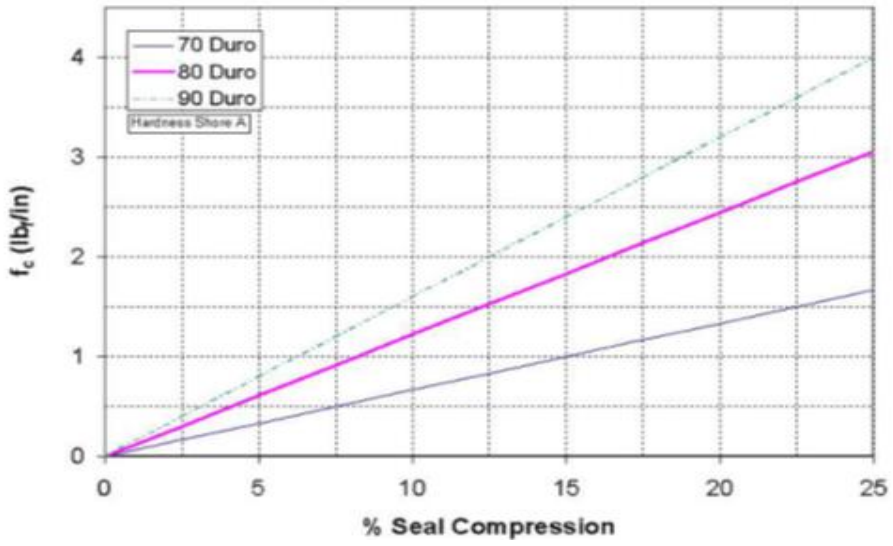

Fig.15. Friction due to seal compression [66]

2.4.5 Lubrication and sliding seals

During sliding of the rubber surface, interaction between the rubber molecules and the substrate will occur in most conditions. Through sliding it is probable that the rubber at the interface is subject to local stick slip motion, while the contamination layer fluctuates between a solid state at stick and a fluidized state through slip. This kind of local stick slip motion occurs for lubricated sliding systems at low sliding velocities [65]. Fig.16. shows the relationship between the coefficient of friction and sliding velocity for NBR rubber against a steel ring under lubricated condition.

Rubber friction under dry sliding condition is higher than that under wet or in the conditions presence of lubricant. The existence of fluid between rubber and a hard substrate reduces the adhesion and hysteretic components of friction. This is because the lubrication reduces the actual contact area between the rubber and hard substrate and this leads to a decrease in the rubber friction coefficient (fig.17) [54].

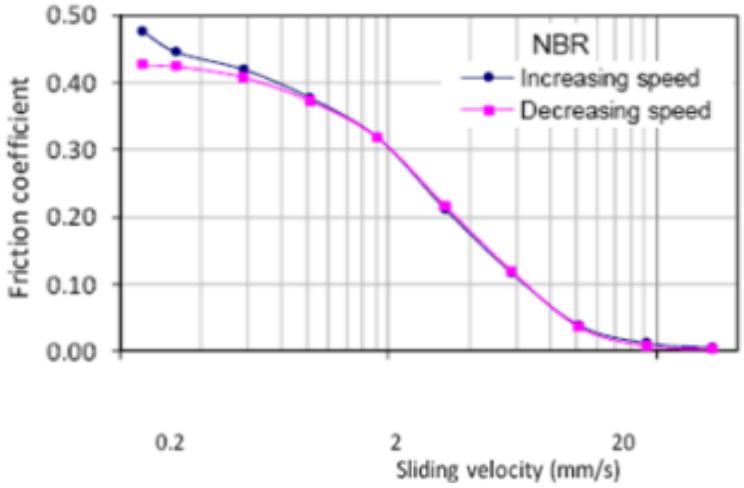

Fig.16. Relationship between coefficient of friction and sliding velocity in lubricant condition, for NBR rubber materials [65].

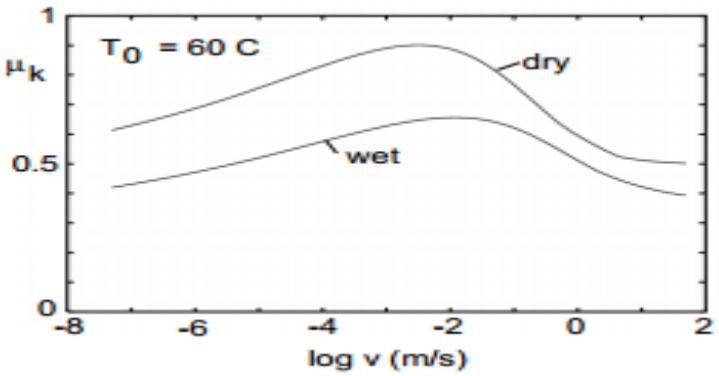

Fig.17. Relationship between dynamic coefficient of friction and logarithm of velocity, for rubber (tire) sliding in dry and wet conditions [67].

Mofidi, Prakash, and Persson. (2008) carried out experiments with rubber operating using eleven kinds of lubricants, and they found that the rubber friction coefficient were almost equal when sliding and operating in different lubricants, this indicates that rubber friction is not through shearing a thin viscous layer, but due to the internal friction of the rubber material [68].

Many previous studies focused on sliding rubber in the presence of the oil as a lubricant. However, a number of researchers studied sliding rubber in the presence of water as a lubricant. The water effectively smooth's the substrate surface, and thus reduces the viscoelastic deformation contribution of the rubber friction from the surface asperities. However there are problems in using water as a lubricant with some kind of rubber. Water has an effect on Nitrile butadiene rubber (NBR) when used as a seal in a lot of machines, similar to those used as a piston seals in water hand pump.

Water changes the mechanical properties of NBR, because water molecules reduce forces between the polymer chains, and this lead to reduction in intermolecular force. This can result in easy material removal during sliding and quickly, increased wear of the seals [69].

Finally, it has been found for dry and wet sliding, that with the lip shaped seal patterns, the friction force increase sharply near the end of the in-stroke and start of the out-stroke over a complete range of duty parameter. If the piston is used to lift or push fluid, and piston seal is a lip shaped pattern, the maximum pressure inclination on the out-stroke is much larger that on the in-stroke, therefore the leaks occur through the out-stroke [70].

2.5 Piston seal of the Water Hand Pump

The task of the piston in a water hand pump is to lift the water from underground to the surface. The piston in our rig divided the pump cylinder into two chambers, during the stroke the water flows through piston valves from the bottom chamber to the upper chamber. When the piston moves down, the valve opens, and when the piston moves up the valve close to raise water by the piston force. The piston seals function is to seal the gap between the piston and the cylinder bore, and also to prevent mixing of inlet and outlet water. This requires critical contact stress with complex design of the lip of the piston seal. During movement of the piston up and down, the piston seals will be under a friction force, and there is a fluctuating forces and stress also acting on the piston seals.

The **ideal and typical friction force on a piston seal of a water hand pumps during operating condition is shown in** Fig.18.

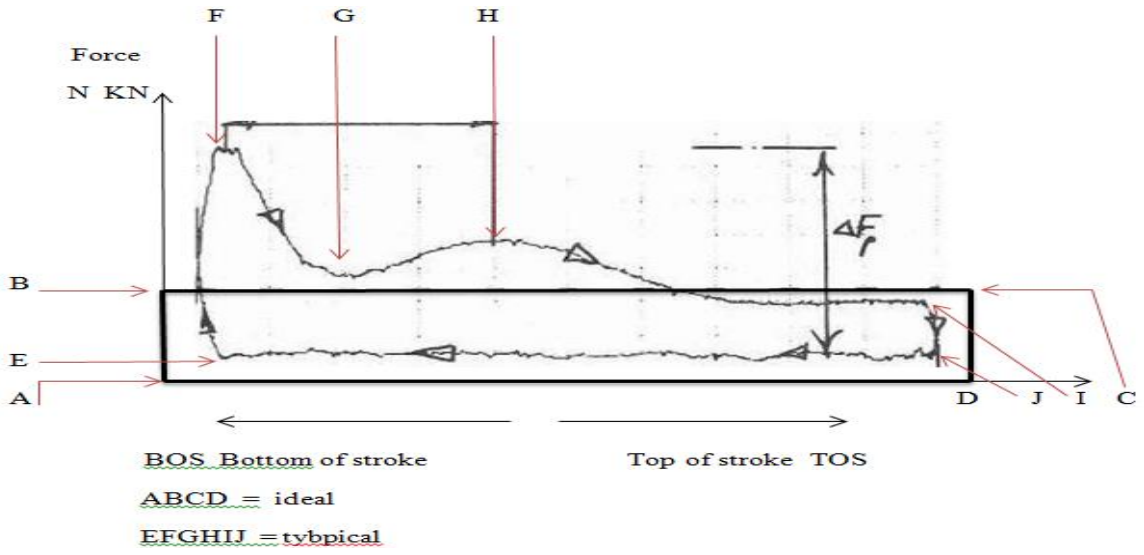

Fig.18. Variation of the load acting on the piston seal during one cycle of the hand pump

From fig.18, the solid line **ABCD** highlights the ideal friction loads, and the dashed curve **EFGHIJ** shows the typical friction loads through one cycle of the piston in a typical water hand pump. Point A; the piston is at the bottom of the cylinder (BDC-Bottom dead centre) before it starts to move, so the friction force acting on the piston seal is zero. When the piston starts to move up, there is a friction force acting on the piston seal until point B. From point B to point C, the friction force is constant as the piston reaches the top of its stroke (TCD-Top dead centre). At point C, the piston starts to move down, resulting in a friction force acting on the piston seal until point D. At point D the piston stops and return to the BDC to complete one cycle. From D to A, the friction is constant because the pistons stops before its second cycle. During the actual stroke as the piston accelerates up it requires a higher force to move up, and the friction force of the piston seal increases rapidly as from point E to point F. The inertial forces required to accelerate the water from rest cause the maximum friction force at point F to exceed the ideal at point B. From point F to point G a reduced external force is required. The problem from point G to point H is the closing of piston value. By point I the piston is decelerating and has reversed direction by point J.

2.6 Wear rates

A number of wear models and equations were studied to analyse their origin, content and applicability. There is no single predictive equation or group of equations that could be found for general analysis of water hand pumps. There are a number of wear models derived using solid mechanics, and most of these depend on material properties [71]. There are three general methods used between 1947 and 1992. Empirical equations up to 1970 are directly built with data taken from experiments. Barwell [72] proposed that the wear rate is a function of time.

Rhee [73] found that the total wear of friction material (elastomers) is a function of the applied load, speed and time. Contact- mechanics based equations were common in the years between 1970 and 1980. They generally began as a model of a system, with account taken of topography of contacting surface in order to calculate the local region of contact. An example of this is due to Archard [74] who published well in advance of the later contact mechanics

$$(V_w = K.S.\frac{N}{P}) \quad (5)$$

where $\mathbf{V_w}$ is the worn volume, **S** is sliding distance, **N** is the applied load and **P** is the pressure which is nearly equal to the hardness, and the ratio of $\frac{N}{P}$ is given as the real contact area, K is a constant. It is rationalised, that the value of K is obtained from experiment and it is known as a wear coefficient [75]. Equations based on material failure mechanism are also common to measure wear and are formulated with observance to (1) mass of removal material from the solid volume of removed material and (2) reduce dimensions of the solid [76].Burbor, 1974: propose that the wear rate is a function of the normal pressure, sliding velocity and temperature. Galin and Goryacheva, 1989: recognised elastic deformations of the surface connecting with rigid foundation. Anisotropic (having a physical property which has a different value when measured in different directions) wear has also been investigated by Zmitrowicz, 1993. Heterogenous wear and wear dependent on the sliding path curvature have been investigated by Zmitrowicz, 2005. The theory of wear rate begins by determing the rate of removal of materials as a function of the hardness of material, sliding velocity, and probability of material to produce a wear particle and also the forces applied [61]. In general, wear can occur in different forms which depend on contact between the surfaces of materials and the contact area, abrasion, adhesion, erosion and fatigue [77].

Fig.19 and Fig 20, show wear rate and wear coefficient versus sliding distance for some materials.

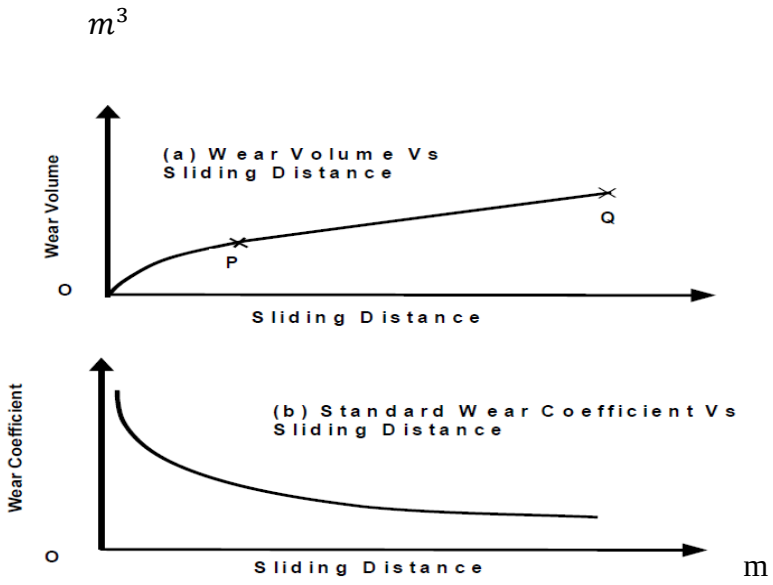

Fig.19. (a) Wear volume versus sliding distance, (b) Wear coefficient versus sliding distance [78].

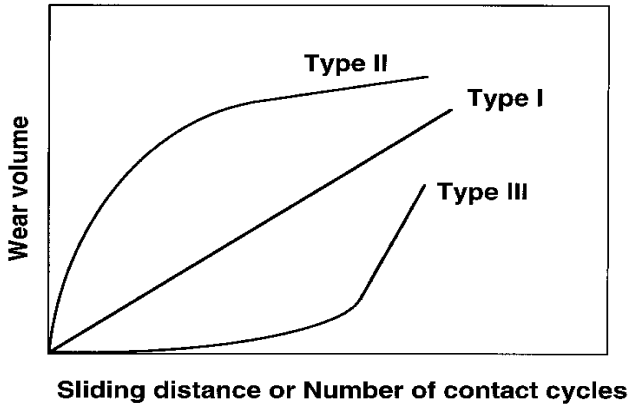

Fig.20. Type I, a constant wear rate during the whole process, Type II. The transition from initially high wear rate to steady wear at low rate(this type is often observed in metals, Chiou, 1985), Type III, catastrophic transition from initial wear of low rate to wear of high rate, such as a fatigue wear (Cho, 1989), [79].

Mofidi [63] and Mofidi. Braham Prakash [62] carried out experiments to find the influence of lubrication on two body abrasive wear of sealing elastomers. Based on their experimental results, they found that the presence the oil resulted in a decrease in coefficient of friction of the sliding elastomers. Fig.21. displays the relationship between elastomers friction coefficient and the sliding conditions.

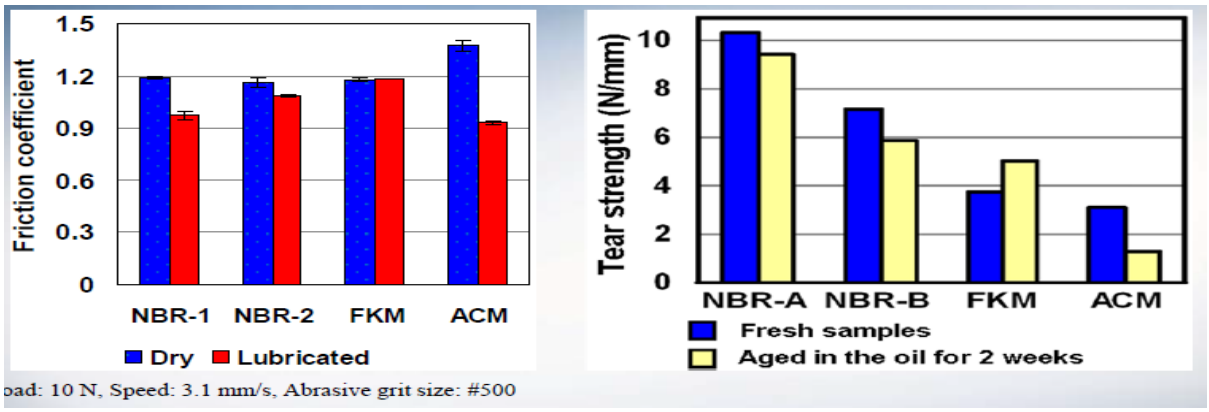

Fig. 21. Elastomers friction coefficients in dry and lubricant sliding conditions [62]

Empirical testing is a very important step for the development of any mathematical model. During these tests the model can be verified and any difficulty or problems highlighted. However there are a lot of variables which effect the wear rate [80]. **Reye** in 1860, said that, the volume of removal of materials from any surface was proportional to energy dissipated into it by the relative motion of two connecting surface

$$(V = K_r.W) \qquad (6)$$

where V is the volume of removal materials, K_r is Reyes wear constant, W is work dissipated into material. Reyes model evaluated wear of materials from an energy consideration stand point [81].

Tabor in 1939, considered that the real amount of contact between two surfaces is less than the apparent contact area. He developed two equations to predict behaviour of the contact area. Using an elastic assumption he stated that the contact area between the surfaces depended on the cubed root of the force applied At the same time, using a plastic assumption, he stated that the contact area between two surfaces dependant on the square root of the load applied. From these hypotheses, the findings showed that the actual contact area increase with increasing load [82]. **Holm** in 1946, posted that the singular atoms on opposing asperities were travel towards each other and then collide. By this hypothesis he stated that the amount of worn material during the atomic interactions was a function of the properties of the materials in contact and the load or the force acting on the contact

$$(V = Z.P / P_m) \quad (7)$$

where V is the volume of removed per unit sliding distance, Z is the probability of removal of an atom per atomic encounter, P is the load applied and Pm is the flow pressure of worn surface [80]. **Archard** [74] decided that key consideration must be used in a wear model. He endeavoured to apply some variables into one predictive equation, and these include: wear mechanism, sliding speed, contact area, contact pressure and material properties. Archards equation of the wear rate depended on a greater number of variables than Holms equation, and Archard equation is very important to analysis and determine the volume of removal materials. The period after 1953 saw a lot of studies applying Archard equations, and a number of wear rate equations derived from it, so Archard equation is still considered an excellent model for calculation of wear rates [83]. **Therefore, according to all previous wear models, there is to date no formula or models found to calculate the material removal rate of NBR piston seals in water hand pumps.**

Due to the frictional forces on rubber, elastic deformation of the specimen occurs. For most materials, the deformation is expected at the contact area under loading, but for rubber and elastomers the elastic deformations is expanded beyond the contact area, this phenomenon is particularly apparent when the reciprocating stroke length is short.

Because of the difficulty in understanding rubber wear mechanisms and rubber deformation, little effort has been focused on the characteristics and wear of the rubber seals, piston seals and sealing systems [11]. **Very limited research has been conducted on the wear of piston seals in the presence of water, and a very few has been reported regarding how to determine and calculate the wear rate of removal material of piston seals used in water hand pump.**

2.7 Finite Element Analyses (FEA) of the wear

Finite element analysis method F.E.A, is a technique for acquisition of numerical solutions to boundary value problems, which predict the response of physical systems subjected to external loads. Analysis of contact problems generally requires the determination of stresses and strains within the contacting surfaces, together with information regarding the distribution of displacements, velocity and stresses at the contact area [45]. Calculating the contact stress distribution is very complex; therefore advanced numerical methods must be used, such as finite element analysis F.E.A [84]. Fig.22. show the F.E.A of elastomer seal.

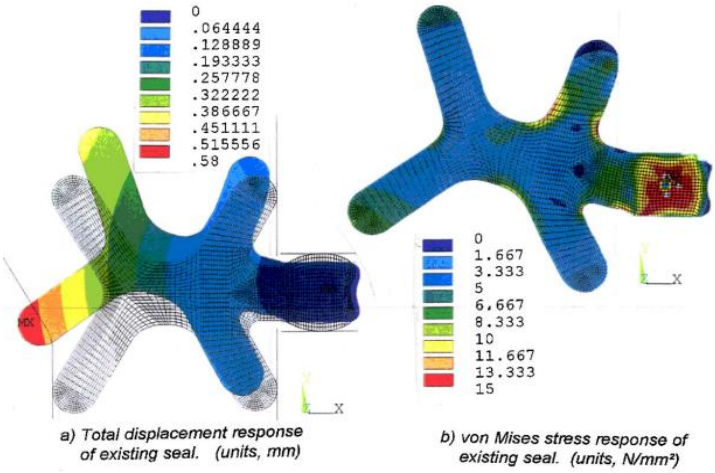

Fig.22. Sample of analysis plots for original seal design. The plot for displacement response shows the seal in the unloaded condition (meshed shape) and the condition after application of pressure load and spool movement (colored shape) [85]

Early theoretical and numerical determination of wear problems were carried out by; Galine and Goryahevae [47], Grib [69], Hugnell [36], Stromberg [37], Franklin [40], Ko Kato [41]

Shillor [42], Mc Coll [43), Kim [44] and Raczelt [39]. All discussed optimization problems with respect to the contact surface geometry generated wear [45].

Rubber is an unparalleled material as it behaves like a highly viscous liquid under fluctuating stress, and rubber can undergo large reversible deformations. The properties of rubber included: large deformation, nonlinear, load-extensions, viscoelastic and damper, nearly incompressible (volume does not change under stress), nonlinear response to stress or strain, exhibiting significant relaxation, and solid hyper-elastic. All these properties are required for F.E.A methods when rubber is in contact with a sliding surface on a hard substrate [87]. Fig.23. displays the stress effected on the O-ring seal after compressed.

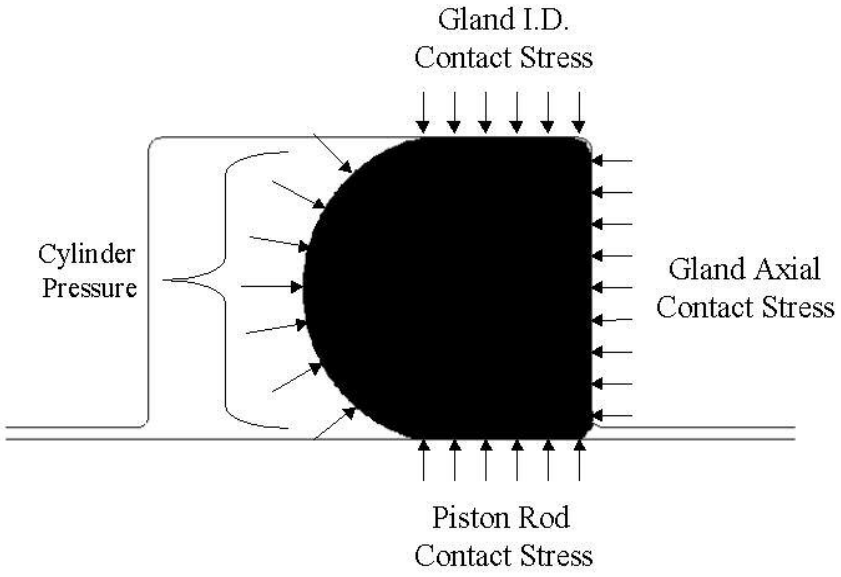

Fig.23. Forces and stresses on the O-ring seal as a result of cylinder pressure [66].

The subject and theory of finite elasticity or non-linear elasticity was developed in 1940s, and is associated with Rivlin,and afterward the development of continuum Mechanics associated with the Truesdell School during 1950s and 1960s.

The impetus for the theoretical developments in finite elasticity came from the rubber industry because of the importance of rubber in many engineering components; one of these is the rubber seals. This impetus was maintained with an increasing use of rubber [86]. There are many types of non-linear elastic models available such as Blatz-ko, Mooney-Rivlin, Neo-Hookean, and Ogden. The description of rubber materials tends to base itself on stretch ratio rather than strain, where stretch ratio $\boldsymbol{\lambda}$ is defined by $\lambda = \frac{L}{L_o}$ where; L is the deformed length of the sample and L_o is the original length. The most widely used finite element model for non-linear elastomer is Mooney-Rivlin model. Mooney-Rivlin model was developed from the Neo-Hookean model. It is usually available in two parameters, although three, five, and nine parameters may provide better results at higher strains [88].

Hyperplastic material (Rubber) has a very low modulus of elasticity and is almost incompressible, so the poisons ratio is very close to 0.5. Also for hyperplastic material loading changes the distance of the atoms with in the lattice of the material and so increase the internal energy, and during loading a stretching and un-balling appears. Loading may lead to deformation such as creeping [89]. Fig.24. shows Non-linear response of a hyperplastic material.

Most seals are made from the rubber and these may include reciprocating and dynamic seals, rod seals, piston seals, and O-ring seals. All of these seals during operation are in contact with the substrate surface, and there is a contact stress. The distribution of the contact stress can be calculated only by using F.E.A method.

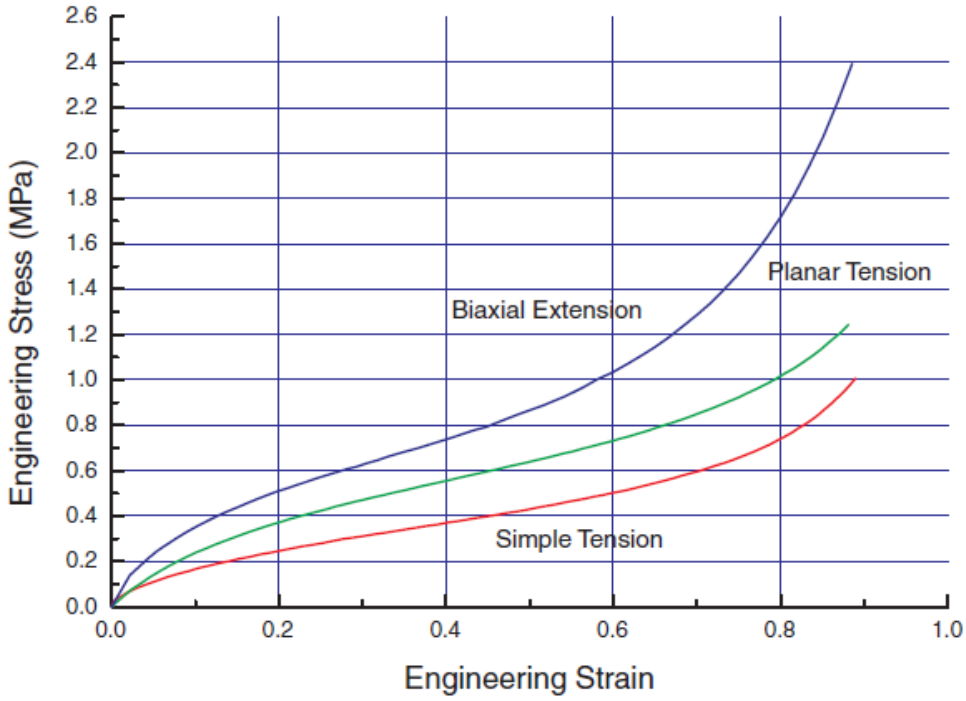

Fig.24. Non-linear response of a hyperplastic material [89]

Many studies has been performed to analysis the operation of reciprocating seals, starting with Kambayashi (1964) as well as Lawire and Dorrogue (1964). There were limitation in their outcomes by the way seals are designed and selected. However, the numerical model were able to determine friction, wear, and leakage within the area where the seal lip attach as to a surface and that resulted in reduction cost and time of design [90]. Sun and Alberson (1996), Peng (1994), their studies the performance of U-Cup hydraulic seals under static loading states and found the frictional forces, and stresses developed within the seal. In 2002,

a study by Claus, discusses the development of a new heavy duty piston seal using F.E.A and comprehensive testing required. Over the years, F.E.A has assisted the designers to reform seals. In 2006, Nicholas discusses the reciprocating rod seals response to dynamic conditions, and how the numerical model competent of simulating the dynamic conditions for seal could be defined [91].

Arthur Bullock in his study [92], combined a F.E.A seal model with dry boundary friction coefficient, and tribology simulations were produced based on the results of a FEA simulation of the rod-seal contact pressure.

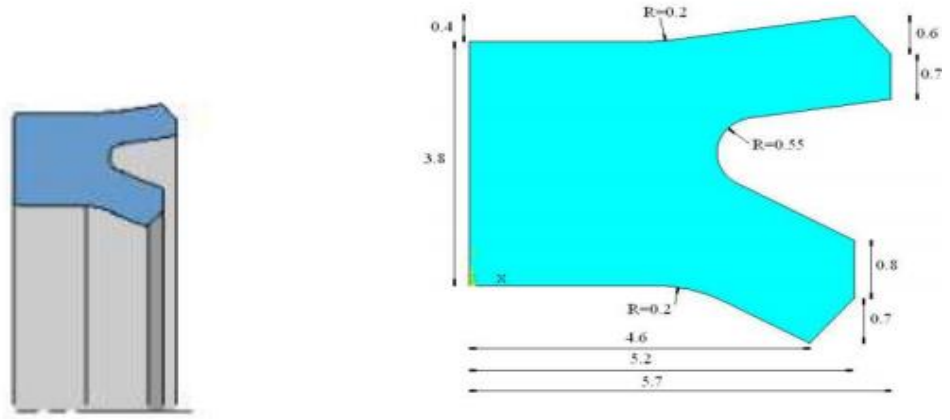

a b

Fig.25 .a-Parker-Hannifin single-lip seal and b- Seal dimensions (mm) assumed in single-lip seal FEA model [92]

The contact pressure is critical in seal modelling, performance evaluation and failure analysis. It is difficult to find and calculate the contact pressure distribution of a lip seal due to the size of the contact area.

Arthur Bullock [92], carried out experiments to measure the constant velocity friction for single-lip and double-lip seals over a range of sliding speeds and sealed pressures with special consideration applied to the instroke-outstroke direction dependence. The results for different seals are presented in the following sections

For the single –lip seal

Increasing the sealed pressure creates an almost equivalent uniform increase in the pressure distribution across the contact above a critical value of sealed pressure (approximately 20 bar (Fig 26). A significantly higher sealed pressure is required to completely flatten the seal against the rod at the change in geometry compared with the lowest sealed pressure required to first induced contact between the rod and main body of the seal. The pressure distribution across the main body of the seal is approximately constant.

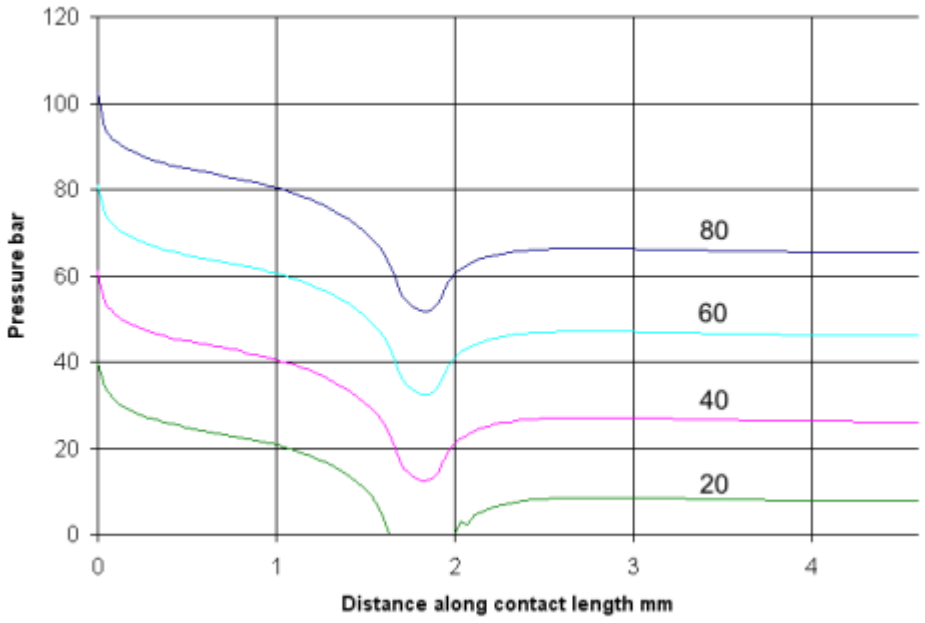

Fig.26. Pressure distribution from FEA of single-lip seal, 0.4 mm radius at the seal corners that form the inlet and outlet. Numerical labels indicate the sealed pressure (bar) [92]

For double-lip seal

The secondary lip produces a region of significantly higher contact pressure than the remainder of the seal, resulting in correspondingly higher normal reaction forcers. At lower sealed pressures, the additional reaction created by the secondary lip is significant relative to the single-lip. For higher sealed pressures, the additional contact pressure along the full lengths of the seals reduce the proportional difference in normal reactions between the single lip and double-lip seals

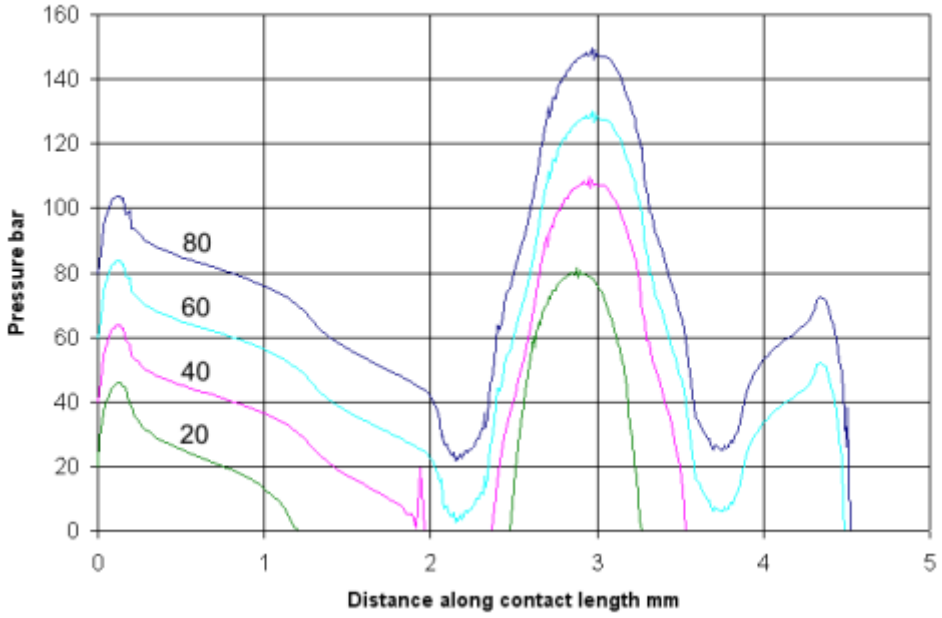

Fig.27. Pressure distribution from FEA of double-lip seal. Numerical labels indicate the sealed pressure (bar) [92]

For the O-ring seal

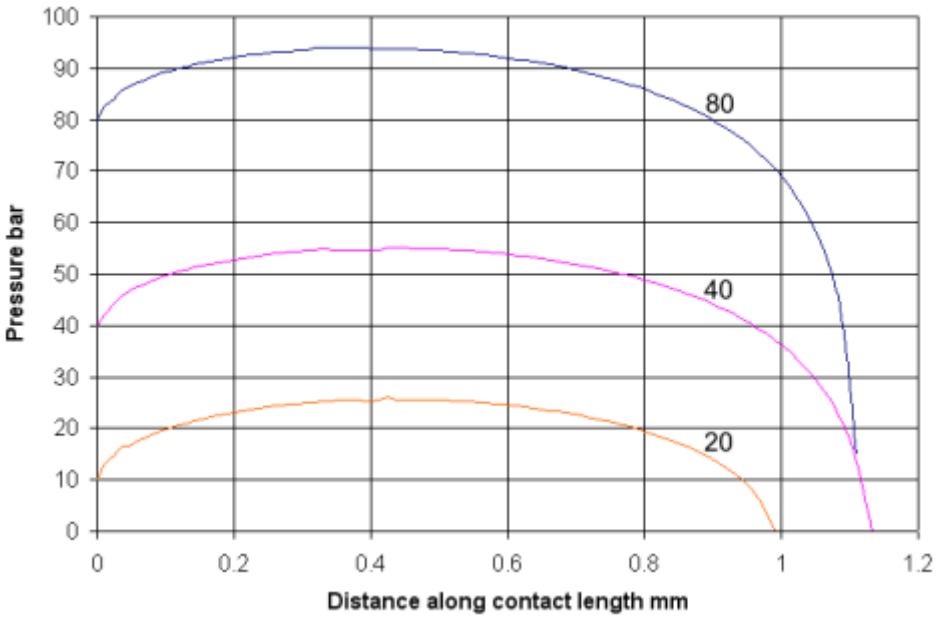

Fig.28. Pressure distribution from FEA of O-ring. Numerical labels indicate the sealed pressure (bar) [92].

F.E.A is a powerful tool to estimate the seal stress, strain, and contact pressure distribution. The amplitude and distribution of contact pressure of a seals is dependent on the contact area of the interface as the contact area changes continuously due to material wear**.** The contact area and seal deformation can be dramatically changed without considering the reduction in thickness of the seal due to wear. The worn off material (removed continuously) must be continuously accounted through the cycles to simulate seal wear [93].

Nandor Bekesi [94], in his study (friction and wear mechanisms of elastomers in dry and lubricated sliding conditions), a tribological tests were carried out tribological tests in order to study the dry sliding friction between an EPDM rubber specimen and a rotating steel shaft.

He found that after applying the normal load the shaft begun to rotate. The contacting nodes were stuck to the shaft at first, then started to slip. The contact pressure values were considerably different in the contact area; in some regions the contacting surfaces separated (fig 29), the rubber became creased and a wrinkle appeared, which remained till the end of the simulation

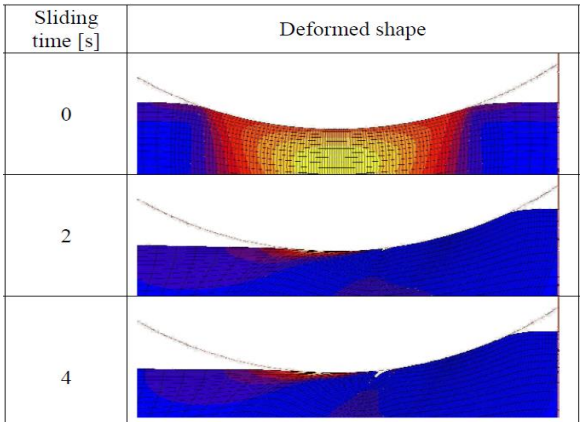

Fig.29. Deformed shape due to sliding time [94]

Nandor studied [94] sliding wear of a seal models of both numerical and experimental to analyse the behaviour of sliding seal experimentally and numerically, he carried out experiments and he investigated EPDM rubber seal are shown in Fig. 30 .

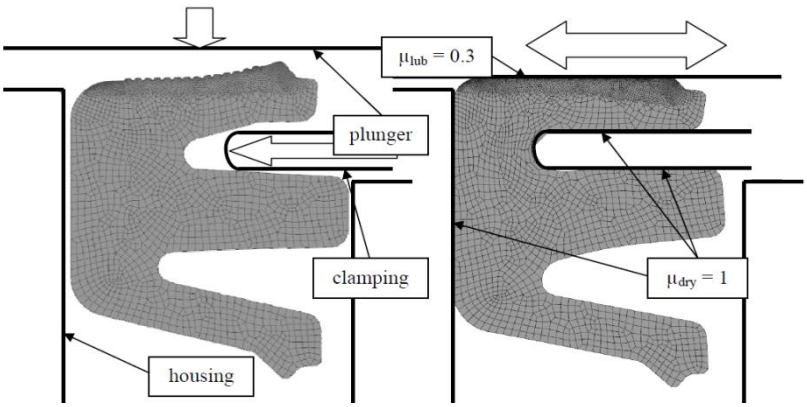

Fig.30. FE model of the seal section before (left) and after mounting in the holder (right) [94]

In the test series, various lubrication conditions were investigated namely dry, boundary and fluid film lubrications. In the case of dry sliding, the specimen was torn into pieces after a few minutes and the test was stopped. When the specimen was fluid film lubricated, no trace of wear was visible on the surface. Based on the results of the researches, Nandor found that the ridges of the seal and the lip edge wear first, and the wear occurs not only in the top layer, but in several layers of elements. Fig. 31. Displays seal worn over the sliding time and due to the number of the cycles

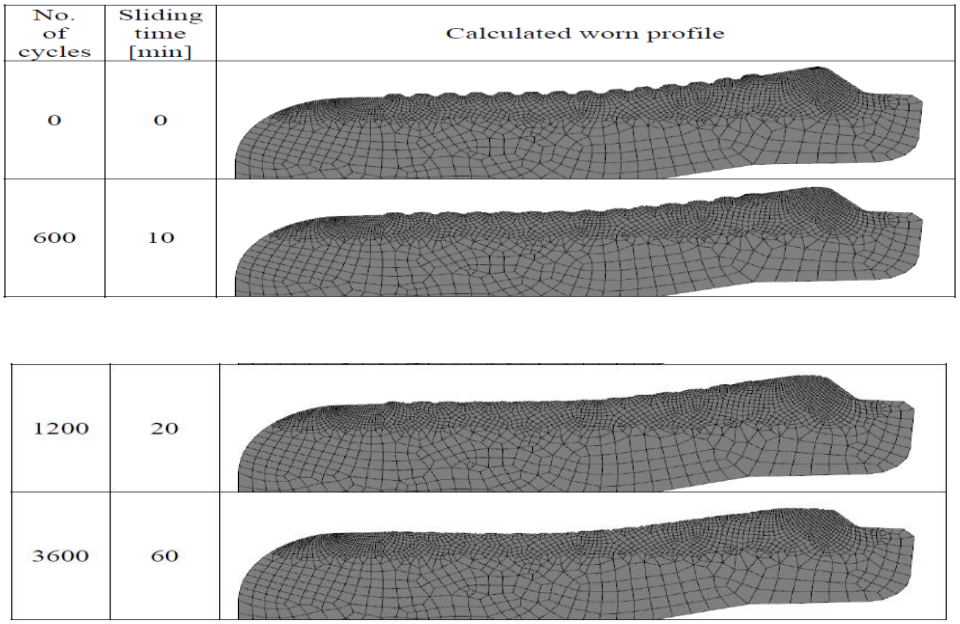

Fig.31. Worn seal area due to sliding time and sliding cycles [94].

The wear process of one ridge can be tracked in the successive images of Fig. 32.

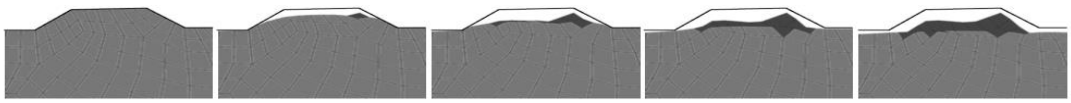

Fig.32.The wear process of one ridge of the seal.

The images show the left ridge of the seal model after 0, 15, 30, 45 and 60 minutes of sliding, respectively [94]. The specification of non-linear material properties for elastomers is very difficult. Theories for large elastic deformations based on strain energy density functions have been developed for hyperplastic materials. These theories, coupled with F.E.A, can be used effectively by design engineers to analysis and design elastomer products operating under highly deformed states. In the case of incompressible materials, the Mooney-Rivlin model remains the most widely used, and this model uses strain energy function in F.E.A modelling [95]. The engineering strain (change in length divided by the original length) is given by,

$$\mathcal{E}=\frac{L_1-L_0}{L_0} \tag{8}$$

the stretch ratio λ is another fundamental quantity, it is length after deformation divided by the original length [96]

$$\lambda=\frac{L_1}{L_0}=\frac{L_1-L_0+L_0}{L_0}=\mathcal{E}+1 \tag{9}$$

The pioneering Mooney-Rivlin model on finite elasticity, it is derived based on the elastic strain energy per unit volume (W), which is a function of the three principle stresses (stretches) of deformation, that is W=W(λ_1,λ_2,λ_3), where $\lambda_1 = l_i / L_i$ (i=1,2,3), and l_i & L_i being deformed and reference length, respectively. It is assumed that the mechanical properties of rubber like solids can be represented in terms of the energy functions. Assuming isotropic solid and isothermal conditions, the energy must be independent of the coordinate system used. Therefore it can be come-cross three strain invariants; $I_1= \lambda_1^2 + \lambda_2^2 + \lambda_3^2$, $I_2 = (\lambda_1.\lambda_2)^2 + (\lambda_2.\lambda_3)^2 + (\lambda_3.\lambda_1)^2$ and $I_3 =(\lambda_1.\lambda_2.\lambda_3)^2$,

for incompressible solid such as rubber: $\lambda_1.\lambda_2.\lambda_3$=1, so I_3= 1 for the rubber [97]. Mooney – Rivlin function for hyperplastic can be displayed by;

$$W = C_1 (I_1 - 3) + C_2(I_2 - 3) \quad (10)$$

where C_1 & C_2 are material constants, and can obtained experimentally through tests, the initial shear and initial bulk modulus is; G=$\frac{E}{2(1+\upsilon)}$, K=$\frac{E}{3(1-2\upsilon)}$, where E is the material young-modulus and υ is passion ratio. For Mooney-Rivlin the initial shear modulus is related to material constant by G = 2(C_1+C_2), and if the material is incompressible, then the initial tensile modulus is given by E= 6(C_1 +C_2). The stress-strain equation can be expressed as:

$$\sigma = 2\{\lambda - \frac{1}{\lambda^2}\}\{C_1 + \frac{C_2}{\lambda}\} \quad (11)$$

this equation can be rewriter as

$$\frac{\sigma}{2\{\lambda - \frac{1}{\lambda^2}\}} = C_1 + \frac{C_2}{\lambda} \quad (12)$$

this equation is the equation for a straight line, and can be plotted as $\frac{\sigma}{2\{\lambda - \frac{1}{\lambda^2}\}}$ against $\frac{1}{\lambda}$ [88]. If the stress-strain curve is not available and only the modulus of elasticity E is known, then according to reference [71], a reasonable approximation to use is; C_1= 4C_2 and E = 3(C_1+C_2), resulting in C_1=$\frac{4E}{15}$ and C_2=$\frac{E}{15}$. Mooney-Rivlin model has been used for problem involving reciprocating seals [84]. Fig.33. Show stress-stretch equation for an incompressible two parameter Mooney-Rivlin model.

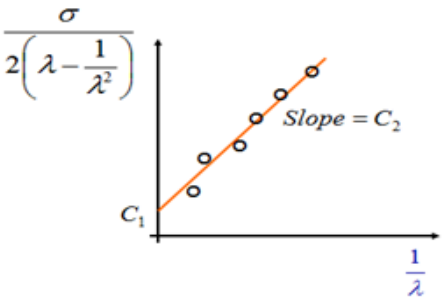

Fig.33.Relationship between uniaxial stress-stretch for two parameter incompressible Mooney-Rivlin Model [89].

Table 3.presented the studies which used the F.E.A method for rubber seals analysis:

Author	Year	Study titel	Ref:
Albrson	1994	Analysed the performance of the U-Cap hydraulic seals under static loading condition.	91
Claus	2002	Analysed the performance of heavy duty piston seals to confirm the seal design.	90
Brian	2005	Analysed dynamic O-ring seals friction in a hydraulic actuator.	66
Nicholas	2006	Analysed the rod seals response to dynamic conditions	91
Arthur	2010	Analysed rod seals: contact pressure, and boundary friction coefficient in dry moving, using a hydraulic actuator.	92
Nandos	2011	Analysed the tribological behaviour of sliding EPDM rubber seal, using aluminium plunger pressed against the seal specimen and moved in reciprocating way.	94

3. Theory

3.1 NBR Piston seals contact area and its friction force

Piston seals used for water pumping are characterised by the deflection angle of the lip (Ø) and by the diameters D_1 and D_2 as shown in Fig .34. These dimensions are very important, because D_1, D_2 and Ø define the function of the piston seal, and the seal compression. This influences the friction force acting on the piston seal. In general, any seal performance is considered to be primarily a result of the sealing force that develops when a seal is compressed.

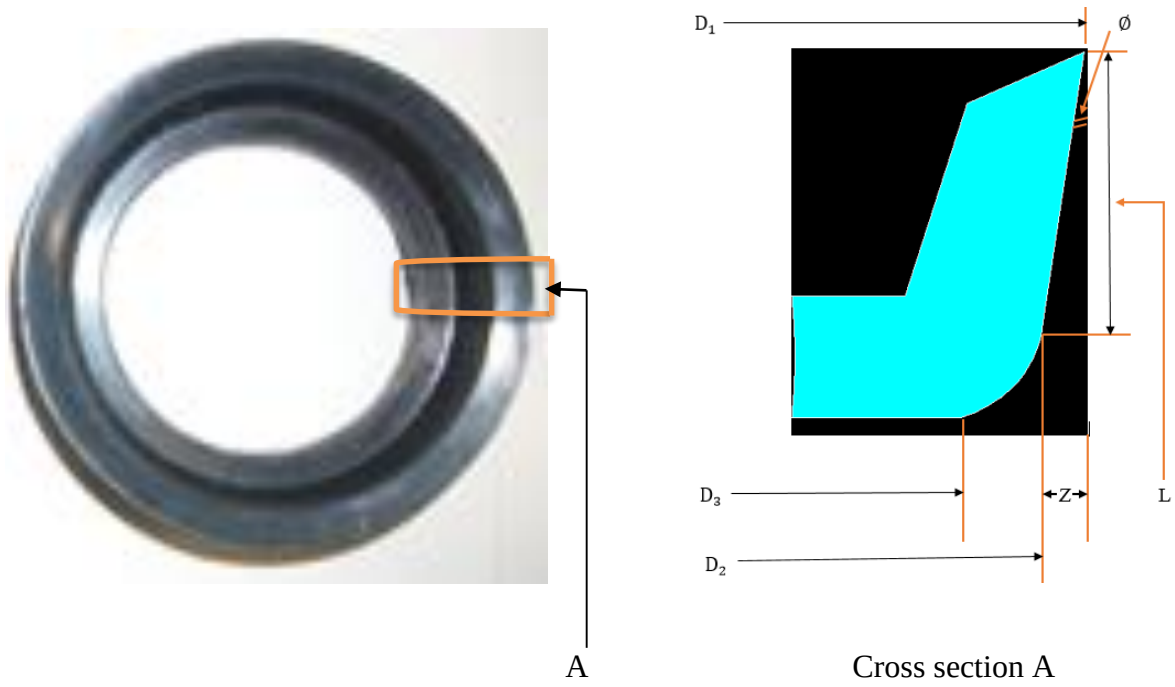

Fig.34: Piston seal and its dimensions.

The initial sealing effect before the operating pressure is applied is produced by the interaction of the seal edges on the cylindrical contact surfaces for any type of seal, and when the operating pressure is elevated the sealing pressure is automatically increased. The evaluation of the NBR piston seal friction force and wear rate is dependent on the seal contact width and piston seal contact area.

Following compression of the piston seal in the cylinder there is a deflection of the lip of the seal, and the distance of the lip deflection defined as X. Due to the lip deflection there is a contact surface (width) defined as Y at the inner wall of the pump cylinder. Fig.35. highlights the shape of the piston seal before and after the compression.

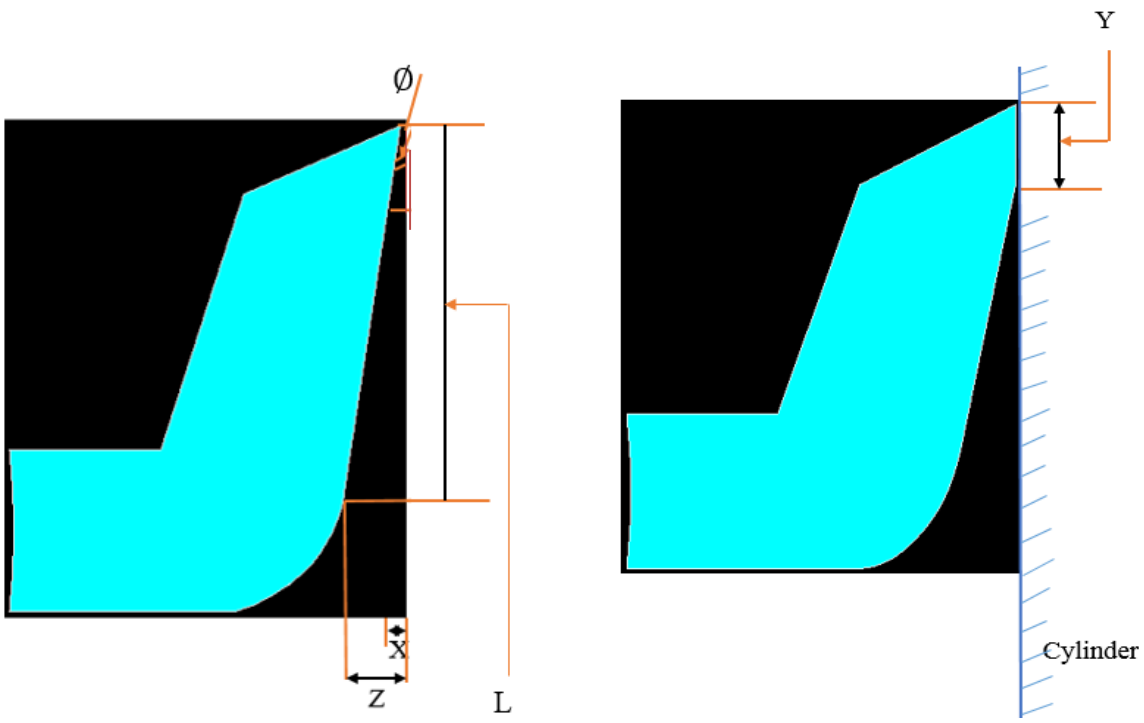

(a) (b)

Fig.35 NBR piston seals shape (a) before compression and (b) after compression

The movement of the lip (X distance) causes a compression. The percentage of compression is different along the seal contact width Y. The amount of the compression depended on the deflections angle of the lip (Ø) and the slope of the seal edge.

The maximum compression is at the top of Y (lips edge) and the minimum compression is at the bottom of Y.

Piston seal compression can be calculated by the equation in the literature:

$$\text{Compression}=\{1-\frac{\text{diameter of the seal before compression}-\text{diameter of the seal after compression}}{\text{diameter of the seal before compression}}\}\times 100\%$$

So the percentage compression of NBR piston seal is:

$$\text{Compression }\%=\{\ 1-\frac{D_1-2X}{D_1}\}\times 100\% \qquad (13)$$

Due to equation (13) the maximum compression is at the top of Y (lips edge) and the minimum compression is at the bottom of Y.

To compute the friction force and wear rate of the NBR piston seal it is necessary to find and calculate the contact area of the NBR piston seal.

$$Z=\frac{D_1-D_2}{2} \qquad (14)$$

$$Ø = tan^{-1}\frac{Z}{L} \qquad (15)$$

$$X=\frac{D_1-Dc}{2} \qquad (16)$$

where Dc is Diameter of the cylinder bore

$$Y=\frac{X}{tanØ} \qquad (17)$$

From equation (13) we can calculate the compression at any point along Y.

The **contact area** CA of the NBR piston seal after compression is given by.

$$CA=\pi.D_S.Y \tag{18}$$

Substituting equation (17) into equation (18), an ***equation for calculating the contact area of the NBR piston seal of the water hand pump is developed.***

$$CA=\frac{\pi.D_S.X}{\tan\emptyset} \tag{19}$$

Forces acting on the NBR piston seals through reciprocating motion up and down are the water load and the weight of (piston and pump rod).

$$F = \rho.g.H\ (Ac - Ar) + W.g \tag{20}$$

F; is the total forces acting on the piston seal (newton), ρ is water density (kilogram per meter square), H is the water column (meter), Ac is the cross section area of the pump cylinder (meter square), Ar is cross section area of the pump rod (meter square), W is the total weight of piston and pump rod and piston seals (kilogram), g is gravity acceleration (meter per second square).

The seal friction force (Fs) is given by

$$Fs = \mu\ (P \times\ CA) = \mu\ (\frac{F}{Ac-Ar} \times\ CA) \tag{21}$$

Where Fs is the seal friction force (newton), μ is the dynamic seal friction coefficient, P is the total pressure acting on the piston seal (newton per meter square), CA piston seal contact area (meter square).

Substituting equation (19) in to equation (21) and using Ac & Ar in term of D, ***the equation for calculating NBR piston seals friction force:***

$$F_S = \mu \left(\frac{F}{\frac{\pi}{4}(D_c^2 - D_r^2)} \times \frac{\pi.Ds.X}{\tan\theta} \right) \quad (22)$$

$$F_S = 4.\mu.F.X. \frac{D_s}{(D_c^2 - D_r^2) . \tan\theta} \quad (23)$$

Where D_s is same D_1 piston seal diameter (meter), D_c; is pump cylinder diameter (meter), and D_r; is pump rod diameter (meter).

The friction force acting on the piston seal of a water hand pump is continually changing through the movement of the piston up and down during one cycle due to the weight of the water column during the piston stroke.

3.2 Wear rate and Volume of removal material of lip shaped piston seal.

Archard equation is still considered to be an excellent model for calculation of wear rates. Applying Archards adhesive wear equation (1953), a new wear rate model can be developed to calculate and determine the wear rate of NBR piston seal over the sliding time.

Archards adhesive wear equation is:

$$V_w = \frac{1}{3} K.S.\frac{N}{P} \quad (24)$$

WhereV_w is volume of removed material (m^3) , S is the sliding distance (m), N is the applied load (Newton), P is the pressure which is approximately equal to the hardness H $\left(\frac{N}{m^2}\right)$. K is the wear coefficient and it is a constant.

By rearrange Archards equation, the wear coefficient can be calculated by the following Equa

$$K = 3\frac{Vw/S}{N/P} \quad (25)$$

$\frac{Vw}{S}$ is the area of removed material A_W (m^2), and $\frac{N}{P}$ is the real contact area A_R (m^2).

Therefore the coefficient of wear (K) is the ratio of the area of removal material per the real contact area, and it is constant:

$$K = 3\frac{A_W}{A_R} \quad (26)$$

For the NBR piston seal of the water hand pump, A_W and A_R change with time of operation, and through the piston sliding distance. They also change due to the fluctuating load of the water acting on the piston seal. This can lead to the value of coefficient of wear (K) changing due to the change in contact area.

The area of the removed material is equal to the difference between the seal contact area before and after testing replaces equation (26) in equation (18) give

$$K = 3\frac{(\pi.D_{sb}.Y_b)-(\pi.D_{sa}.Y_a)}{\pi.D_{sb.}Y_b} \quad (27)$$

In general Y can be calculated from equation (**17)**: $Y = \frac{X}{tan\theta}$

Where $(D_{sb}$ and $Y_b)$ are the piston seal diameter and length of piston seals contact surface before the test, and D_{sa} and $Y_a)$ are the piston seal diameter and length of piston seals contact surface after the test. By removing π, ***the equation for calculating wear coefficient can be expressed by the following.***

$$K = 3\frac{(D_{sb}.Y_b)-(D_{sa}.Y_a)}{.D_{sb.}Y_b} \quad (28)$$

Substituting equation (28) in equation (25), results in the ***Equation for the Volume of removed material***

$$V_w = \pi\{(D_{sb}.Y_b) - (D_{sa}.Y_a)\} \times S \quad (29)$$

Equation of the Wear rate of NBR piston seal

$$A_w = \pi\{(D_{sb}.Y_b) - (D_{sa}.Y_a)\} \quad (30)$$

These equations will be applied for calculating wear volumes and wear rates.

4. Experimental set up

4.1 Rig Design

The purpose of this research is to study and analyse the wear of NBR piston seals and to investigate the mechanisms of wear under sliding conditions in the presence and absence of water. To carry out this research, a custom built pump rig was designed and developed which operate similarly to the water hand pumps used in developing countries. Two similar hand pumps operate with the same stroke using pneumatic cylinders to reciprocate. Fig 36 shows a photograph of the test rigs. By used this rig and over operating time the wear will occur and increase with time of operation also by increase the stroke of the piston can find and determine its effect on wear of the piston seal.

The pump rig has been designed to conduct experiments on frictional and wear behaviour of NBR piston seals first under dry condition with short stroke 56.74 mm and long stroke 200 mm, and with different loads acting on the piston seals. Second, in wet condition with short stroke 56.74 mm and long stroke 200 mm, using water as a lubricant.

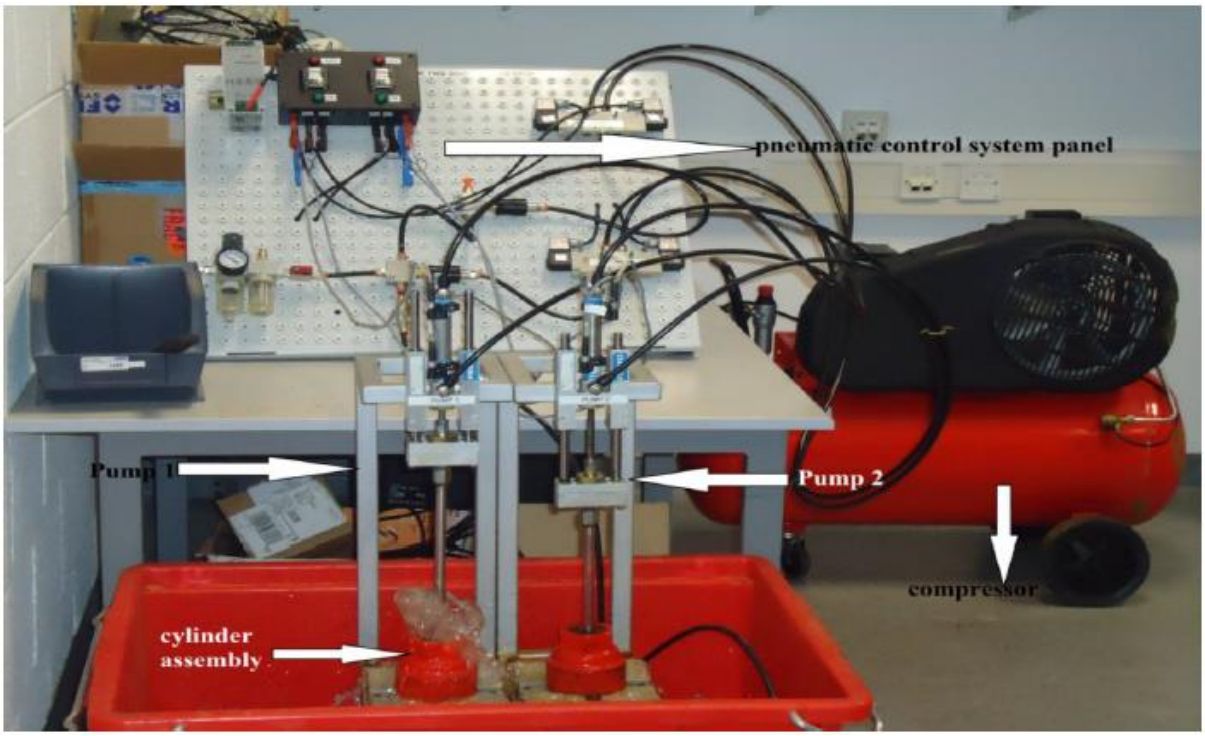

Fig.36 Wear test rigs

In this study, an investigation of uncoated NBR piston seals were used to measure the seal friction and wear rate. For each pump, there are two NBR piston seals, one at top and one at bottom of the piston chamber dividing the pump cylinder into two areas. The motion of the pneumatic cylinders rig allowed the piston to move up and down at a specific stroke length.

4.2 Pump rigs components and specifications

The Cylinder was made from cast iron with a Brass-lined inner wall. The inner diameter of the cylinder was 63.03 mm, and there are upper and lower caps made from cast iron. The inner diameter of outlet of the upper cap was 39.68 mm, the inner diameter of the inlet cap was 39.68 mm, Fig.37. shows pump cylinder and caps.

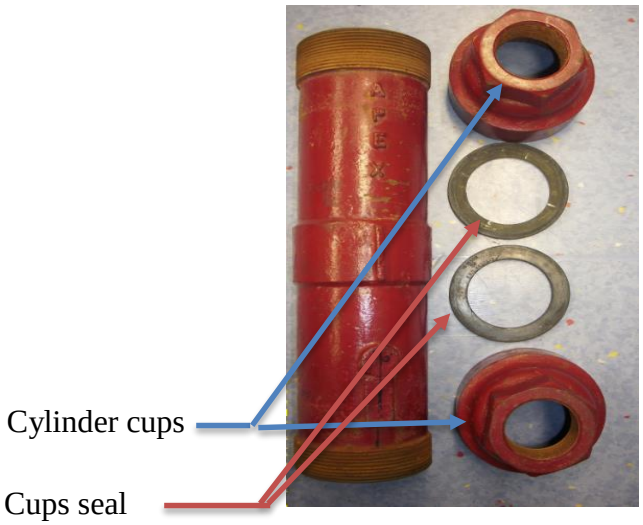

Fig.37. Pump cylinder, caps and Cap seals

Pump rod was the rod made from steel with a 12.05 mm diameter and 41 mm length. This connects the piston in the pump cylinder to the rod of pneumatic piston. The pump rod of the piston can extend and retract.

Piston was made from brass and included a housing contains the piston seals and piston valve. The piston is connected to the pump rod. The piston lifts the water by the piston motion. Fig.38 shows the piston and piston valve. Piston valve is a one way valve and the water flows through the valve into the upper chamber of the cylinder.

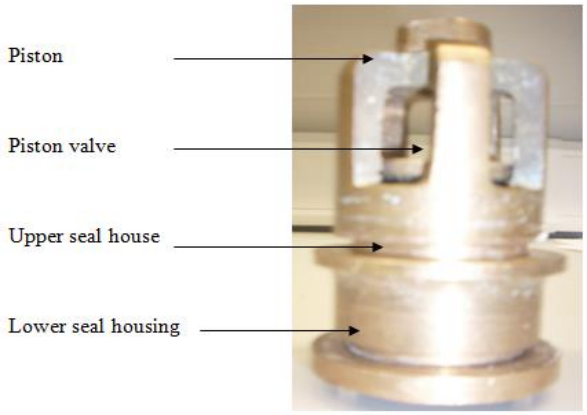

Fig.38. Piston housing and valve assembly

Fig.39: Top and bottom piston seals

Foot valve: It is a one way valve and is located at the lower cap. The water flows through the foot valve up-ward into the lower cylinder. The foot valve is open on the up stroke and close sealed on the down stroke. Fig.36 show foot valve.

Fig.40. Foot valve assemply

4.3 Pneumatic system

The pump rig operates by using a pneumatic system which contains: 1-Double acting cylinder (Type 20×57 for the short stroke 56.74 mm and type 32×200 for the long stroke 200 mm). 2- U- type guide unit of 20 mm DIA cylinder up to 57 mm for short stroke, and U-type guide unit of 32 mm DIA cylinder up to 200 mm for long stroke. 3. Reed switches two for the short stroke and two for the long stroke. The pneumatic system is supplied with air pressure to a maximum of 10 bars. The piston rod of the pneumatic piston connects with the pump rod of the rig, so when the pneumatic system operates, the pump rod moves with a reciprocating motion. The air supply is controled by using 5/2 solenoid operated valve. This pneumatic system allowed the pump rig to operate continuously simulating the operation of a hand pump used in developing countries. To calculate the pressure drop, the piston is provide with two pressure gauges, one at air inlet pipe and other at air outlet pipe.

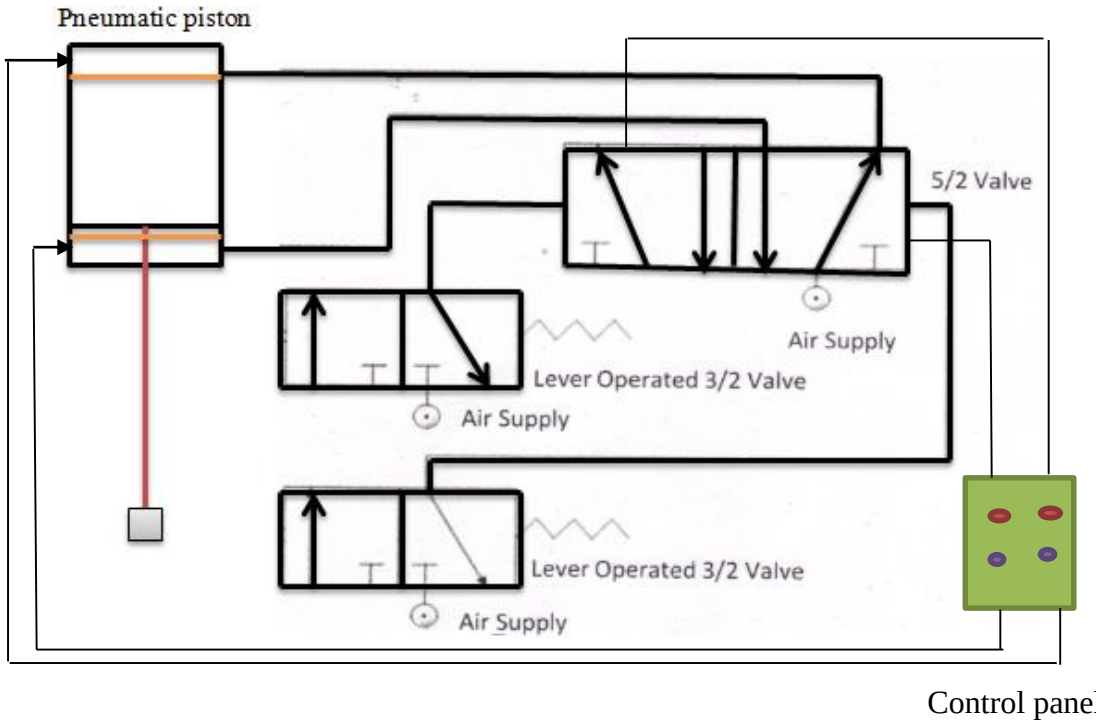

Fig.41.Schemetic diagram of the pneumatic circuit of the wear test rig

5. Result and Discussions

5.1 Experimental Results for Pumps Rig with Short Stroke (56.74 mm)

In this study two methods were used for analysis of wear of the NBR piston seals of the water hand pump, under wet and dry sliding conditions. These methods are experimental analysis and Finite Element Analysis (F.E.A). The validity of the equations outlined in Chapter 5 for seal contact area, seal friction force, coefficient of seal wear, and volume of removed material from seal were tested using the experimental rig. **Three experiments** were carried out and each experiment included a number of tests. **The first experiment** was conduct under wet sliding and in the presence of water, where the pump rig ran to pump clean water, similar to the mode of operation of water hand pumps used in the developing countries. At the same time, the water played an important role as it acted as a lubrication fluid for the piston seals. This experiment was carried out with different piston speeds 115, 144, 153, 165, 189 (mm/sec) each test at a constant speed and the operating time for each test was 3 hours. Forces acting on the piston seals were water loads and weight of piston plus pump rod. **The second experiment** was under dry sliding condition which included two tests. The same velocity (153 mm/sec) was used for these tests, operating times for the test was two hours and four hours respectively. Forces acting on the piston seal were weight of piston plus pump rod. **Third experiment** was also conducted under dry sliding condition with effect of a mass of 0.5 Kg added (to increase the load on the piston seal and find its effect), this experiment included two tests. Same velocity was used for the tests and the operating time for test one was 2 hours and four hours for the second. Forces acting on the piston seal were: weight of piston plus pump rod and mass of 0.5 Kg was added to the pump rod.

Due to the deflection angle of the lip of the piston seal the compression of the seal after insertion into the cylinder is not homogeneous and not equal on all the regions of the seal contact surface (Y). To prove that the piston seal contact surface (Y) was divided into 5 equal regions (6 points), the diameter and the travel distance (X) of each point were evaluated. Table 4, presents the results of the NBR piston seal compression. The % compression along the contact surface was calculated and found that the % compression (starting from the lips edge) was 2.446% and at the remaining points was 1.939%, 1.460%, 0.977% and 0.489 however at the bottom point of the contact surface (Y) the compression was zero because at the last point the seal diameter is 63 mm which is equal to the diameter of the pump cylinder (63 mm).

Table 4. % Compression of the lip of the NBR piston seal due to the travel distance X and for a different points along the contact surface (Y).

Contact surface Y divided to 5 regions (6 points) starting from the lips edge	Seal Diameter mm	Travel distance X mm	% Compression
Point 1	64.58	0.79	2.446
Point 2	64.246	0.623	1.939
Point 3	63.934	0.467	1.460
Point 4	63.622	0.34	0.977
Point 5	63.31	0.155	0.489
Point 6	63	0	0

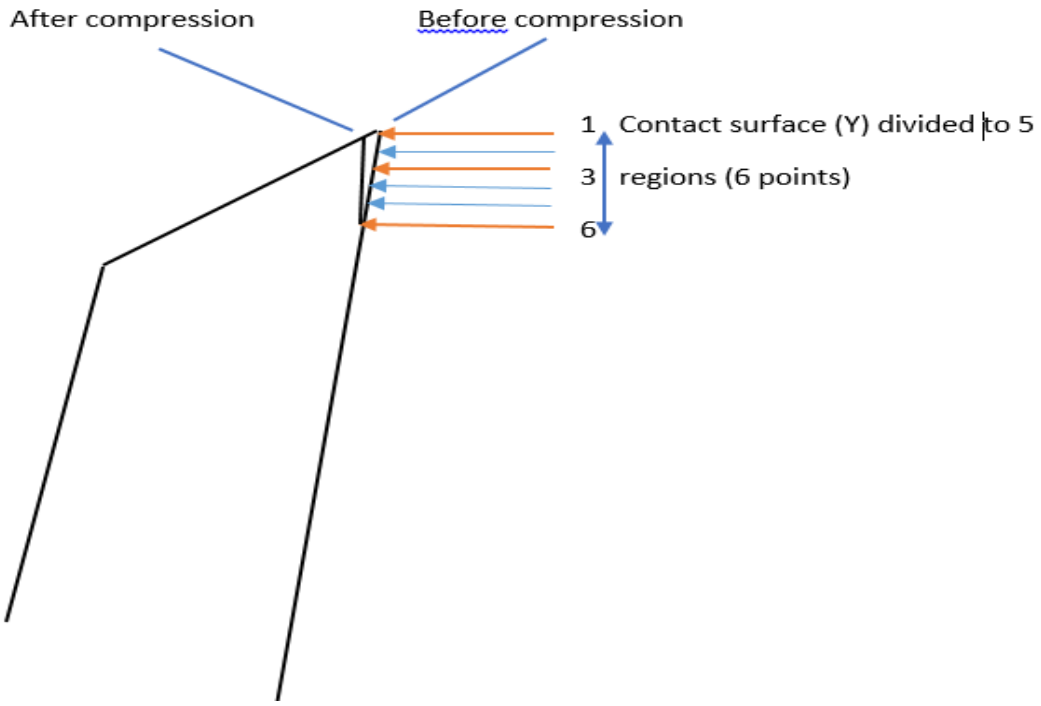

Fig.41 Piston seal before and after compression

The compression of the piston seal is not homogeneous, and this influence on the behaviour of the piston seal during sliding conditions. The maximum compression was at the top point (lips edge) of the piston seal contact surface (Y), The compression will reduced until the bottom point of seal contact surface which has the minimum compression. That mean higher wear will occur at the top of the seal edge. This is in a good agreement with research's results of ALghathiam (2005) (64] and Nandor (2011) [94].

5.1.1 Wet sliding wear in presence of the water:

The results obtained from this experiment confirm that the forces acting on the piston seal are fluctuating forces. During the reciprocating motion, the piston seal was influenced by the weight of the water. Due to the change in water column during the sliding distance, the influence of the loads acting on the upper piston seal changed throughout each cycle.

A change was noted when the piston was at the bottom of its stroke and started to move up, The load decreased when the piston was moving up, the water was forced out until the end of the half stroke (56.74 mm). Afterward the load increased during the downword stroke. Water will flow through piston valve from the lower chamber of the pump cylinder to the upper chamber until the end of the stroke (113.8 mm). This change of the loads is same and equal for each cycle. Table 5 shows the change of load acting on the piston seals during the first, second, and third cycles.

Table 5. Loads acting on piston seal over sliding distance and through each cycle.

First Cycle		Second Cycle		Third Cycle	
Load acting on piston seal (N)	Piston seals sliding distance (mm)	Load acting on piston seal (N)	Piston seals sliding distance (mm)	Load acting on piston seal (N	Piston seals sliding distance (mm)
19.289	0	18.985	124	18.985	252
18.985	10	18.691	134	18.691	262
18.691	20	18.397	144	18.397	272
18.397	30	18.103	154	18.103	282
18.103	40	17.603	171	17.603	299
17.603	57	18.103	188	18.103	309
18.103	74	18.397	198	18.397	319
18.397	84	18.691	208	18.691	329
18.691	94	18.985	218	18.985	339
18.985	104	19.289	235	19.289	356
19.289	114				

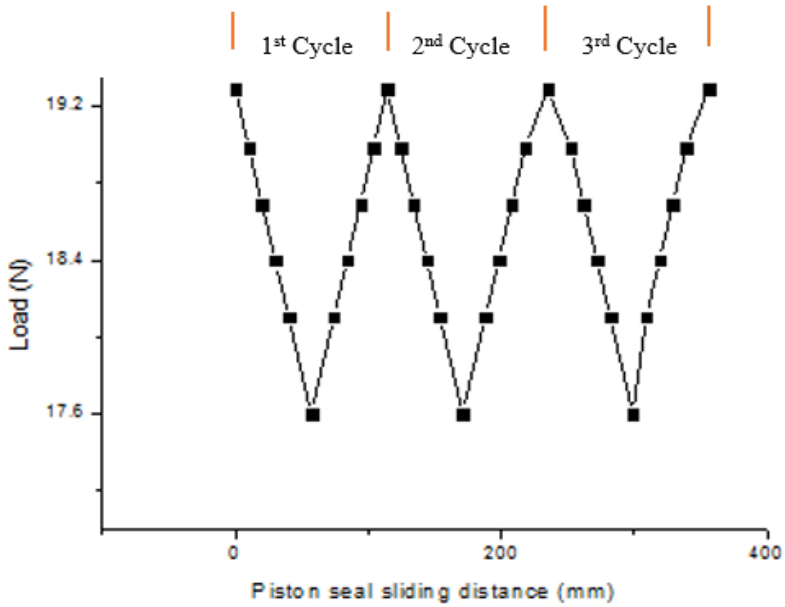

Fig.42. Fluctuating load acting on the upper piston seal, for wet sliding in presence of the water.

Fig.42. shows the maximum and minimum water loads acting on the upper piston seal and also shows the fluctuating load over the sliding time. This fluctuating load results in wear of the seal material, then removal of material and a fatigue wear. The lower piston seal is not under the same fluctuating load because the water is acting only on the upper seal.

It can be established that the: NBR piston seal under wet sliding condition and in presence of the water will be under the influence of fluctuating load and this will increase the oscillating stress at the top surface of the piston seal resulted in fatigue wear, and higher wear rates than that focuses on the lower piston seal

Table 6 (a), 4(b) and 4(c.) show the results which obtained from wet sliding experiment in presence of water. The loads acting on the upper piston seal are water load and piston plus pump rod weights.

Table 6 (a). Piston seal contact area under wet sliding conditions

Piston seal Dia (mm)	Operating hours (H)	Load acting on the seal (N)	θ lip seals deflection angle	X Travel distance of the seal edge (mm)	Y Contact surface (mm)	CA Contact area $(m^2)\times 10^{-4}$	No of Cycles
64.58	0	19.289	11.9	0.79	3.7	7.5	0
64.19	3	19.289	11.51	0.59	2.9	5.8	11102
64.09	6	19.289	11.47	0.54	2.6	5.4	22204
64.05	9	19.289	11.41	0.51	2.5	5.1	33306
63.99	12	19.289	11.36	0.48	2.4	4.9	44408

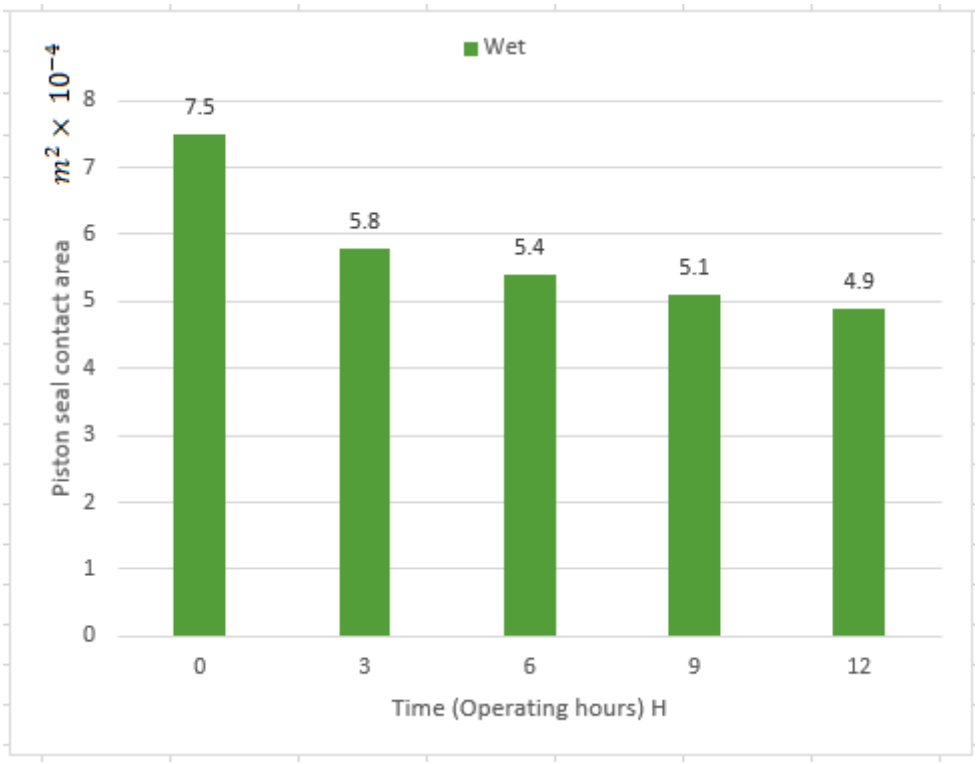

Fig.43. Piston seal contact area for wet sliding conditions.

The contact area of the piston seal is large at the beginning of the experiment and then gradually (Fig 43). For the first 3 hours, the reduction was higher. This is due to the higher friction at start of the experiments. Water then acts as a lubricant fluid and formed a low friction layer. This reduced the seal friction and led to a decreases in the deformation of the uncoated NBR piston seal. This would eventually reduce the seal wear. This is a good agreement with the research results of Mofidi [63] and Mofidi . Prakash [62].

Table 6 (b). Friction force and coefficient of friction of the piston seal for the wet sliding conditions

Piston seal Dia (mm)	Load (N)	μ Coefficient Of friction	Seal friction force (N)	Total load (N)	Strain	Stress ($\frac{N}{m^2}$)	Operating hours (H)
64.58	19.289	0.25	4.89	24.5 At start	0.2069	25116	0.25
64.19	19.289	0.19	3.78	23.3	0.1997	33862	3
64.09	19.289	0.18	3.52	23.1	0.1989	35925	6
64.05	19.289	0.17	3.3	22.9	0.1985	37039	9
63.99	19.289	0.16	3.1	22.7	0.1971	40416	12

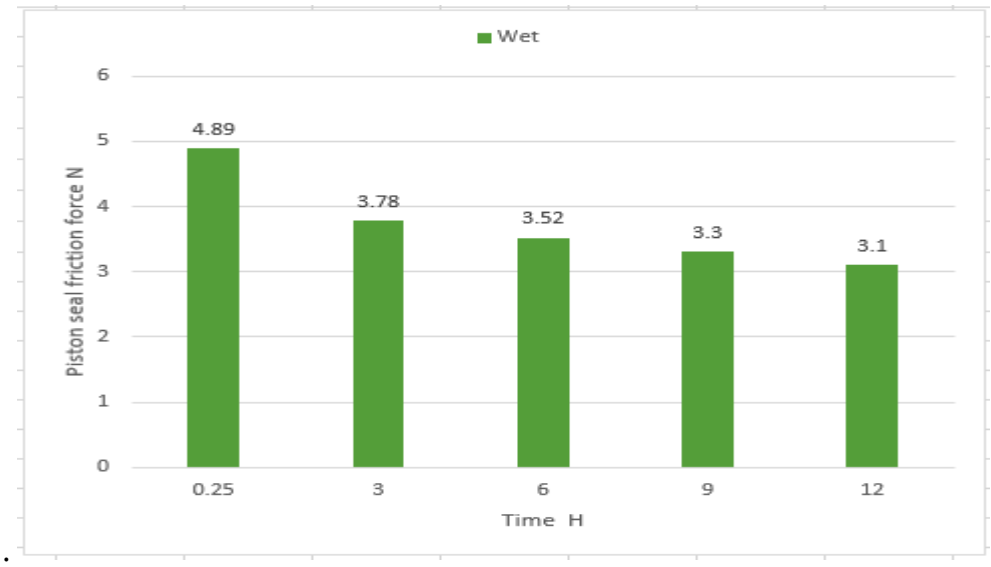

Fig.44. Seal friction force for the wet sliding conditions.

NBR piston seal friction was higher at start of the experiment and then decreases gradually over time. (Fig 44) The seal contact area was large at the beginning as a result of the piston seals compression. This led to a higher force during the initial running in period. After that over time the seal friction decreases because the water influence on sliding condition and formed low friction layer.

Table 6 (C). Volume of removed material and wear rates for the wet sliding conditions.

Piston seal DIA (mm)	Operating Hours (H)	Sliding Distance (m)	Vw volume of removal material $(m^3)\times 10^{-6}$	Total Vw Volume of removed material $(m^3)\times 10^{-6}$	Aw Wear Rate $(m^2)\times 10^{-4}$	Total Aw wear rate $(m^2)\times 10^{-4}$	K Wear Coefficient
64.58	0	0	0	0	0	0	0
64.19	3	1252	19.21	19.21	1.7	1.7	0.68
64.09	6	2808	4.52	23.73	0.4	2.1	0.206
64.05	9	4514	3.39	27.12	0.3	2.4	0.166
63.99	12	6555	3.39	30.31	0.3	2.7	0.117

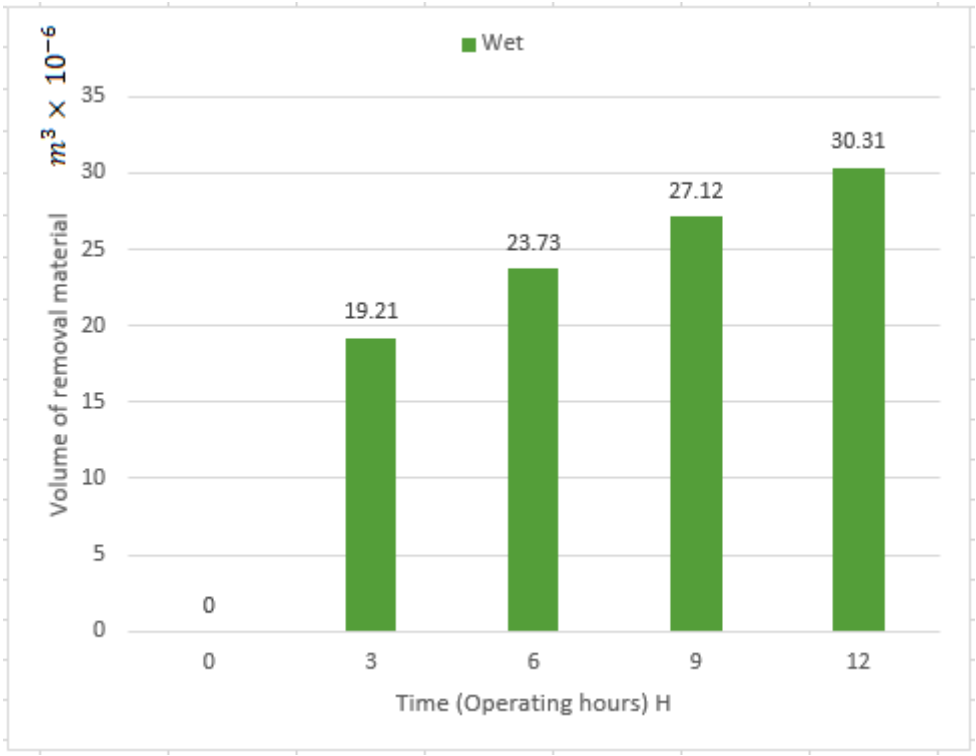

Fig.45. Volume of the removed material of uncoated NBR piston seals for wet sliding in presence of the water.

Fig.45 highlights gradual increase in the volume of removed material of uncoated NBR piston seal over time. The reason of this removal is the wear of the uncoated NBR piston seal through the wet sliding condition. The fluctuating load of the water on the top surface of the piston seal could lead to fatigue wear. Again the friction of the piston seal contact surface against wall of the pump cylinder could cause wear of the seal.

.

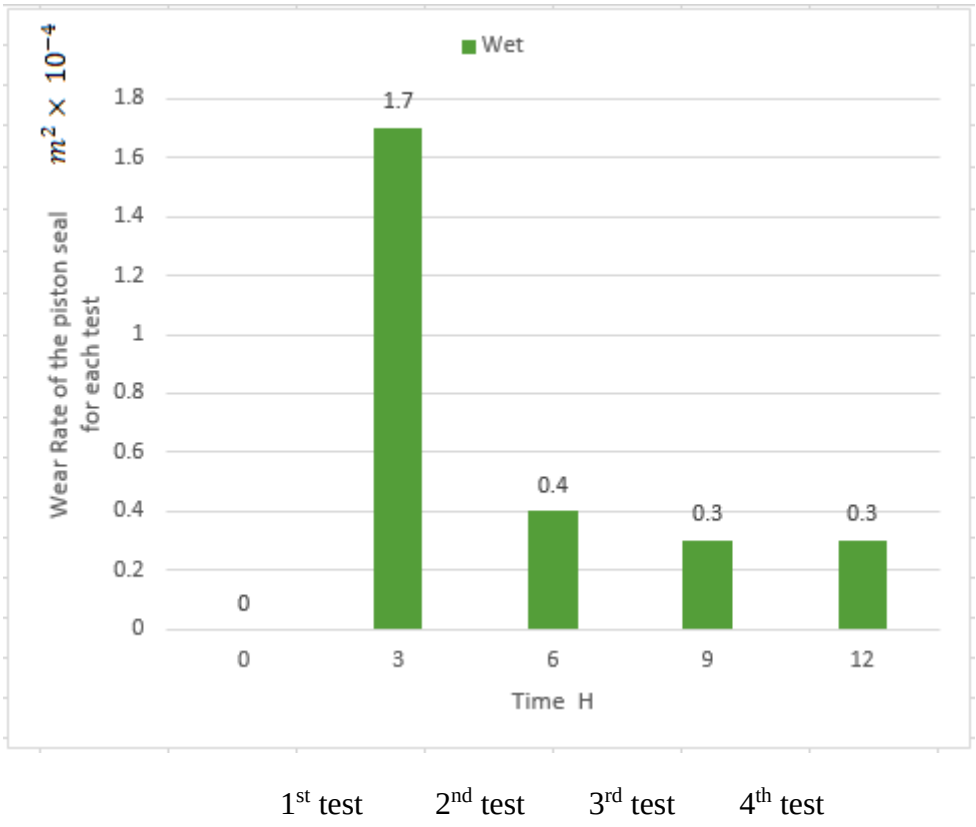

1st test 2nd test 3rd test 4th test

Fig.46. Wear rate of uncoated NBR piston seal in wet sliding conditions.

The wear rate of the uncoated NBR piston seal was extremely high at the first test (first 3 hours) than at the other tests, and the wear rate gradually decreased for 2nd, 3rd, and 4th tests (Fig 46). This is due to the higher removal seal material (through the first 3 hours of the operating), as a result of: initial large contact area of the piston seal, initial higher seal compression, higher seal friction at starting of piston movement and increased water penetration over time resulting in a reduction in piston seal friction.

5.1.2 Dry Sliding Wear and Dry Sliding wear with Added mass.

Table 7, Table 8 and Table 9 presented the results obtained from the second and third series of experiments under dry sliding conditions without and with the added weight to the piston rod respectively.

Table 7 (a) Piston seal contact area under Dry sliding conditions

Piston seal Dia (mm)	Operating hours (H)	Load (N)	θ Lip seals deflection angle	X travel distance of the seal edge (mm)	Y contact surface (mm)	CA contact area $(m^2)\times 10^{-4}$	No of Cycles
64.50	0	12.811	11.98	0.75	3.5	7.08	0
64.20	2	12.811	11.36	0.6	2.98	6.01	6336
63.21	6	12.811	9.82	0.105	0.602	1.194	19008

Table 7 (b) Piston seal contact area under Dry sliding conditions with added mass o5 Kg.

Piston seal Dia (mm)	Operating hours (H)	Load (N)	θ Lip seals deflection angle	X travel distance of the seal edge (mm)	Y contact surface (mm)	CA contact area $(m^2)\times 10^{-4}$	No of Cycles
64.19	0	17.716	11.99	0.59	2.801	5.64	0
63.74	2	17.716	11.82	0.37	1.767	3.53	6336
63.01	6	17.716	10.067	0.005	0.028	0.055	19008

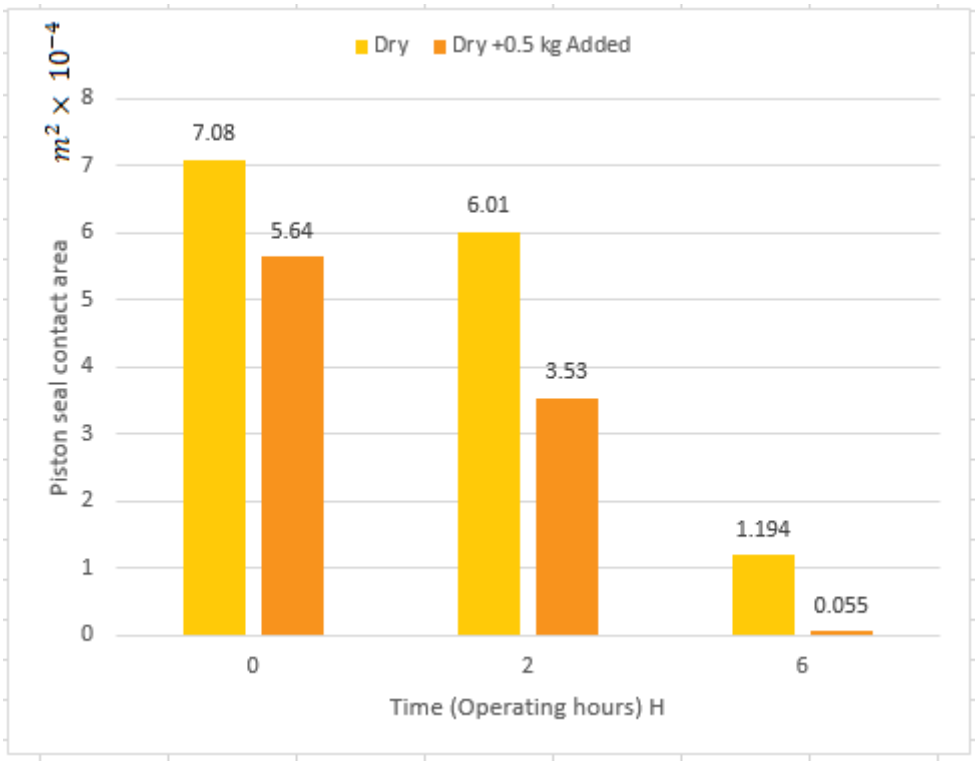

Fig.47. Piston seal contact area of the uncoated NBR piston seal under dry sliding condition and during dry sliding condition with the effect of 0.5 kg mass added to the pump rod.

The initial contact area was found to be $7.00 \times 10^{-4}\ m^2$ for dry sliding. This reduced to $6.01 \times 10^{-4}\ m^2$ over the first 2 hours of operation. As a considerable drop, a real contact area was noted to be $1.194. \times 10^{-4}\ m^2$ after 6 hours of pump operation.

For the dry sliding condition with the influence of added mass of 0.5 kg to the pump rod mass, the reduction of the contact area of the piston seal was higher than that with no added mass. The added mass of 0.5 kg to the pump rod mass led to an increase in the load acting on the piston seal and that cause higher material removal.

These results are in a good agreement with research results of A. D. Ropert [48] and M. Mofidi [63] and Mofidi. Prakash [62].

Table 8 (a) Friction force and coefficient of friction of the piston seal for the dry sliding conditions

Piston seal Dia (mm)	Operating hours (H)	Load (N)	μ Coefficient Of friction	Seal friction force (N)	Total load (N)	Strain	Stress Stress ($\frac{N}{m^2}$)	Young modulus E ($\frac{N}{m^2}$) $\times 10^6$
64.50	0.25	12.811	0.26	3.22	16.02	0.207	18094.6	0.0871
64.20	2	12.811	0.201	2.575	15.38	0.196	21316.1	0.1082
63.21	6	12.811	0.039	0.511	13.322	0.171	107294.8	0.6245

Table 8 (b) Friction force and coefficient of friction of the piston seal for the dry sliding conditions with added mass of 0.5 Kg.

Piston seal Dia (mm)	Operating hours (H)	Load (N)	μ Coefficient Of friction	Seal friction force (N)	Total load (N)	Strain	Stress Stress ($\frac{N}{m^2}$)	Young modulus E ($\frac{N}{m^2}$) $\times 10^6$
64.19	0.25	17.716	0.1887	3.343	21.059	0.207	31383.5	0.151
63.74	2	17.716	0.118	2.09	19.806	0.204	50186.9	2.45
63.01	6	17.716	0.00185	0.032	17.748	0.174	3186330	18.23

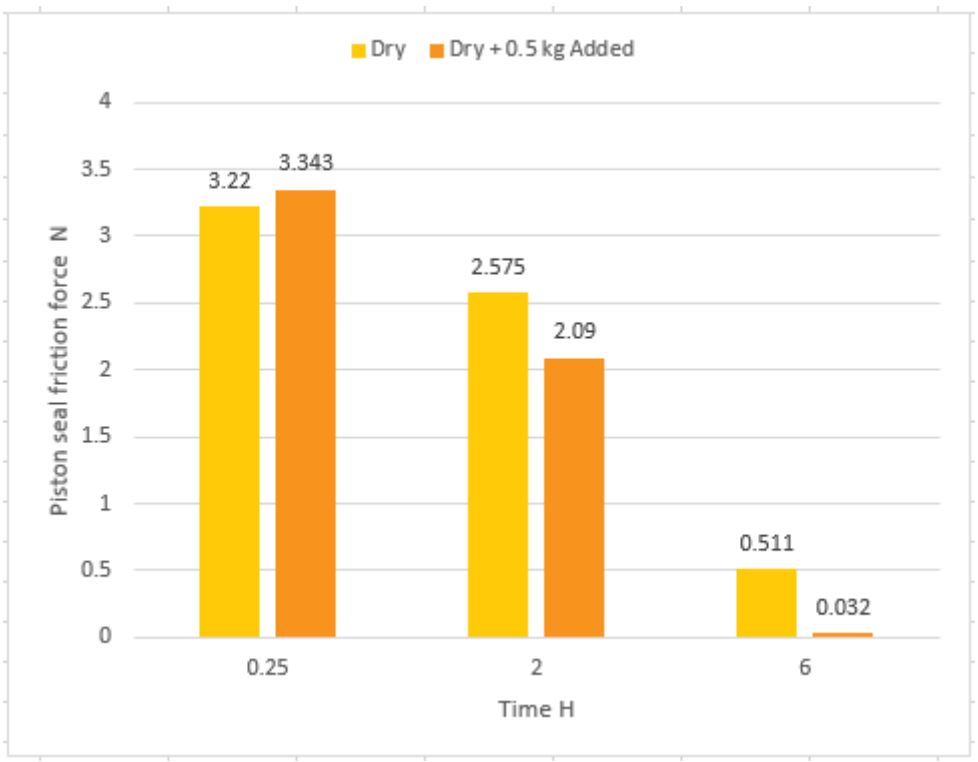

Fig. 48. Piston seals friction force during dry sliding condition and dry sliding condition with the effect of 0.5 kg mass added to pump rod mass.

Due to the seal diameter in dry sliding condition was higher than in dry sliding condition with added mass the friction force at the beginning of operation was higher under dry sliding condition as shows in (Fig 48) The seal friction force ranged from 3.22 N for dry sliding conditions to 3.34 N for dry sliding with increased load during the initial experimental phase. These figures dropped considerably after 2 hours of operation and rapidly following 6 hours of running. This can be explained due to:

1-Areduction in real diameter due to wear.

2-Adecrease in the piston seal friction coefficient.

3-Areduction in the adhesion force between the real surface and pump cylinder.

The results obtained from the experiment show that the reduction of NBR piston seals friction force was higher in dry sliding condition with effect of 0.5 kg mass added than in dry sliding condition.

Table 9 (a) **Volume of removed material and wear rates for the dry sliding conditions**

Piston seal Dia (mm)	Operating hours (H)	Sliding distance (m)	Vw volume of removal material $(m^3)\times 10^{-6}$	Total Vw removal material $(m^3)\times 10^{-6}$	Aw Wear Rate $(m^2)\times 10^{-4}$	Total Aw Wear Rate $(m^2)\times 10^{-4}$	K coefficient of wear
64.50	0	0	0	0	0	0	0
64.20	2	720	12.09	12.09	1.07	1.07	0.453
63.21	6	2180	54.4	66.49	4.816	5.88	2.403

Table 9 (b) **Volume of removed material and wear rates for the dry sliding conditions with added mass of 0.5 Kg**

Piston seal Dia (mm)	Operating hours (H)	Sliding distance (m)	Vw volume of removal material $(m^3)\times 10^{-6}$	Total Vw removal material $(m^3)\times 10^{-6}$	Aw Wear Rate $(m^2)\times 10^{-4}$	Total Aw Wear Rate $(m^2)\times 10^{-4}$	K coefficient of wear
64.19	0	0	0	0	0	0	0
63.74	2	720	23.89	23.89	2.115	2.115	1.12
63.01	6	2180	39.25	63.14	3.474	5.58	2.95

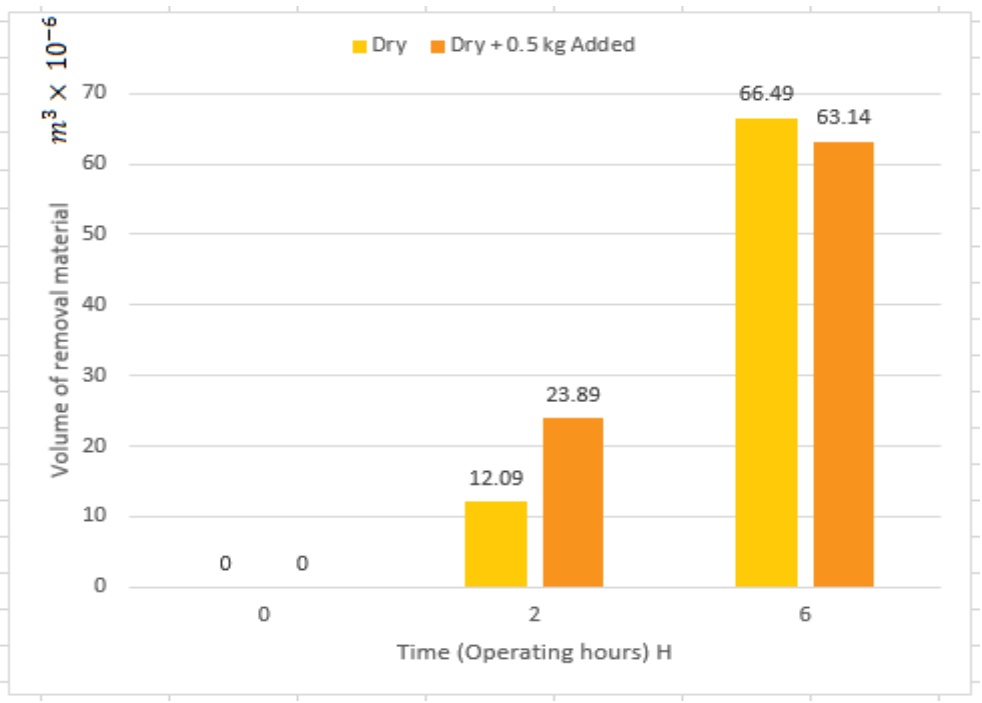

Fig.49. Volume of removed material of the uncoated NBR piston seal during dry sliding condition and dry sliding condition with 0.5 kg mass added to pump rod.

The initial volume of material removed was slow for both dry and dry plus 0.5 Kg additional mass experiments. However following 2 hours of operation the rate of volume removal was considerably higher when the o.5 Kg mass was added. This rate decreased towards the end of the experiments resulting in a value of removal of $63.14 \times 10^{-6}\ m^3$ (Fig 49).

Higher removal of material of uncoated NBR piston seal with operating hours for both sliding conditions, is because of higher fiction between the seal surface and cylinder surface. The results obtained from the experiment show that at dry sliding condition with the effect of 0.5 kg mass added and after 6 hours of sliding the diameter of the NBR piston seal reduced to 63.01mm which is almost equal to the cylinders bore diameter (63mm).

Comparison of the results obtained from the experiments under dry sliding and wet sliding showed that the volume of material removed during wet sliding was less than during dry sliding, the volume of material removed after 6 hours of operation for wet sliding was $23{,}73\times 10^{-6}\ m^3$ while the volume of material removed during dry sliding after 6 hours operation was $66.49\times 10^{-6}\ m^3$, that is because of the water act as a lubricant in wet sliding condition which reduce the seal friction and that led to reduce removal material.

Fig.50. Presents the graph of the wear rate of uncoated NBR piston seals for each test due to the operating hours for Dry sliding condition and Dry sliding condition with the effect of 0.5 kg mass added to pump rod mass.

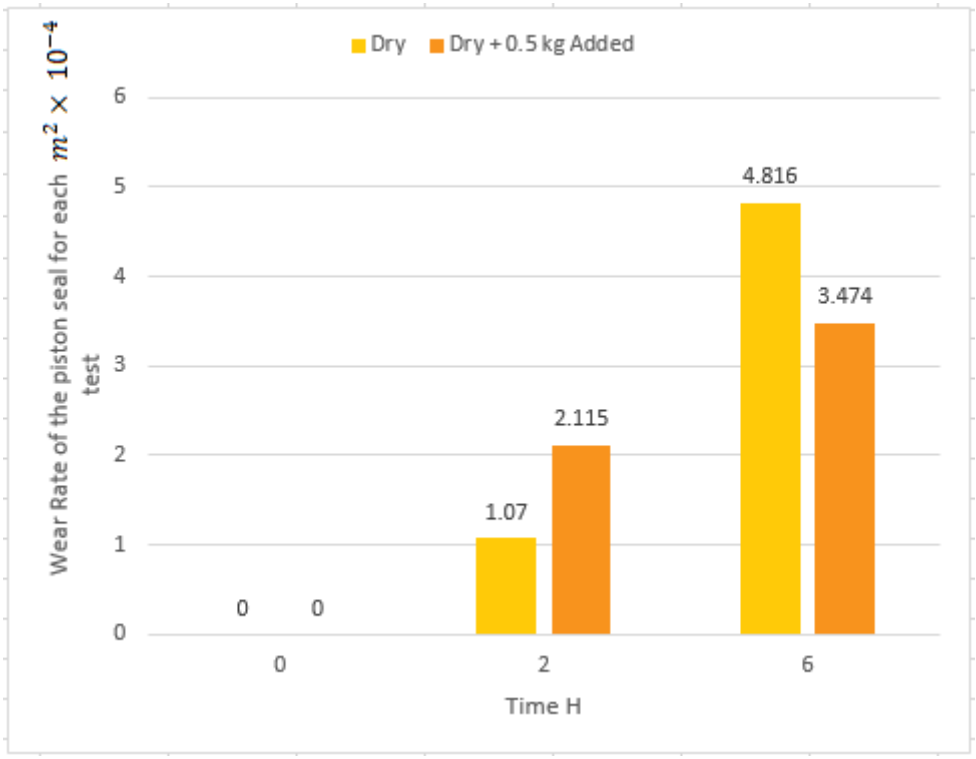

Fig.50. Wear rate of NBR piston seal during dry sliding condition and dry sliding condition with 0.5 kg mass added to pump rod.

The wear rate of the piston seal was initially low. However this increase to $1.07\times 10^{-4}\ m^2$ and $2.11\times 10^{-4}\ m^2$ respectively for non-loaded and loaded (0.5 Kg) experiments. The result was noted after 6 hours of operation was that the loaded dry sliding wear rate was considerably lower than that of the dry sliding experiment, this may be explained due to fatigue wear during the experiments or to unbalanced loading of the piston rod.

5.1.3. Comparison of the Results obtained from the experiments of the three sliding conditions.

Based on the results of my experimental tests on Analysis of the wear of uncoated NBR piston seal the following can be stated. It can be established that:

1-The reduction in contact area of the uncoated NBR piston seal in wet sliding condition and in presence of the water is lower than in dry sliding conditions.

Presence of the water has a contribution to decrease the reduction of the seal diameter. The uncoated NBR piston seals diameter decreased from 64.58mm to 63.99mm during 44408 cycles of wet sliding condition in presence of the water. While the diameter of uncoated NBR piston seal decreased from 64.50mm to 63.21mm during 19008 cycles of dry sliding condition.

The higher reduction of uncoated NBR piston seals diameter was in dry sliding condition with effect of 0.5 kg mass added to pump rod mass, the diameter decreased from 64.19mm to 63.01mm during 19008 cycle, that mean the piston seal diameter become equal to the cylinder diameter after 19008

A relationship was found between the contact area and travel distance (X) of the lip of uncoated NBR piston seal after compressed, and I found that the contact area increases when X increasing.

2- The presence of the water in wet sliding reduced the friction of the uncoated NBR piston seal with roll of the edge of the piston seal formation. And the friction of the uncoated NBR piston seal in dry sliding was higher with parallel line on the piston seal contact surface formation and with higher worn of the lip.

The friction in dry sliding increases when increasing mass of the pump rod.

A relationship exists between the friction force and the travel distance (X) of the lip of the uncoated NBR piston seals after compressed, and I found that the friction force decreases when X decreasing.

3- Higher removed of material of uncoated NBR piston seal during operating hours of dry sliding, and lower removed of material of uncoated NBR piston seal during operating hours of wet sliding in presence of the water.

4- Uncoated NBR piston seal in dry sliding condition (with effect 0f 0.5 kg mass added to the pump rod mass) failed after 19008 cycles, while for the wet sliding in presence of the water the uncoated NBR piston seal not failed after 44408 cycles.

6- In wet sliding condition and in presence of the water the wear rate decreases after each test, while in dry sliding condition the wear rate increases after each test.

A relationship exists between the wear rate and the length of the contact surface(Y) of uncoated NBR piston seal, and I found that removed of material increases when Y is large, and the removed of material decreases when Y reducing.

5.2. F.E.A of uncoated NBR piston seals.

The study of wear has been conducted for many years. In material science, wear is defined as the material degradation generated when materials are in contact. This section will describe the process of simulating the mechanism of wear that occur when using an NBR piston seal by using finite element analysis.

Finite element method (FEA) is a numerical technique for finding approximate solutions to boundary value problems for differential equations. It uses various methods to minimise an error function and produce a stable solution. FEM encompasses all the methods for connecting many simple element equations over many small subdomains, named finite elements, to approximate a more complex equation over a larger domain. Finite Element Analysis is used in problems where analytical solution are not easily obtained. Mathematical expressions required for solution are not simple because of complex: geometries, loadings, and material properties. This study uses F.E for analysis 2D Rubber and dry contact, where an axisymmetric model of an NBR piston seal of the water hand pump is compressed by the cylinder surfaces and then the loaded uniformly with distributed pressure. The NBR piston seal has an inner diameter 42 mm and outer diameter of 64.5 mm, and is bounded by 4 contact surfaces. The piston seal contact edge moves a total distance of 1.58 mm compressing the piston seal. A total load of 24 N was applied and this included water load of 6.24 N applied in the Y direction for wet sliding condition. For dry sliding conditions a total load was 17.76 N. Piston seal was analysed using 2-parameters Mooney-Rivilen model. The Mooney –Rivilen material parameters were assigned values of C1 (N/mm^2) & C2 (N/ mm^2) and d = 2/k (mm^2 /N) . Using stress-strain equation :$\dot{O} = 2\{\lambda - \frac{1}{\lambda^2}\}\{C_1 + \frac{C_2}{\lambda}\}$, this equation can be rewritten as,

$$\frac{O'}{2\{\lambda - \frac{1}{\lambda^2}\}} = C_1 + \frac{C_2}{\lambda} \qquad (31)$$

this equation is the equation for a straight line, and can be plotted as $\frac{O'}{2\{\lambda - \frac{1}{\lambda^2}\}}$ against $\frac{1}{\lambda}$, and then coefficient C_1 and C_2 easily calculated.

The geometry and dimensions for the piston seal model used for this study is presented in fig 51.a.

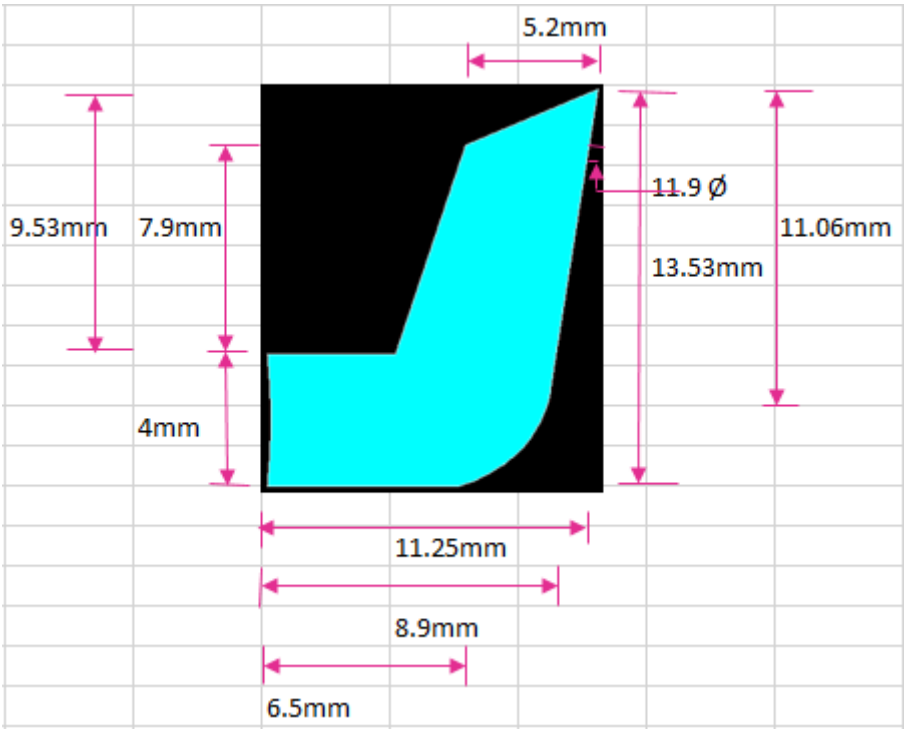

Fig.51 a. Piston seal geometry before compression

To obtain the contact pressure distribution for the piston seal the appropriate was modified and produced in ANSYS 12. (Fig 51 b)

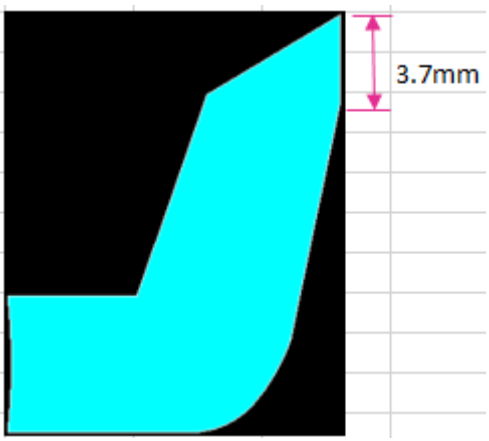

Fig .51 b. Piston seal contact after compression

Constraints were applied to the geometry as shown in Fig (51.C).

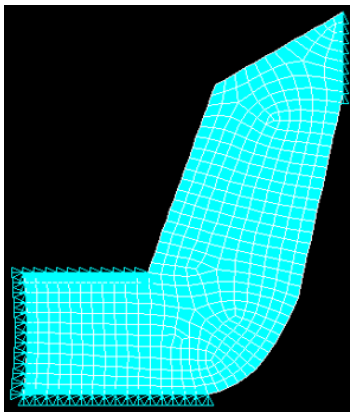

Fig.51.C Constrain applied to the geometry of piston seal.

A uniform sealed pressure was applied to the piston seal edge on the lip of the piston seal to simulate the loading from the compression and a load of the water was applied to the top surface to simulate the loading from the pressurized water for the wet sliding condition. For dry sliding there is no loading from the pressurized water

The material was assumed to be non-linear elastic with poissons ratio of 0.49.

A mesh was used along the piston seal as shown in fig (51.d). This mesh had 169 nodes across the piston seal interface for respective geometries.

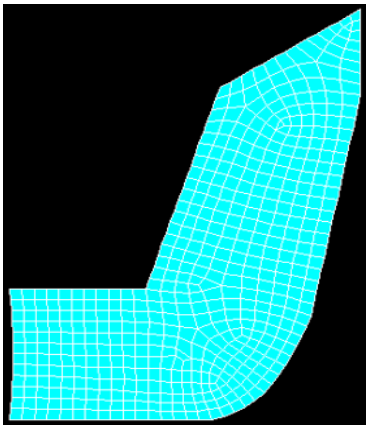

Fig.51.d. Mesh of the geometry of piston seal.

Plane 182 element was used to allow the use of solvers designed for rubber materials.

5.3. Finite Element Analysis (F.E.A) Results and Discussion.

5.3.1 Wet and dry sliding conditions.

Distribution of the contact stresses is very complex and can be analysed only by using F.E.A method. The distribution of the stresses acting on the uncoated NBR piston seal in wet and dry sliding conditions was analysed. Also, the behaviour of the seal friction and the wear (in wet and dry sliding conditions) was analysed.

Uncoated NBR piston seal is non-linear elastic (hyperplastic) material and it is incompressible (volume does not change significantly with increasing stress). This type of material is able to undergo large reversible elastic deformations and has unique damping properties. Its behaviour is time dependant. Because of these reasons and due to the sliding conditions, ANSYS 12 Mechanical APDL software was used and the suitable F.E.A model was 2D Mooney- Rivlin, hyper 4 node plan 182 with axisymmetric behaviour

5.3.2 Results of the Wet sliding condition

Finite element analysis was carried out by using load conditions, water loads and piston and

Pump rod weight. Table.8. presents the stretch $\lambda = (\varepsilon+1)$, and engineering stress of the uncoated NBR piston seal $\frac{\sigma(\boldsymbol{stress})}{2[\lambda-\frac{1}{\lambda^2}]}$ through the wet sliding. Also, the table shows Mooney-Rivlin constant values.

Table 10. Engineering strain (ƛ), engineering stress and Mooney-Rivlin constants for the Wet sliding condition in the presence of water.

Piston seal Dia mm	No of cycles	ƛ = (Ɛ + 1)	1/ ƛ = 1 / (Ɛ + 1)	$\frac{\sigma(\boldsymbol{stress})}{\mathbf{2}[ƛ - \frac{\mathbf{1}}{ƛ^{\mathbf{2}}}]}$ N/m^2
64.58	0	1.2069	0.82856	24132.67
64.19	11102	1.1997	0.83354	33532.82
64.09	22204	1.1989	0.83409	35697.91
64.05	33306	1.1985	0.83437	36868.21
63.99	44408	1.1971	0.83535	40473

Table 11. Mooney-Riviln constant

C10	C01	d =2/k $\frac{m^2}{N}$
12000	3834310.6	$\mathbf{5.199\times 10^{-10}}$

At the start of the stroke and over the operating time of wet sliding time, the NBR piston seal will be effected by the load of the water and by the weight of the piston and pump rod. This effect will remain till the end of the cycle and as a result the piston seal will deform. The deformation is dependent on the contact pressure values.

5.3.2. 1. NBR piston seal after 3 hours of the wet sliding time.

Figures: 52 displays F.E.A of the an NBR piston seal after 3 hours of the wet sliding time in the presence of water.

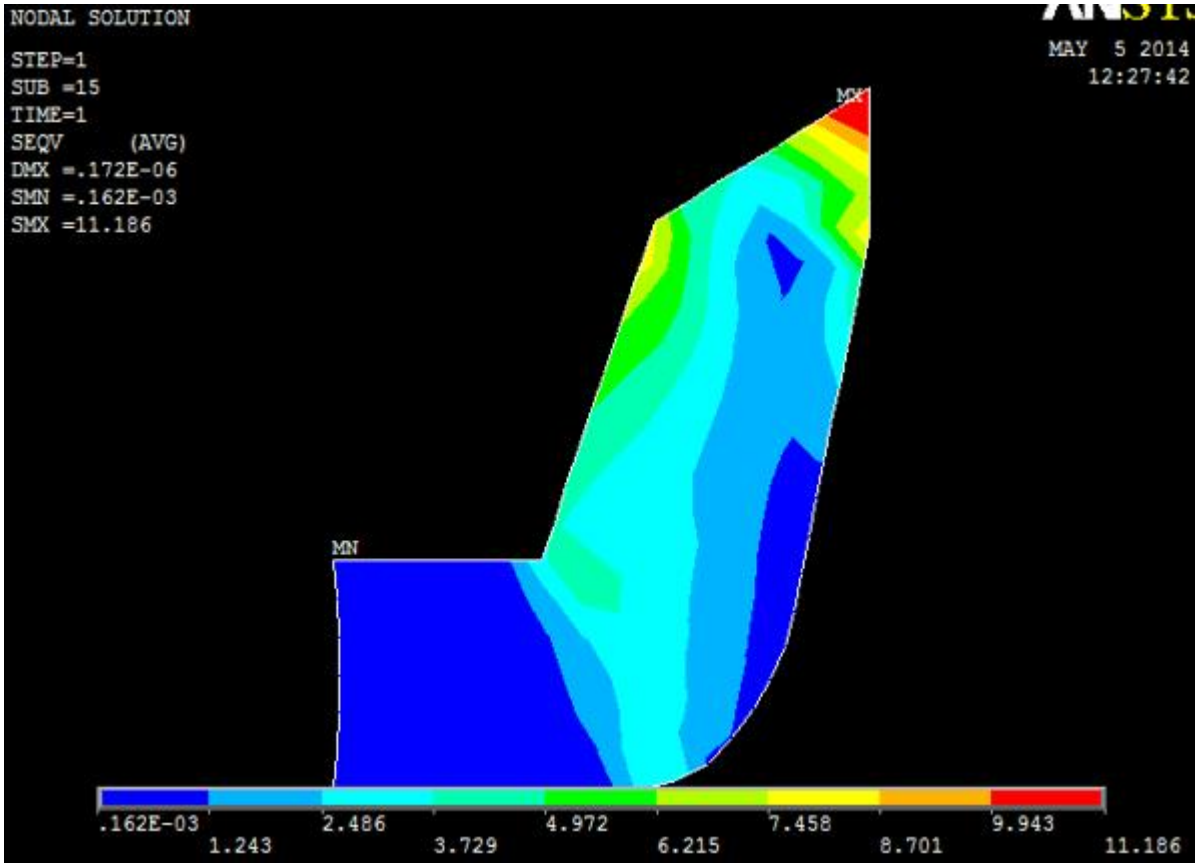

Fig. 52. Von.mises stress distribution the NBR piston seal after 3 hours of the wet sliding time in the presence of water.

The results of the analysis show that the Von-Mises stress was different in the seal contact area. Several layers of the piston seal were influenced by the stress. The higher was stress distributed at the lips edge of the piston seal and along the seal contact surface high stress values were also noted along the top surface of the seal. This is because of (1) higher squeeze of the lip (2) higher friction along the seals contact surface, and (3) The influence of the fluctuating load of the water along the top surface.

The maximum von-mises stress (11.186 MPa) was at the top surface of the lip specifically at small distance from the lips edge. Von-mises stress along the seal contact surface (starting from the lips edge) gradually decreased further away from the cylinder wall. The measurement is taken also decreases along the top surface of the seal.

Table.10. presented Von mises stress values for the NBR piston seal after 3 hours of the wet sliding time. Table 12 (a). presents distribution of the von-mises stress along the contact surface of the NBR piston seal (starting from the lips edge), Table 12 (b). presents distribution of the von-mises stress along the top surface of the NBR piston seal (starting from the lips edge), and Table 12 (C). presents distribution of the von-mises stress along the horizontal depth from the piston seal contact surface.

Table 12. Distribution of the Von-Mises Stress values in the NBR piston seal, after 3 hours of the wet sliding in the presence of water.

Distance mm	Von-Mises stress MPa
2.9	10.934
2.6	10.704
2.3	10.704
2	10.32
1.95	9.943
1.716	9.348
1.6	8.701
1.311	7.993
1.1	7.458
0.9813	7.458
0.6399	8.0553
0.4	8.701
0.2631	8.701
0.1997	7.458
0.1	7.458
0.07	7.458
0.0374	7.458

a

Distance mm	Von-Mises stress MPa
4.91	10.934
4.6799	11.186
4.46	11.186
4.01	9.943
3.699	8.701
3.3	7.458
2.9	6.215
2.6	4.972
2.2	3.729
1.9	4.972
1.5866	4.972
1.139	4.972
0.837	5.175
0.6	6.215
0.35	7.458
0.129	8.701
0.07883	8.701

b

Distance mm	Von-Mises stress MPa
0	9.943
0.6	8.7010
1.1	7.458
1.55	6.215
2.15	4.972
2.3	3.729
2.5	2.48

C

Fig. 53. displays graphs of the von-mises stress in the NBR piston seal due to the distance along the: seals contact surface, seals top surface, and horizontal depth which start from the contact surface, after 3 hours of the wet sliding time.

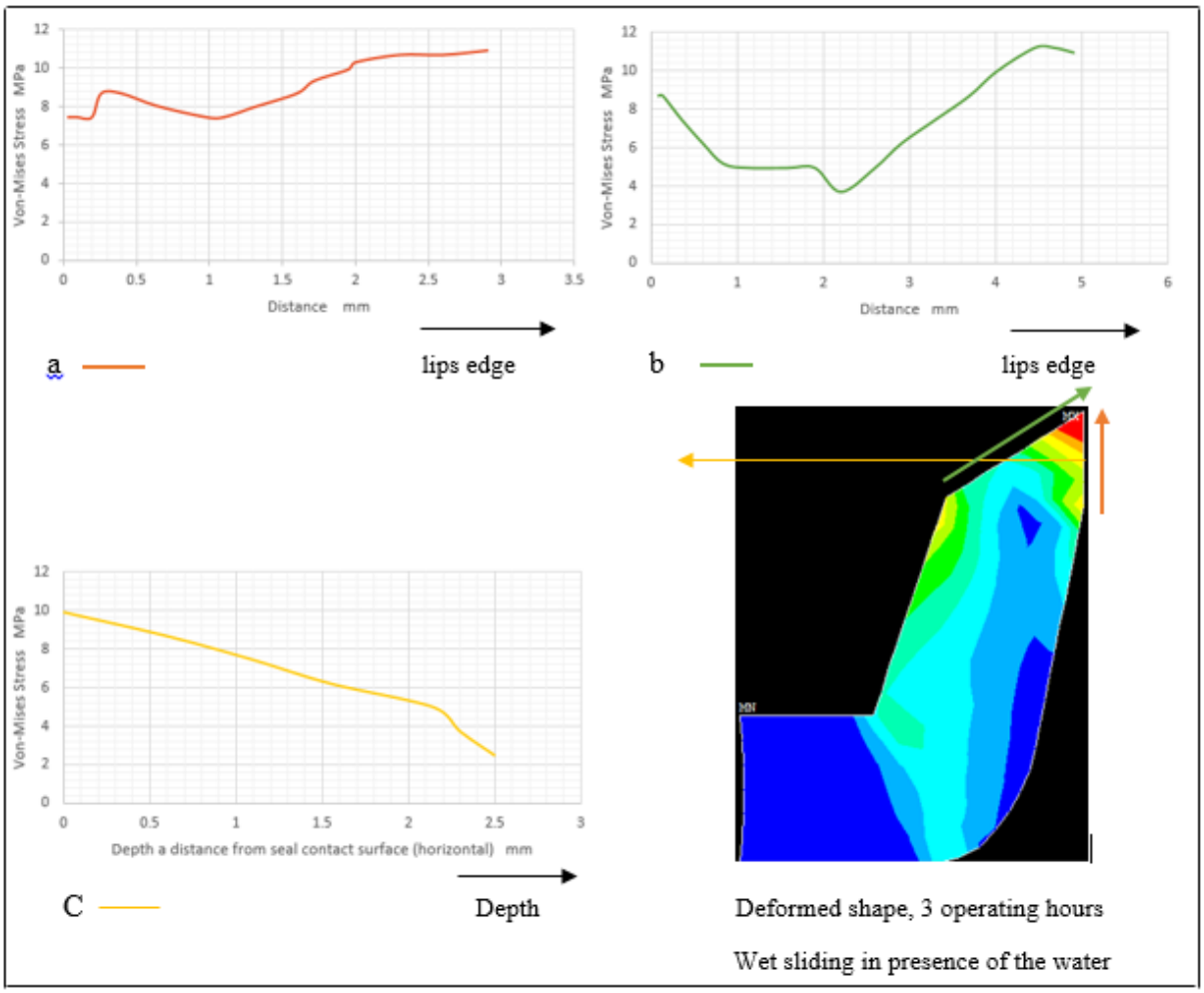

Fig 53. Von mises stress in NBR piston seal after 3 hours of the wet sliding time

5.3.2.2. NBR piston seal after 6 hours of the wet sliding time.

Figures 54 displays F.E.A of the uncoated NBR piston seal after 6 hours of the wet sliding time and in the presence of water.

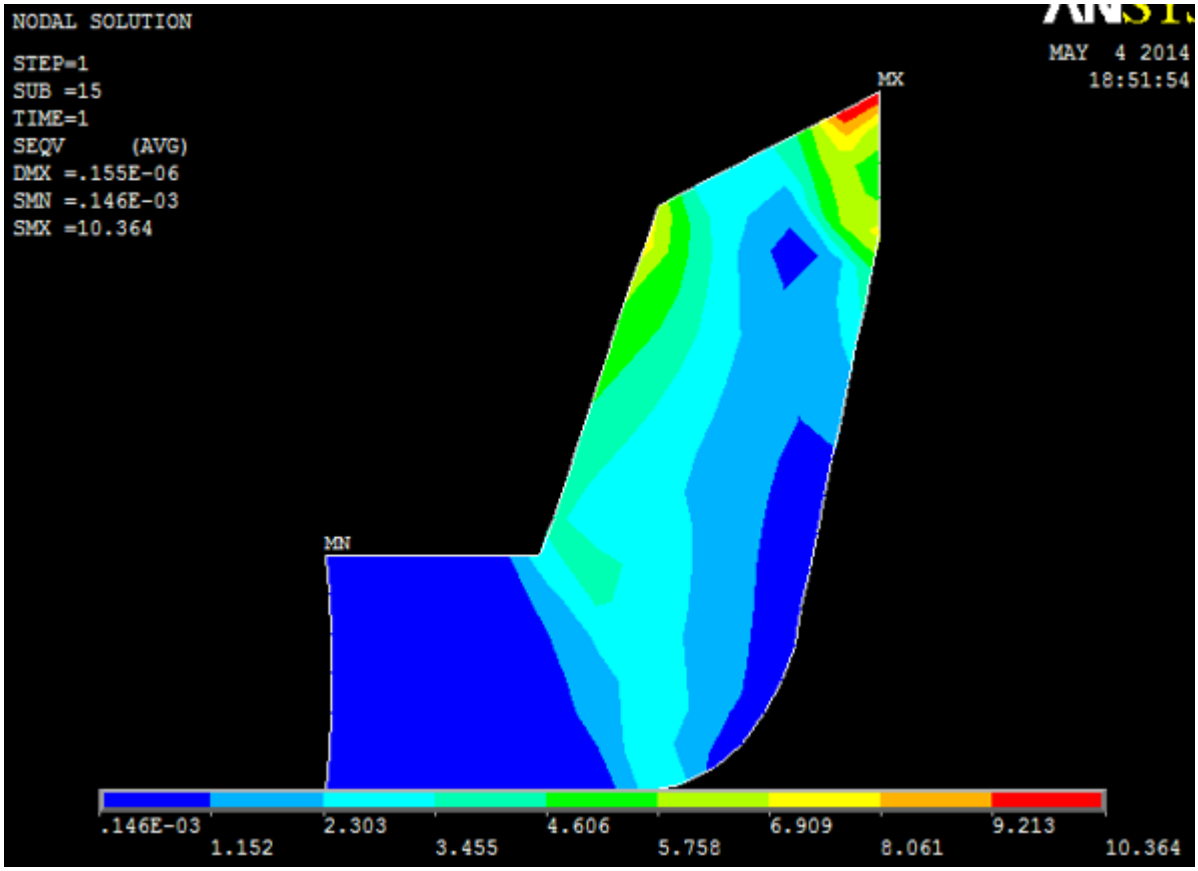

Fig. 54. Von mises stress distribution in NBR piston seal after 6 hours of the wet sliding time in the presence of water.

The condition of the NBR piston seal after 6 hours of the wet sliding time is different than after 3 hours. Von-mises stress was different in the piston seal contact area and several layers of the NBR piston seal were influenced by the stress.

The higher von-mises stress was found to be distributed at the lips edge of the seal and along the seal contact surface also along the top surface of the seal.

Along the top surface of the seal (starting from the lips edge) the von-mises stress was found to decreased away from the lip. The maximum von-mises stress (10.364 MPa) was found at the top surface of the seal. This illustrates that the fluctuating load of the water remained effected on the piston seal (at the top surface of the seal). While the effect of the seal compression and the effect of the seal friction decreased, and due to this reasons the von-mises stress at the seal contact surface decreased.

Table.13 presents Von mises stress values for the uncoated NBR piston seal after 6 hours of wet sliding time. Table 13 (a) presents the distribution of the von-mises stress along the contact surface of the NBR piston seal (starting from the lips edge), Table 13 (b). presents the stress distribution along the top surface of the NBR piston seal, and Table 13 (c) presents the stress distribution along the horizontal depth.

Table 13. Distribution of the Von-Mises Stress values responses for uncoated NBR piston seal after 6 hours of wet sliding time in the presence of water.

Distance mm	Von-Mises stress MPa
2.6	10.364
2.5	10.364
2.4	9.213
2.25	8.061
2.11	6.909
1.976	6.909
1.61	5.758
1.3877	5.758
1.0627	6.315
0.76	6.909
0.6028	6.909
0.338	7.399
0.26	8.061
0.1607	8.061
0.03	8.061

a

Distance mm	Von-Mises stress MPa
4.325	10.364
4	10.316
3.475	9.213
3.325	8.061
3.175	6.909
3.025	5.758
2.82	4.606
2.375	3.455
2.087	3.455
1.633	3.455
1.201	3.686
0.775	4.606
0.5	5.758
0.2	6.909

b

Distance mm	Von-Mises stress MPa
0	5.4979
0.45	5.7156
0.9	2.38
1.2	3.2314
1.5	3.1932

C

Fig. 55. displays graphs of the von-mises stress for uncoated NBR piston seal due to the distance along the seals contact surface, seals top surface, and horizontal depth which start from the contact surface after 6 hours of the wet sliding time

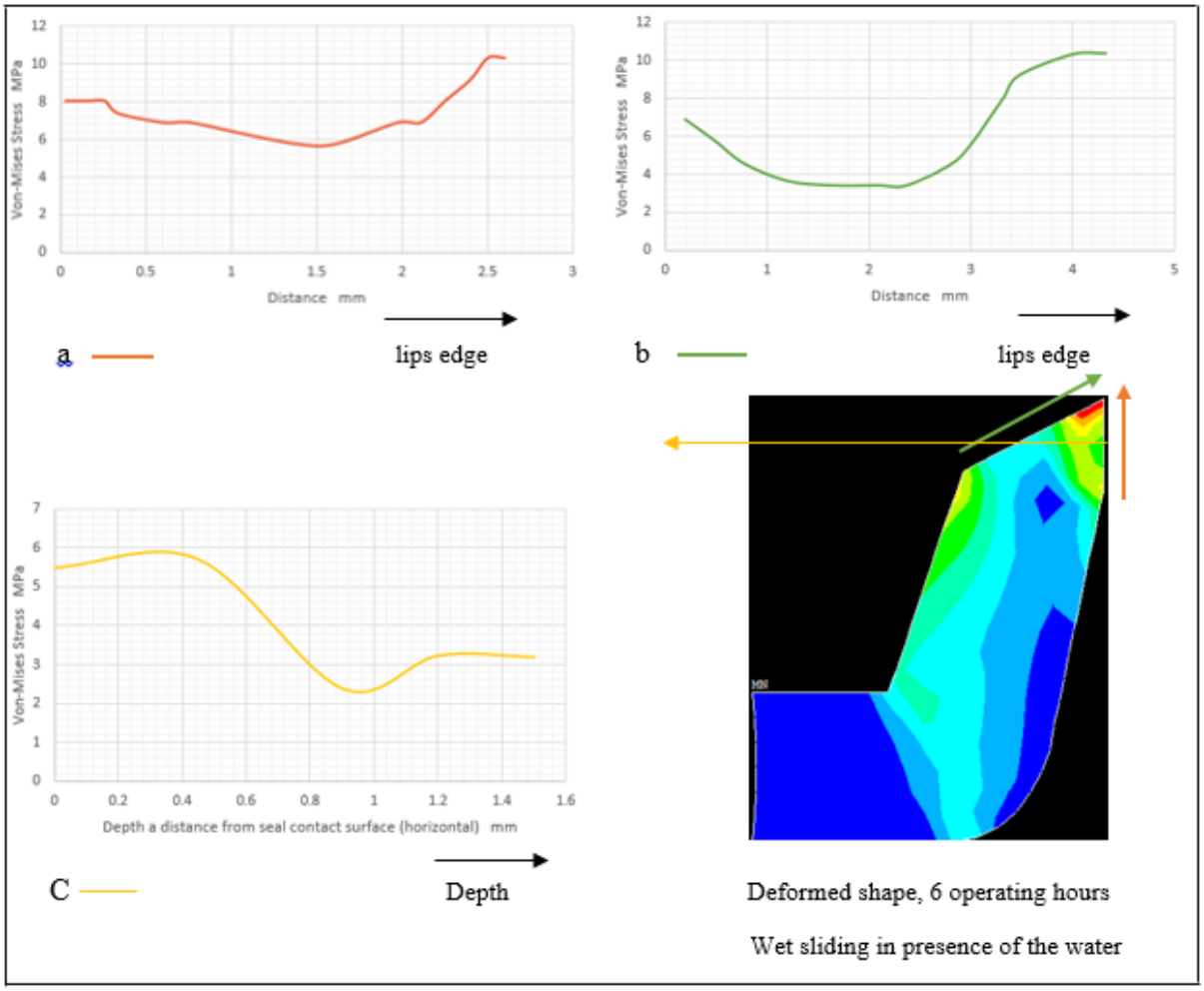

Fig.55.Graphs show the von-mises stress values in the NBR piston seal at the seal contact surface, seal top surface, and horizontal depth after 6 hours of wet sliding time.

5.3.2 3. NBR piston seal wear after 12 hours of the wet sliding time.

Figures 56 displays F.E.A of the uncoated NBR piston seal after 12 hours of the wet sliding time and in the presence of water.

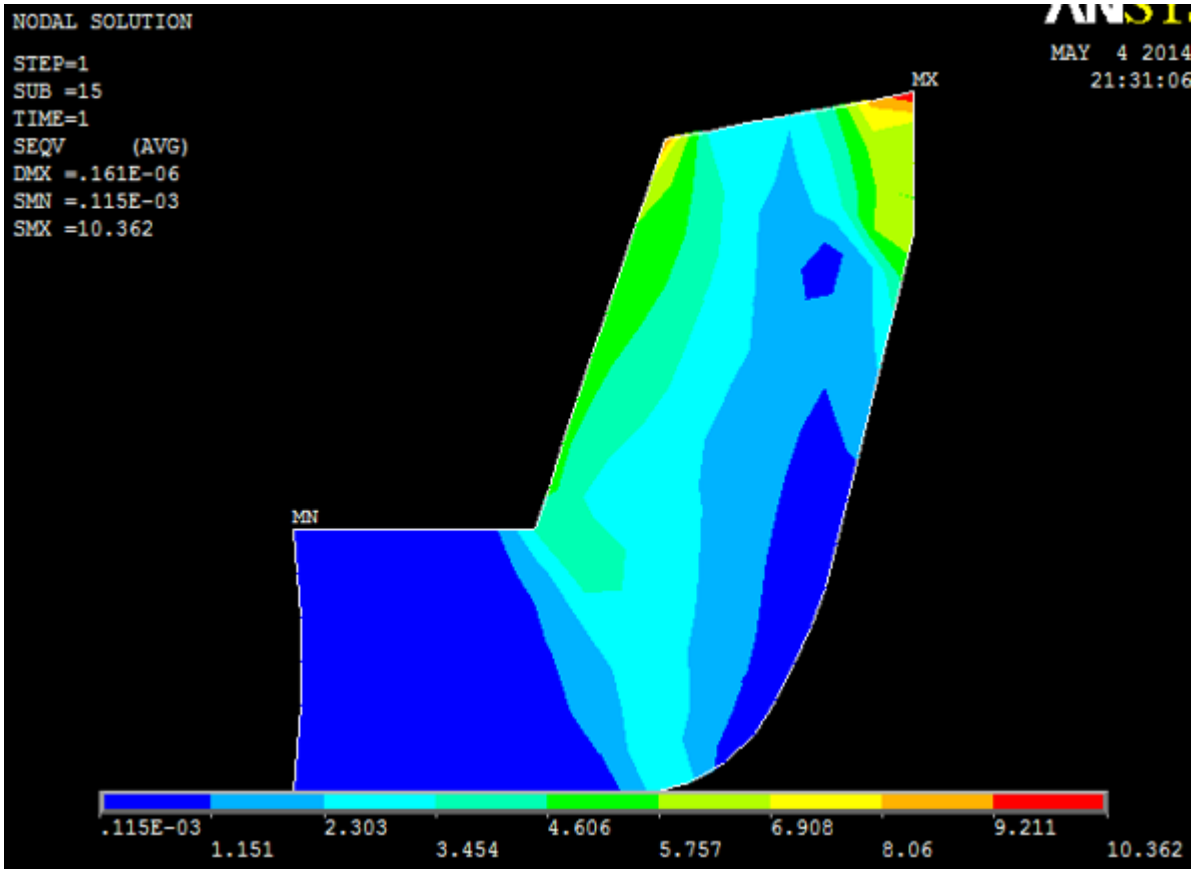

Fig.56. von mises stress distribution in the uncoated NBR piston seal after 12 hours of the wet sliding time in the presence of water.

After 12 hours of the sliding time, the effect of the stress in the all regions of the piston seal contact decreased. The maximum von-mises stress (10.362 MPa) was found at the lips edge. The highest of stress was found only at the small region of seal edge. This is because of higher removal of seal material occurred over the 12 hours of the sliding time, and due to the decrease in seal contact area. Decreasing of the piston seal contact area led to a decrease in the seal squeeze and the seal friction.

Table.14 presented Von mises stress values for the uncoated NBR piston seal after 12 hours of the wet sliding time. Table 14 (a). presentes distribution of the von-mises stress along the contact surface of the NBR piston seal, Table 14 (b) present the stress distribution along the top surface of the NBR piston seal, and Table 14 (c) present the stress distribution along the horizontal depth which start from the piston seal contact surface.

Table 14. Distribution of the Von-Mises Stress values in the uncoated NBR piston seal after 12 hours of the wet sliding time in presence of the water.

Distance mm	Von-Mises MPa
2.4	10.362
2.25	9.211
2.1	8.06
1.95	6.908
1.683	6.384
1.453	5.757
1.3	5.757
1	5.757
0.72	5.757
0.369	5.757
0.11	5.757

a

Distance mm	Von-Mises MPa
4.25	10.362
3.85	9.211
3.44	8.06
3.25	6.908
3.05	5.757
2.85	4.606
2.5	3.454
2.13	3.454
1.399	3.5322
0.899	3.871
0.6	4.606
0.4	5.757
0.2	6.908
0.1	8.06

b

Distance mm	Von-Mise stress MPa
0	6.0589
0.75	6.213
1	3.52
1.3	2.0531
1.9	2.6907
2.15	4.323
2.4	6.7238

C

After 12 hours of the wet sliding, along the piston seals contact surface (starting from the lips edge) von-mises stress values decreased and then remained at a constant value, while along the top surface von-mises stress first decreased and afterward increases. At the horizontal depth which starts from the seal contact surface the von-mises stress decreased afterward increased.

Fig. 57. displays graphs of the von-mises stress in the uncoated NBR piston seal due to the distance along the seals contact surface, seals top surface, and horizontal depth start from the contact surface after 12 hours of the wet sliding time.

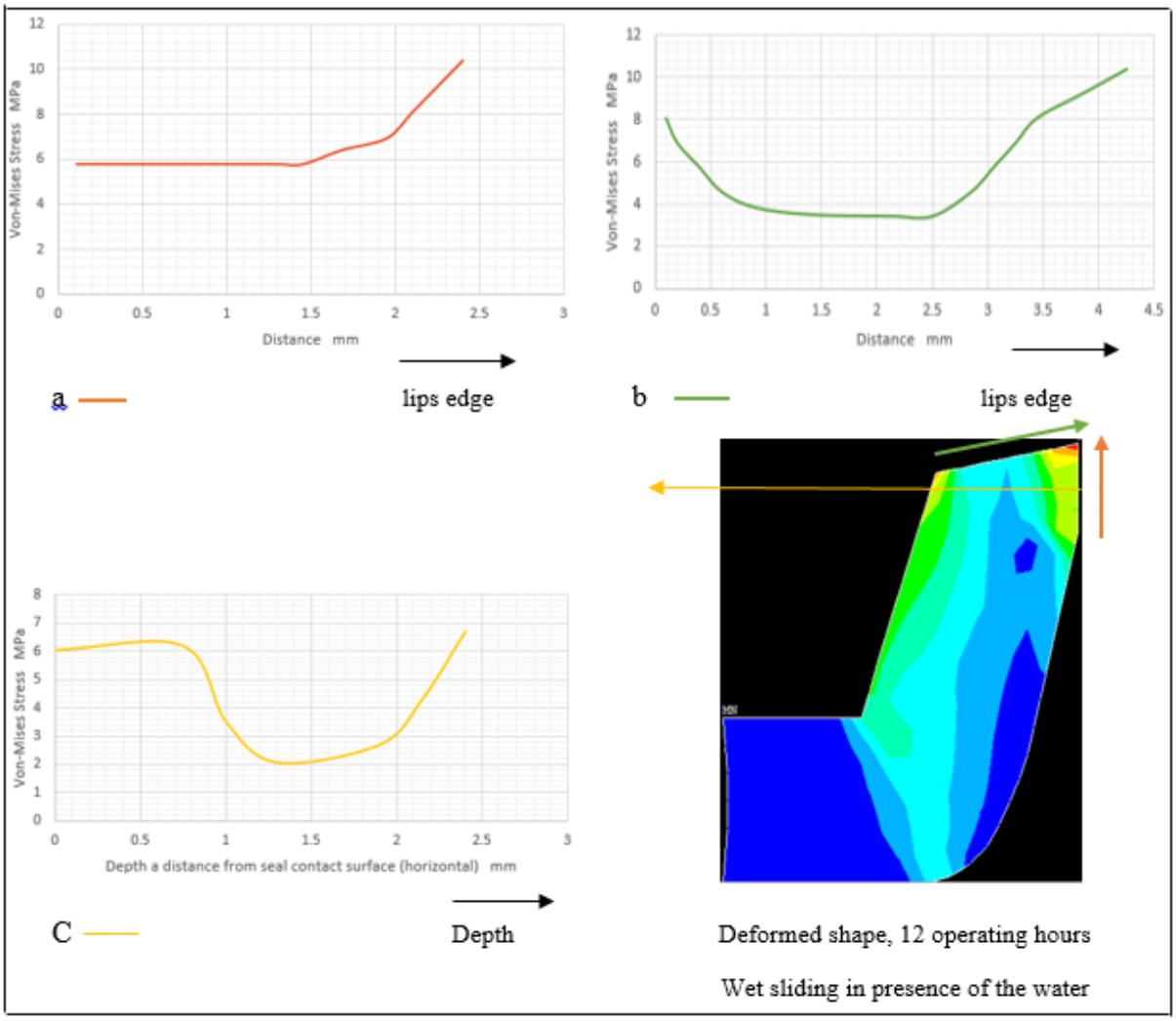

Fig.57.Graphs show the von-mises stress values for NBR piston seal following 12 hours of wet sliding time.

As a result, some regions of the piston seals contact area deformed after 12 hours of wet sliding time due to the influence of piston seals compression, coefficient of friction of piston seals, and fluctuating load of the water. The deformation was higher at the lips edge of the piston seals and that led to increased wear of the piston seals material.

Fig. 58. presented the deformation conditions of the uncoated NBR piston seal over the time during the wet sliding in the presence of water.

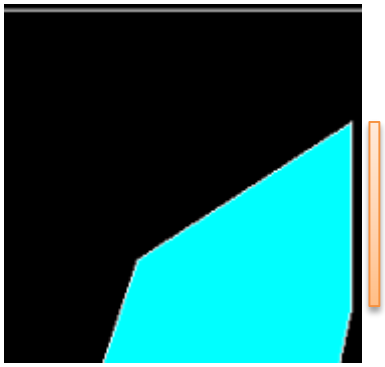

a-Sliding time is 0 (no stress)

contact surface length 3.7 mm

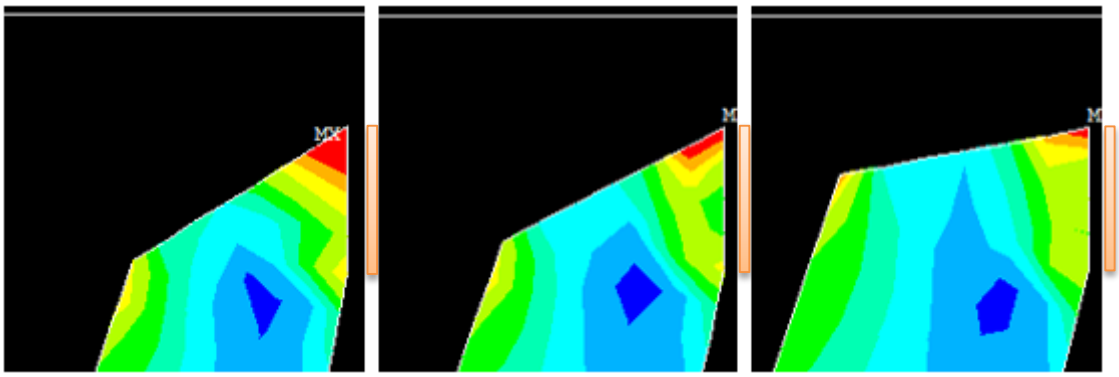

b- Sliding time is 3 hours *contact surface length 2.9 mm*

c – Sliding time is 6 hours *contact surface length2.6 mm*

d- sliding time is 12 hours *contact surface length 2.4 mm*

Fig. 58. Deformed shapes of the uncoated NBR piston seal after 0, 3, 6 and 12 hours of operation.

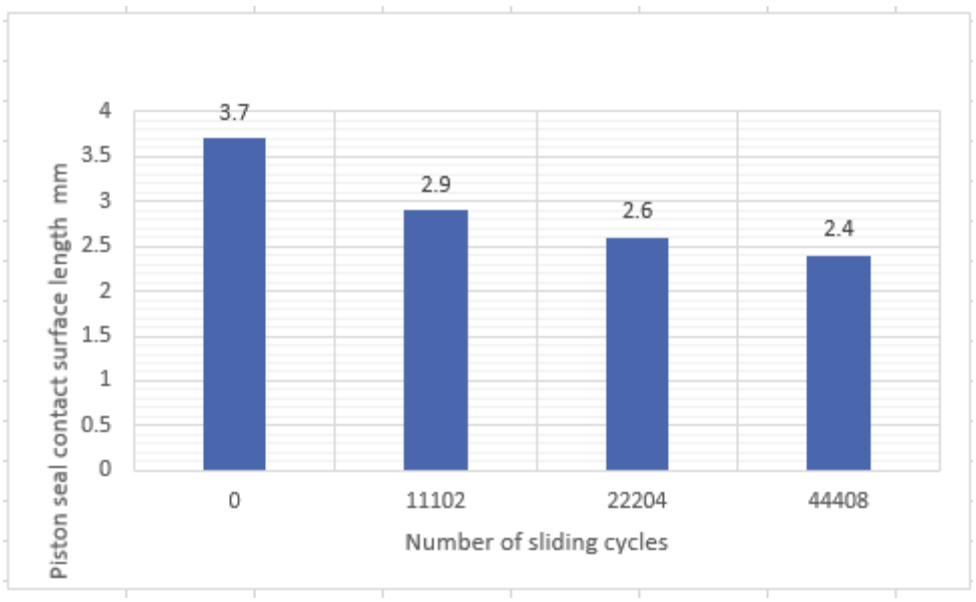

Fig.59. The contact surface length of the NBR piston seal in the presence of water.

There was a reduction in seal contact surface length over sliding time which means that there was a wear in the seal.

The F.E.A results on the contact surface length of the NBR piston seal over the wet sliding time are in a good agreement with the experimental results of my experiments and also with research results of Bullock [92], and Bekesi [94].

5.3.3 Dry sliding condition.

Finite element analysis was carried out by using different loading conditions, (piston + Pump rod) weight under dry sliding condition. Table.13. presented: (stretch) ƛ= (Ɛ+1), and engineering stress $\frac{\boldsymbol{Stress}\ \sigma}{\mathbf{2}[\lambda-\frac{\mathbf{1}}{\lambda^{\mathbf{2}}}]}$, of the piston seal through the dry sliding. Also the table shows Mooney-Rivlin constants value.

Table 15. Engineering strain, engineering stress and Mooney-Rivlin constants. For the dry sliding condition.

Piston seal Dia mm	No of cycles	λ = $(\varepsilon + 1)$	$1/\lambda$ = $1/(\varepsilon + 1)$	$\frac{\boldsymbol{Stress}\ \sigma}{\mathbf{2}[\lambda - \frac{\mathbf{1}}{\lambda^{\mathbf{2}}}]}$ N/m^2
64.50	0	1.207	0.82850	17379.03
64.20	6336	1.196	0.83612	21448.96
63.21	19008	1.171	0.85397	121447.4

Table 16. Mooney Rivlin constants

C10	C01	d = 2/k $\frac{m^2}{N}$
4000	4085724.2	$\mathbf{4.89\times 10^{-10}}$

At the early stage of operation and over the dry sliding time, the piston seal will be influenced by the weight of the piston plus pump rod. This influence will remain till the end of the operating time and as a result of this influence the piston seal will deform. The deformation depends on the contact pressure values.

5.3.3 1. Uncoated NBR piston seal after 2 hours of dry sliding time.

Figures 60 displays F.E.A of the uncoated NBR piston seal after 2 hours of the dry sliding time.

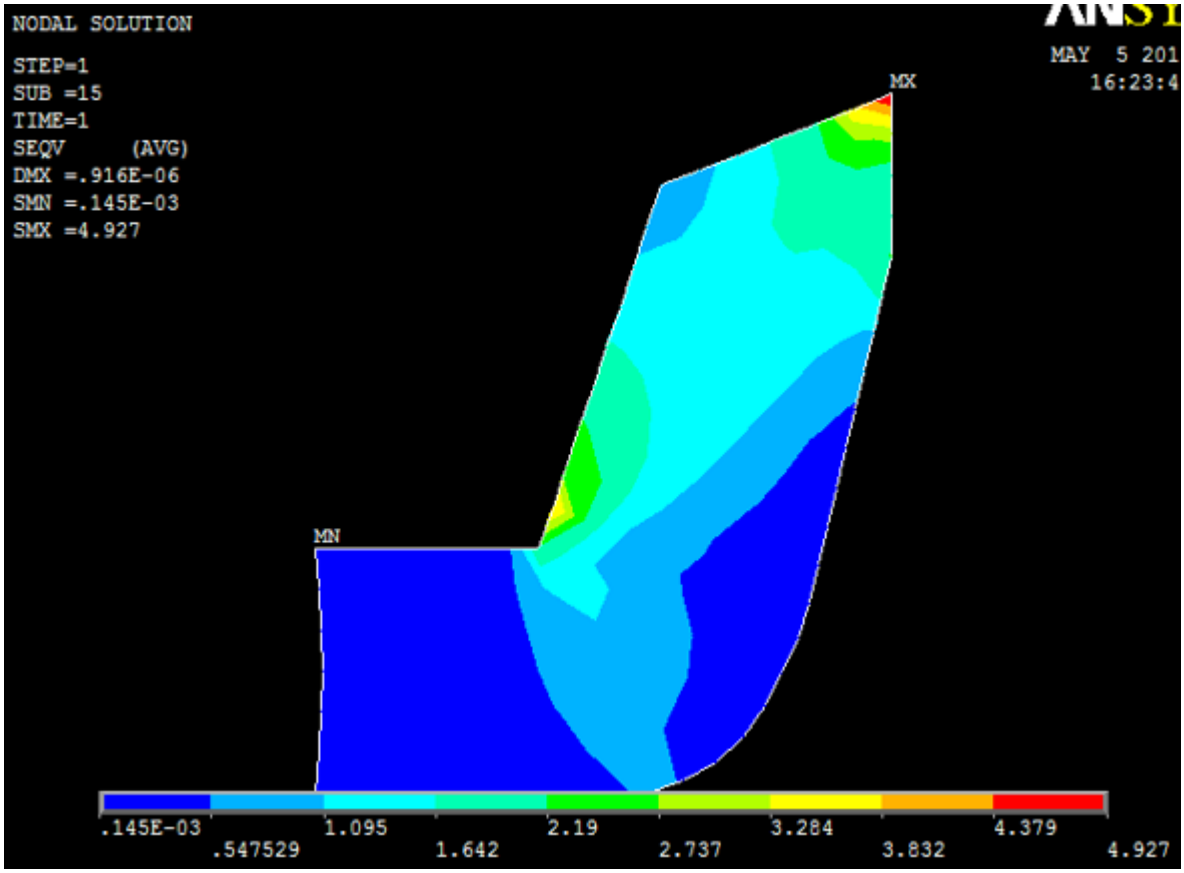

Fig. 60. Von mises stress distribution in the uncoated NBR piston seal after 2 hours of the dry sliding time.

The results of the analysis show that the Von-Mises stress was different in the piston seal contact area and several layers of the piston seal were influenced by the stress. The higher stress was developed at the lip of the piston seals and also along the piston seal contact surface. The maximum Von-Mises stress (4.927 MPa) was found at the tip of the seal. This is due to the higher squeeze of the lips seal and due to higher friction of lips seal.

The von-Mises stress gradually decreased along the contact surface and the top surface of the seal. Table 17 presented Von-Mises stress values for the uncoated NBR piston seal after 2 hours of the dry sliding time.

Table 17. Distribution of the Von-Mises Stress values in the uncoated NBR piston seal after 2 hours of the dry sliding time

Distance mm	Von-Mises stress MPa
2.986	4.9266
2.784	4.379
2.636	3.832
2.436	3.284
2.133	2.737
1.9399	2.25
1.785	2.19
1	2.19
0.5	2.19

A

Distance mm	Von-Mise stress MPa
4.5	4.9266
4.25	4.379
4	3.832
3.7	3.284
3.5	2.737
3.2	2.19
2.2	1.642
1	1.095
0.5	0.547529
0.2	0.547529

b

Distance mm	Von-Mises stress MPa
0	1.773
0.75	1.9728
1.493	1.9175
2.166	1.6505
2.9	1.3741
3.621	1.159

C

.

.

Fig.61. displays graphs of the von-Mises stress after 2 hours of the dry sliding time

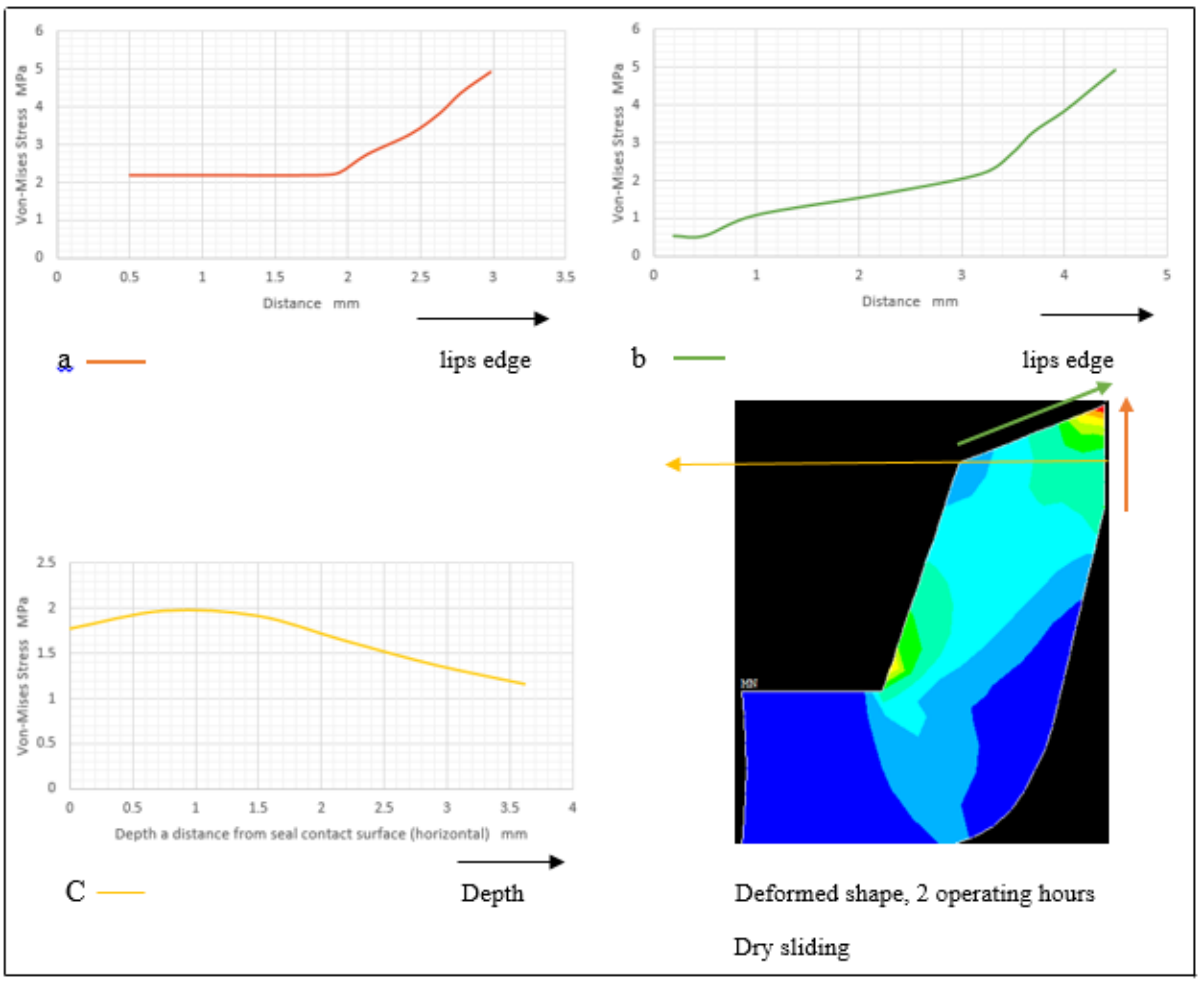

Fig.61.Graphs show the von-Mises stress values in the uncoated NBR piston seal after 2 hours of dry sliding time.

Cooperation the von –Mises stress under dry sliding condition and wet sliding condition:

Von Mises stress was highest on the top surface of the seal under wet sliding condition due to the fluctuating load of the water acting on the top surface of the seal, but under dry sliding condition the highest von-Mises stress was on the edge of the lip of the seal because there was no water and there was higher friction between the contact surfaces of the vseal and cylinder.

5.3.3.2. Uncoated NBR piston seal after 6 hours of the dry sliding time.

Figures 62 displays F.E.A of the uncoated NBR piston seal after 6 hours of the dry sliding time.

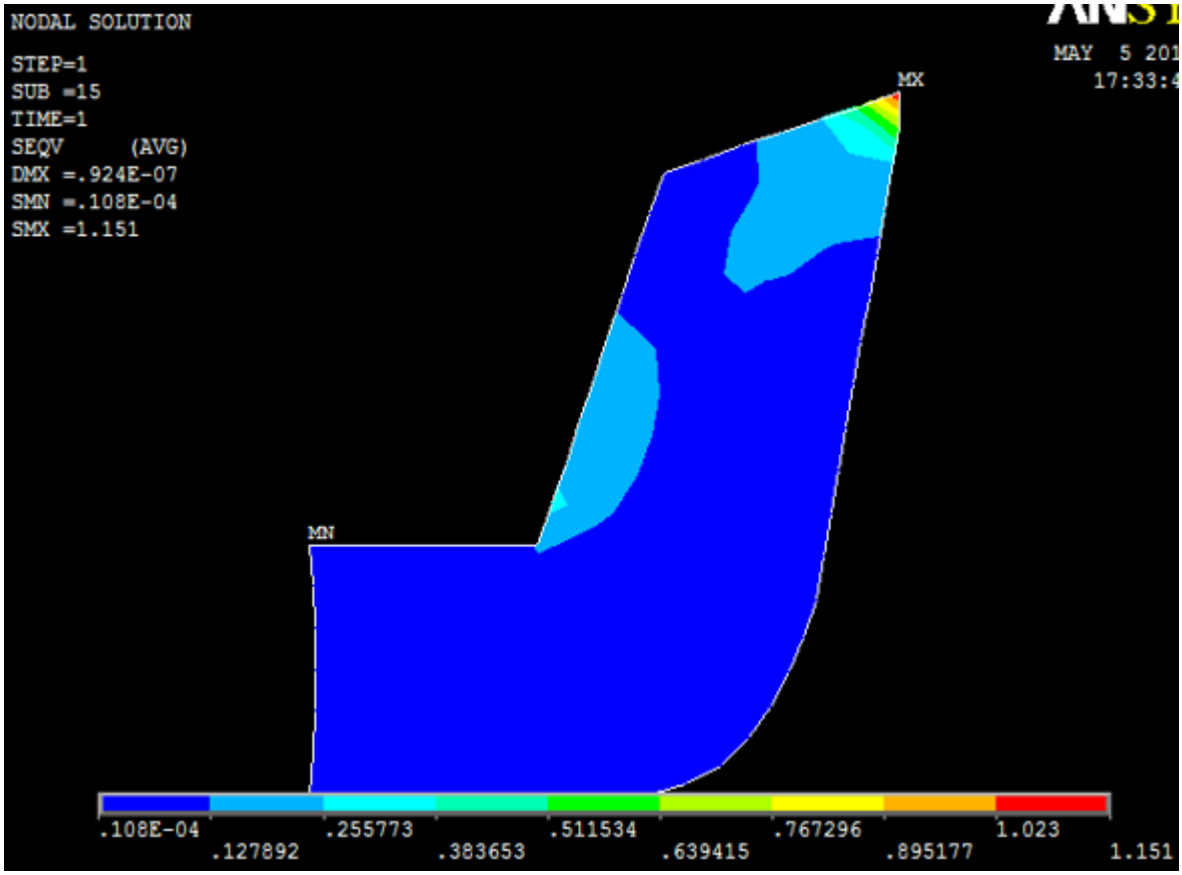

Fig. 62. Von-Mises stress distribution in the uncoated NBR piston seal after 6 hours of the dry sliding time.

The results of the analysis show that the Von-Mises stress after 6 hours of dry sliding time were less than that after 2 hours of dry sliding time. There was a higher reduction of the seals contact surface which lead to more wear and less in contact surface then less in stress. The maximum von-Mises stress (1.151 MPa) was found at the tip of the piston seals.

Table 18 presented Von Mises stress values for the uncoated NBR piston seal after 6 hours of the dry sliding time.

Table 18. Distribution of the Von-Mises Stress values in the uncoated NBR piston seal after 6 hours of the dry sliding time.

Distance mm	Von-Mises stress MPa
0.602	1.151
0.499	1.023
0.405	0.8951
0.3	0.76729

a

Distance mm	Von-Mises stress MPa
3.45	1.151
3.325	1.023
3.249	0.8951
3.1	0.76729
3	0.63941
2.9	0.51153
2.7	0.38365
2.4	0.25577
1.4	0.12789
0.9978	0.000108
0.65	0.000108
0.2	0.000108

b

Distance mm	Von-Mises stress MPa
0	1.1509
0.15	0.895177
0.3	0.76729
0.425	0.639415
0.631	0.511534
0.8262	0.3865

c

Fig. 63. displays graphs of the von-Mises stress for NBR piston seal after 6 hours of the dry sliding time.

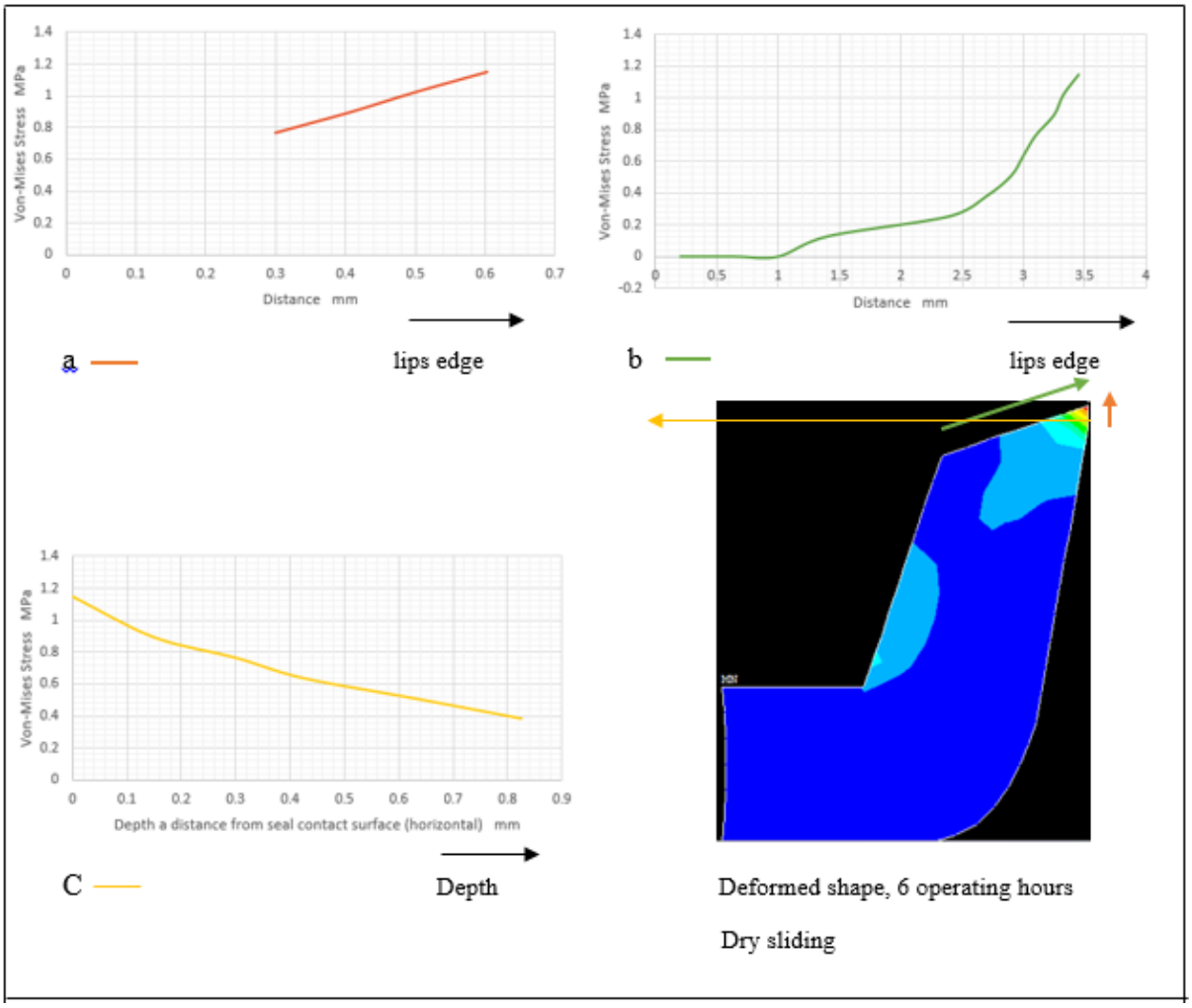

Fig.63.Graphs show the von-Mises stress values in the uncoated NBR piston seal after 6 hours of dry sliding time.

As a result, some regions of the piston seal contact area deformed in the uncoated NBR piston seal after 6 hours of dry sliding time due to the influence of the piston seals squeeze and the friction coefficient of the piston seals. The deformation was higher at the lips edge and along the piston seal contact surface. This deformation led to wear of the piston seal material and afterward removal of seal material. The higher removal of seal material causes higher reduction in piston seal contact area (Fig.64).

Fig. 64. Presents the deformation conditions of the uncoated NBR piston seal over the time of the dry sliding.

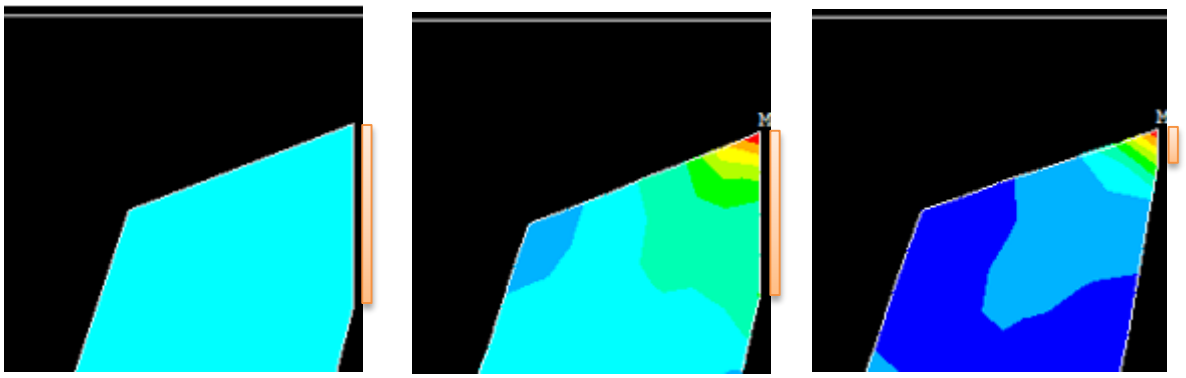

a-Sliding time is 0 (no stress) *contact surface length 3.5 mm*

b-Sliding time is 2 hours *contact surface length 2.9 mm*

c-Sliding time is 6 hours *contact surface length 0.6 mm*

Fig. 64. Deformed shapes of the uncoated NBR piston seal over the time of dry sliding,

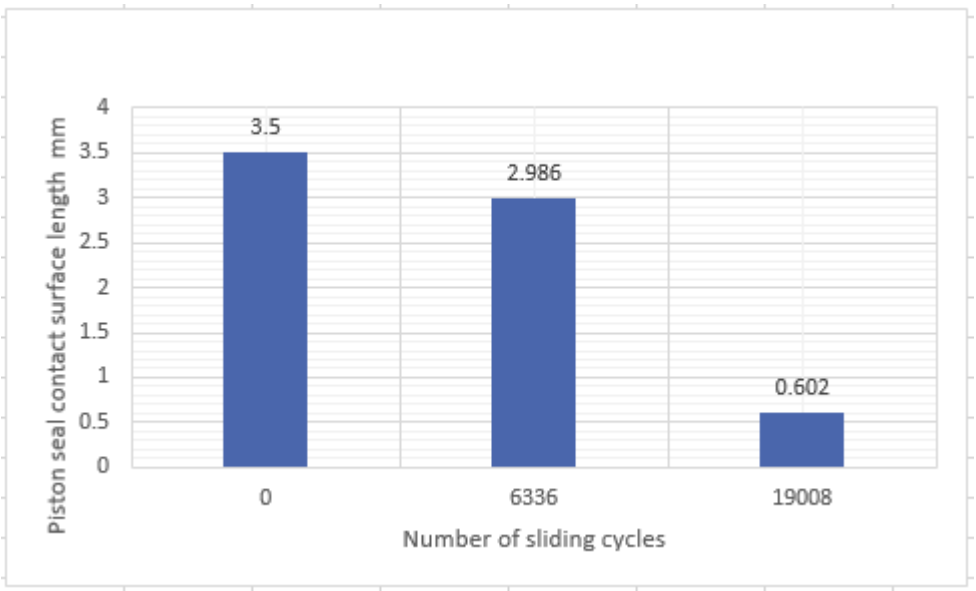

Fig.65. The contact surface length of the uncoated NBR piston seal over the dry sliding cycles.

The reduction in seal contact surface length over the time of dry sliding was higher than that in the wet sliding. This confirm that the wear of the piston seal during dry sliding operation was more than during wet sliding operation and that may be due to the higher seal friction.

The F.E.A results on the contact surface lengths of the uncoated NBR piston seal over the dry sliding time are in a good agreement with the experimental results and also with the research results of Bullock [92], and Bekesi [94].

5.3.4. Dry sliding condition with effect of mass of 0.5 kg added to pump rod mass.

Finite element analysis was carried out by using different loading conditions, {(piston + Pump rod) weight + a mass of 0.5 kg }. Table.17. presented: stretch $\lambda = (\varepsilon+1)$, and engineering stress $\frac{\sigma(stress)}{2[\lambda-\frac{1}{\lambda^2}]}$, of the uncoated NBR piston seal through the dry sliding. Also the table shows Mooney-Rivlin constants values.

Table 19. the engineering strain, engineering stress, and Mooney-Rivlin constants, for the dry sliding condition with effect of a mass of 0.5 kg added to the pump rod mass.

Piston seal Dia mm	No of cycles	$\lambda = (\varepsilon+1)$	$1/\lambda = 1/(\varepsilon+1)$	$\frac{\sigma(stress)}{2[\lambda - \frac{1}{\lambda^2}]}$ N/m^2
64.19	0	1.207	0.82850	30142.4
63.74	6336	1.204	0.83056	48804.5
63.01	19008	1.174	0.85178	3552556.5

Table 20. Mooney-Rivlin constants

C10	C01	d = 2/k $\frac{m^2}{N}$
26000	9059143.2	2.201×10^{-10}

5.3.4 1. Uncoated NBR piston seal after 2 hours of the dry sliding time with the effect of a mass of 0.5 kg added to the pump rod mass.

Figures 66 displays F.E.A of the uncoated NBR piston seal after 2 hours of the dry sliding time with the effect of a mass of 0.5 kg added to the pump rod mass.

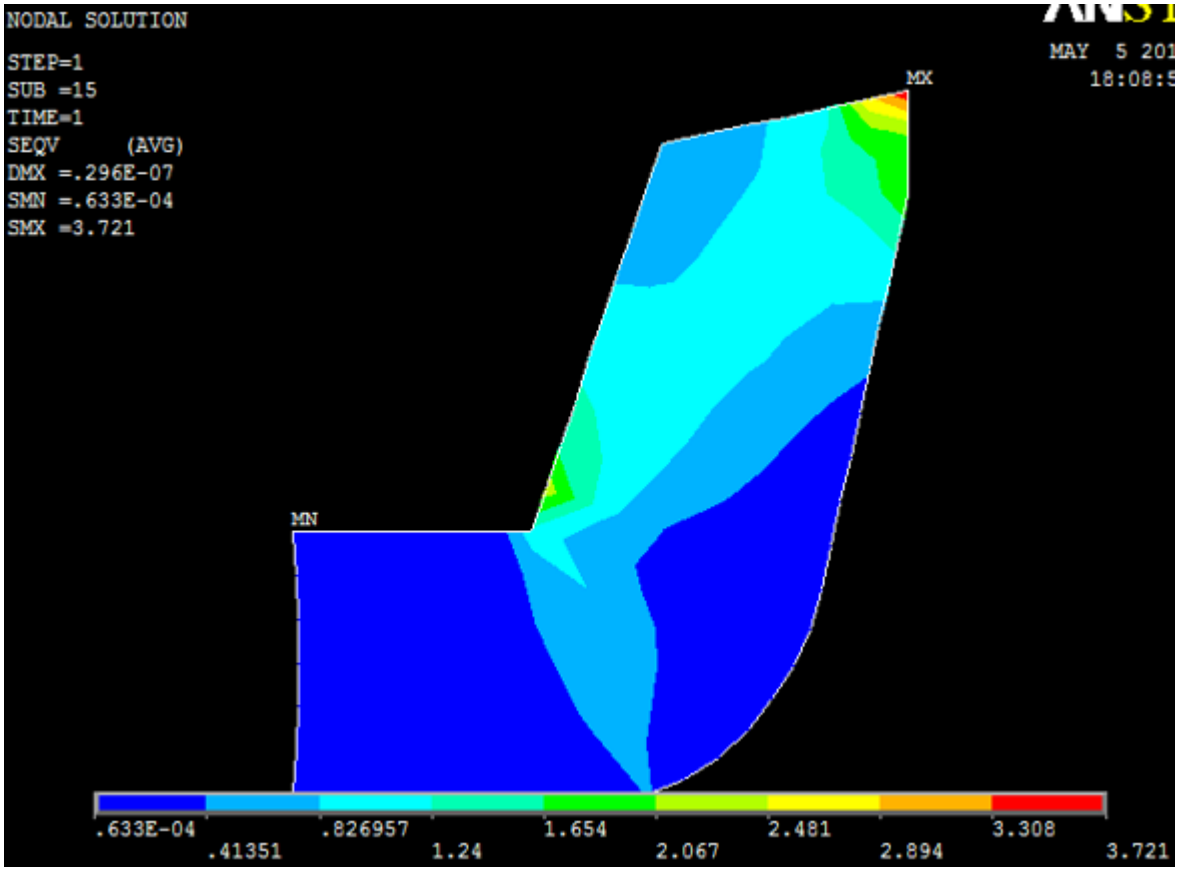

Fig. 66. F.E.A of the NBR piston seal, and the condition after 2 hours of the dry sliding time with effect of mass of 0.5 kg added to the pump rods mass.

.

The maximum Von-Mises stress (3.721 MPa) was at the tip of the seal. Von-mises stress gradually decreased along the contact surface, along the top surface of the seal, and along the horizontal depth of the seal.

Table 21 presents Von Mises stress values in the uncoated NBR piston seal after 2 hours of the dry sliding time with the effect of a mass of 0.5 kg added to the pump rods mass.

Table 21. Distribution of the Von-Mises Stress values in the uncoated NBR piston seal after 2 hours of the dry sliding time with the effect of a mass of 0.5 kg added to thepump rod mass.

Distance mm	Von-Mises stress MPa
1.767	3.7211
1.617	3.308
1.467	2.894
1.317	2.481
1.117	2.067
0.75	2.067
0.49	2.067
0.25	2.067

a

Distance mm	Von-Mises stress MPa
4.2	3.7211
4	3.308
3.8	2.894
3.5	2.481
3.35	2.067
3.2	1.654
3	1.2433
1.9	0.8269
1.45	0.41351
1	0.41351
0.5	0.41351

b

Distance mm	Von-Mises stress MPa
0	2.2203
0.6	2.0677
1.4	1.6542
2.4	1.2455
3.84	0.82695

C

Along the contact surface (starting from the lips edge) von-Mises stress values gradually decreased and afterward remained constant. Also along the top surface (starting from the lips edge) von-Mises stress varies in a similar way. However along the horizontal depth starting from the seal contact surface the von-Mises stress continually decreased.

Fig. 67 displays graphs of the von-Mises stress in the uncoated NBR piston seal along the seals contact surface, seals top surface, and horizontal depth starting from the contact surface, after 2 hours of the dry sliding time with the effect of a mass of 0.5 kg added to the pump rod mass.

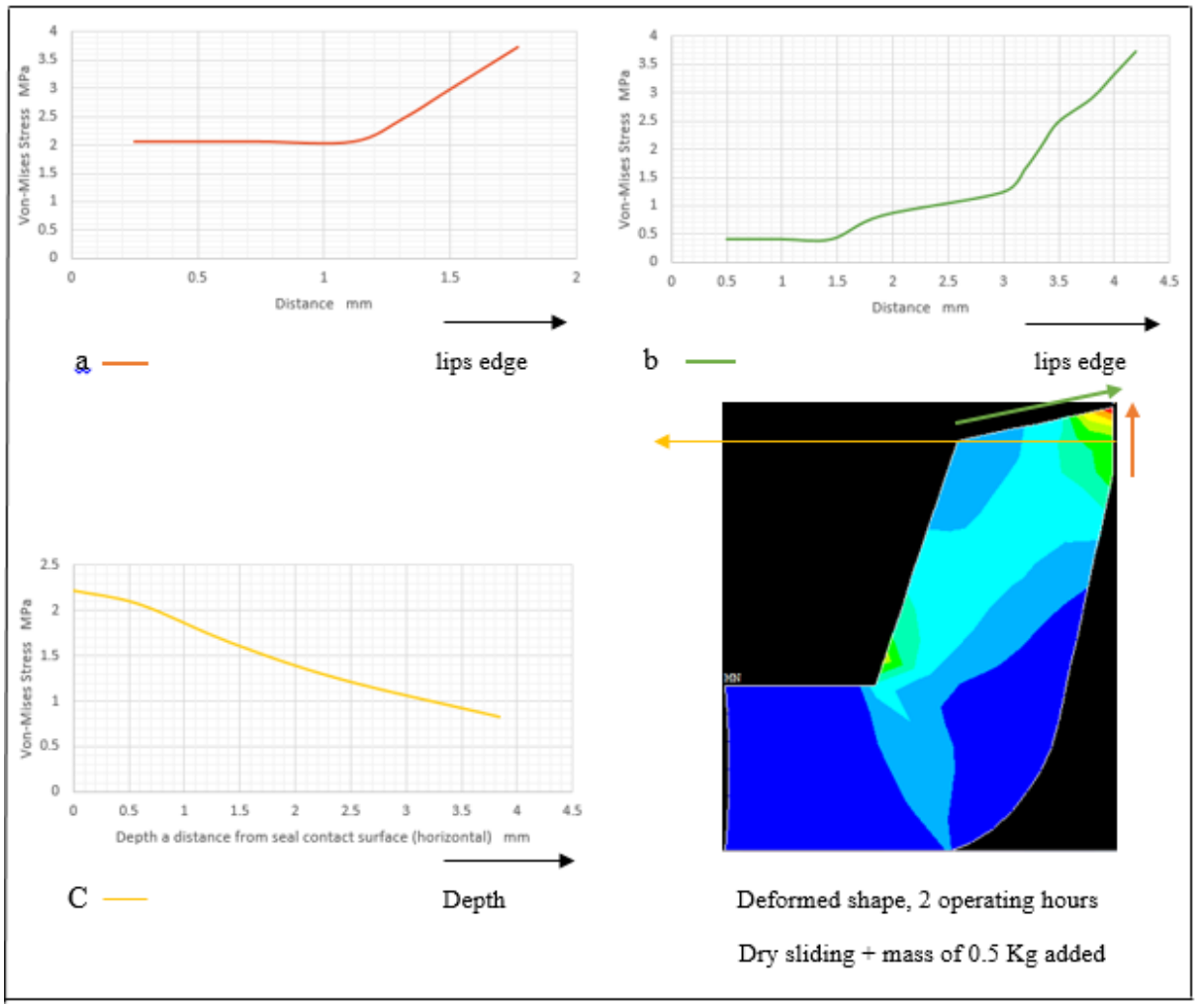

Fig.67.Graphs show the von-Mises stress values in the uncoated NBR piston seal due to the distance along the (a) seals contact surface (b) seals top surface, and (c) horizontal depth starting from the contact surface, after 2 hours of dry sliding time with the effect of a mass of 0.5 kg added to the pump rod mass.

5.3.4.2. Uncoated NBR piston seal after 6 hours of dry sliding time with the effect of a mass of 0.5 kg added to the pump rods mass.

Figures: 68 displays the von-Mises stress distribution in the uncoated NBR piston seal after 6 hours of dry sliding time with the effect of a mass of 0.5 kg added to the pump rod mass.

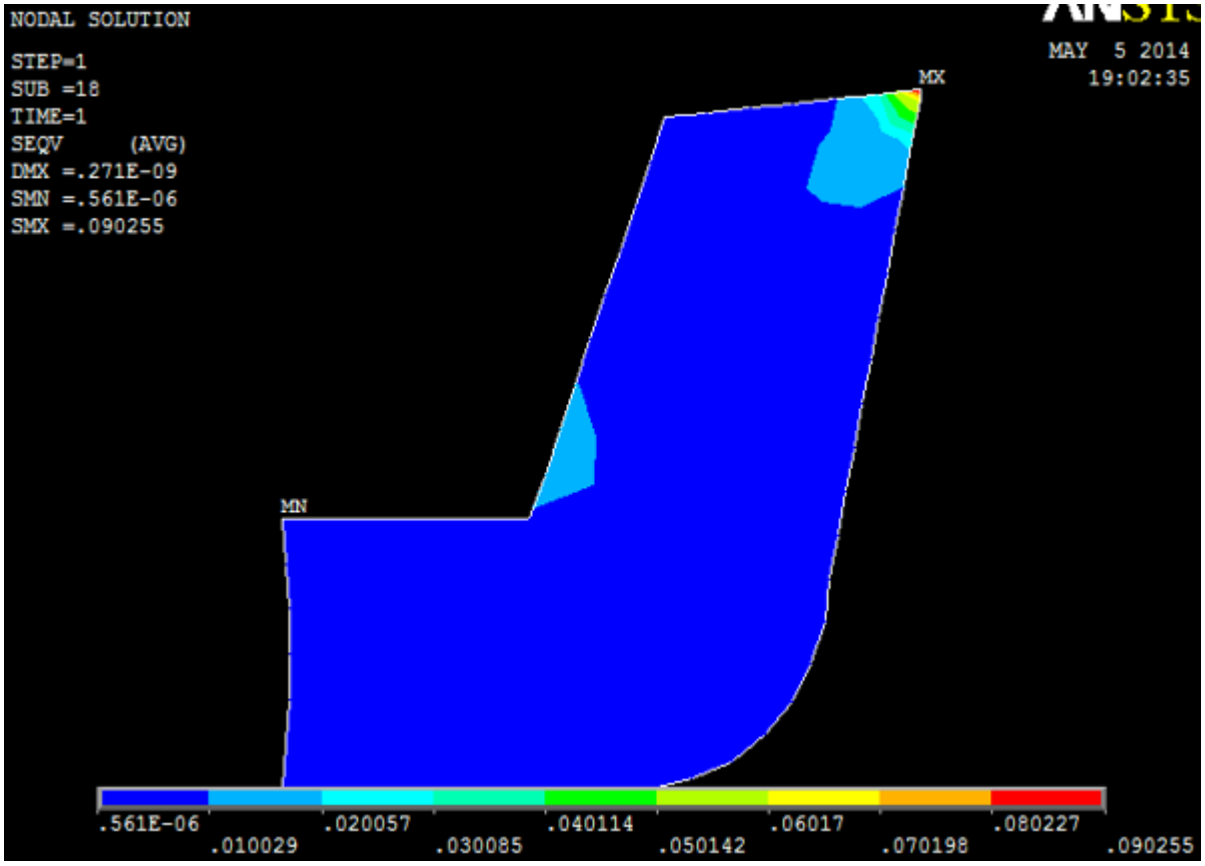

Fig. 68. Von-Mises stress distribution in the uncoated NBR piston seal, and the condition after 6 hours of the dry sliding time with effect of the mass of 0.5 kg added to the pump rod mass.The maximum von-mises stress (0.090255 MPa) was at the lips edge of the piston seals. Von-mises stress gradually decreased along the contact surface of the piston seal (starting from the lips edge), along the top surface of the piston seal (starting from the lips edge),

and along the horizontal depth starting from the seal contact surface. There was a higher reduction in piston seal contact surface (it was nearly to zero). This indicated that there was a higher amount of material removed through the 6 hours of the sliding time.

Table 22. presents Von-Mises strress values for the uncoated NBR piston seal after 6 hours of the dry sliding time with effect of the mass of 0.5 kg added to the pump rod mass**Table.20**. Distribution of the Von-Mises Stress values in the uncoated NBR piston seal after 6 hours of the dry sliding time with the effect of the mass of 0.5 kg added to the pump rod mass.(a) along the contact surface (b) along the top surface.

Table 22. von-Mises stress distribution

Distance mm	Von-Mises stress MPa
0.028	0.90255
0.014	0.080227
0.011	0.070198

a

Distance mm	Von-Mises stress MPa
3.4	0.90255
3.3	0.08227
3.15	0.070198
3.05	0.0617
2.95	0.050142
2.65	0.040114
2.3	0.030085
2.15	0.020057
1.95	0.010029
1.8	0.00000561
1.2	0.00000561
0.6	0.00000561
0.2	0.00000561
0.05	0.00000561

b

.Fig. 69 displays graphs of the von-Mises stress in the uncoated NBR piston seal along the seals contact surface and seals top surface, after 6 hours of the dry sliding time with effect of the mass of 0.5 kg added to the pump rod mass.

Along the contact surface of the NBR piston seal (starting from the lips edge) von-mises stress values gradually decreases and afterward remained constant. However along the top surface (starting from the lips edge) von-Mises stress sharply decreased and afterward remained constant

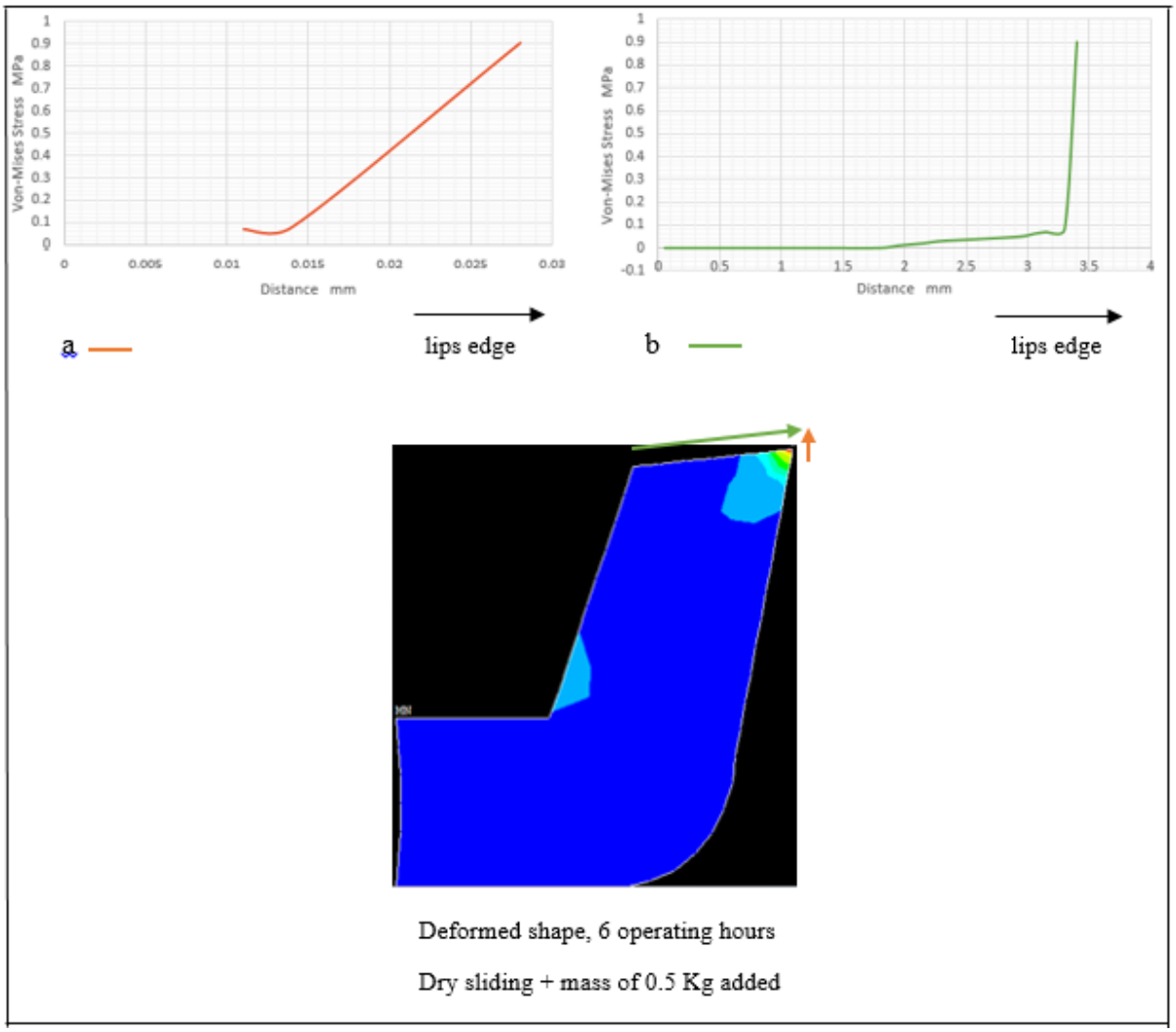

Fig.69.Graphs show the von-Mises stress values along (a) seal contact surface (b) seal top surface after 6 hours of dry sliding time with the effect of the mass of 0.5 kg added to the pump rod mass.

Fig. 70. Presented the deformation conditions of the uncoated NBR piston seal over the time of the dry sliding with effect of the mass of 0.5 kg added to the pump rod mass. The deformation was higher at the lips edge and at the piston seal contact surface.

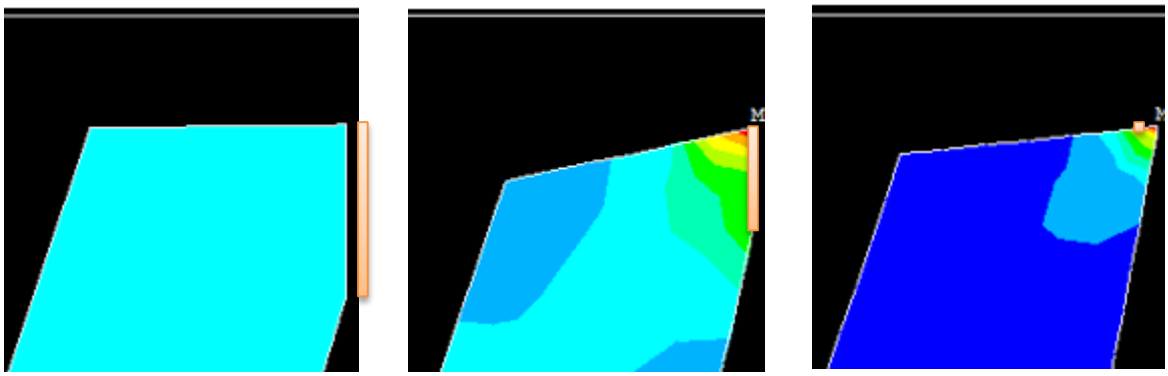

a-Sliding time is 0 (no stress) *contact surface length 2.8 mm*

b-Sliding time is 2 hours contact surface length 1.7mm

c-Sliding time is 6 hours *contact surface length 0.02 mm*

Fig. 70. Deformed shape of the uncoated NBR piston seal over the time of dry sliding with the effect of a mass of 0.5 kg added to the pump rod mass (a) sliding time = 0 hours (b) sliding time = 2 hours (c) sliding time = 6 hours.

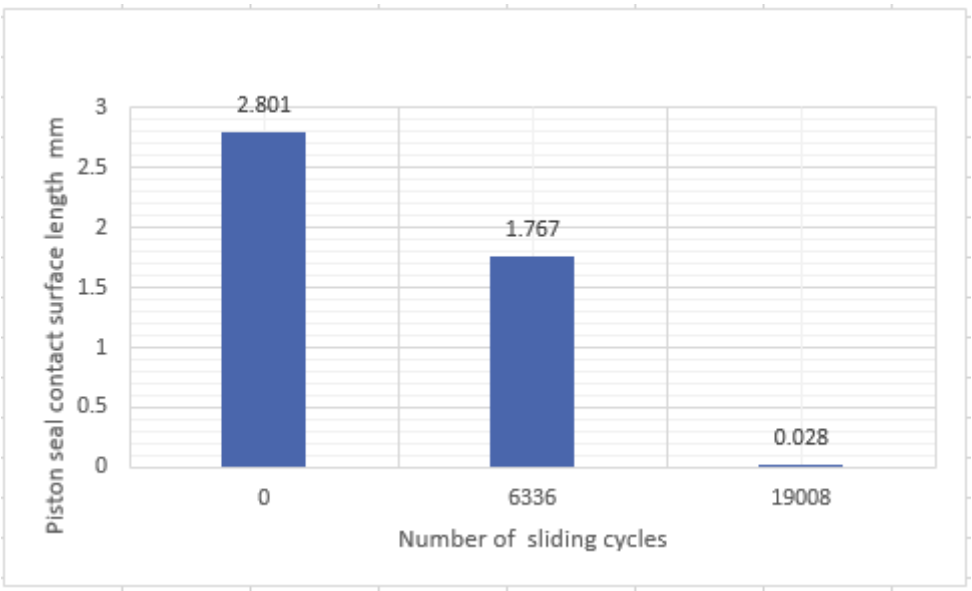

Fig.71. The contact surface length of the uncoated NBR piston seal over the dry sliding cycles with the effect of mass of 0.5 kg added to pump rod mass.

Higher wear of the piston seal during the dry sliding operation with 0.5 Kg added, there was no seal compression after 19008 cycles of the piston seal (Fig 71).

The F.E.A results on the contact surface lengths of the uncoated NBR piston seal over the dry sliding time with effect of the mass of 0.5 kg added to the pump rod mass are in a good agreement with results of the experimental and also with the research results of Bullock [92], and Bekesi [94].

Fig. 72. displays the contact surface lengths over the sliding time of the uncoated NBR piston seal during wet and dry sliding conditions. Over the wet and dry sliding time the length (mm) of the contact surface of the NBR piston seal decreases. This decrease was different due to the sliding condition. The decreasing contact surface lengths occurred as a result of the wear of NBR piston seal.

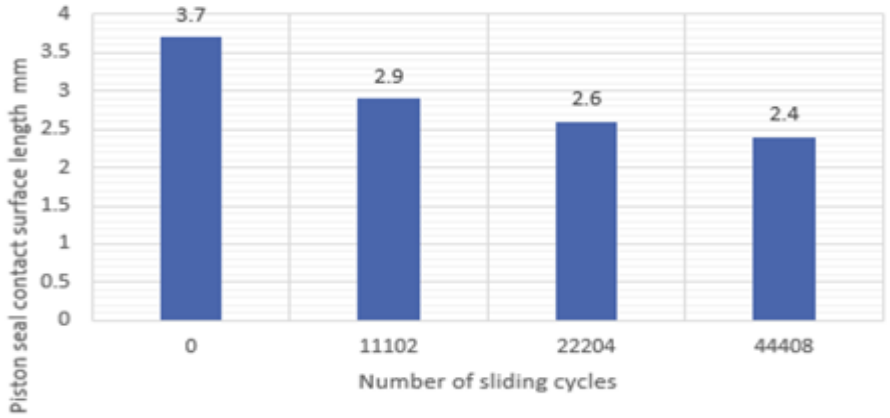

(1) Wet sliding conditions

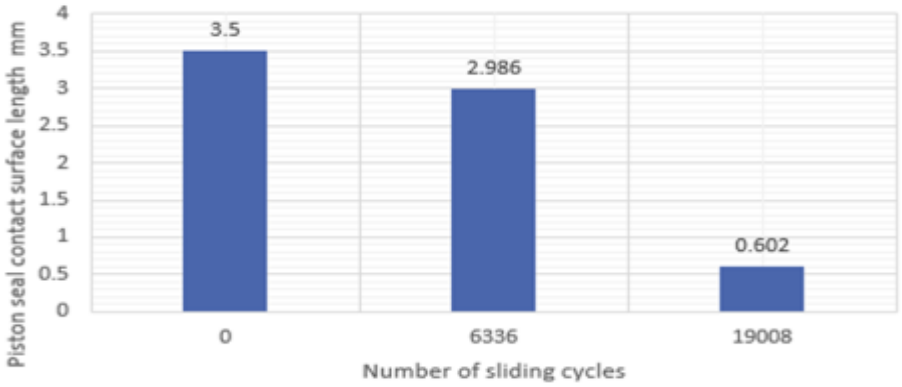

(2) Dry sliding conditions

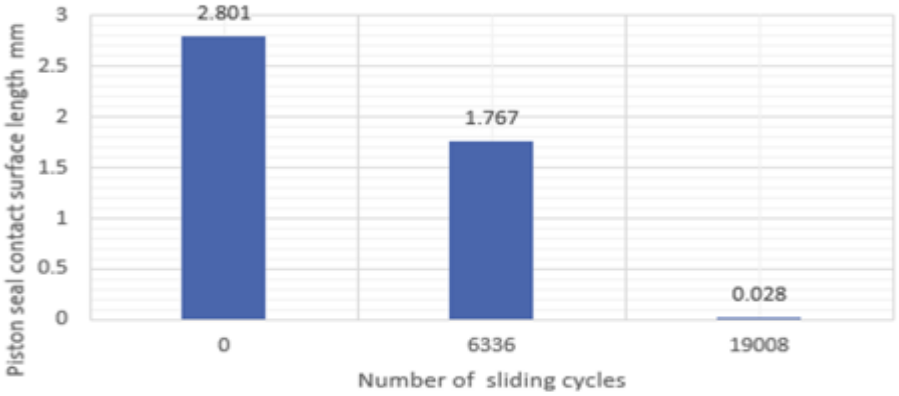

(3) Dry sliding conditions with 0.5 Kg added

Fig.72. contact surface lengths with different sliding conditions

6.1 Conclusion.

Based on the results of the experimental tests carried out on the Analysis of the wear of uncoated NBR piston seal can be drawn, the following can be stated. It can be established that:

1-The reduction in contact area of the uncoated NBR piston seal in wet sliding condition in the presence of water is found to be lower than that in dry sliding conditions.

The presence of water contributes to a decrease in the seal diameter. The uncoated NBR piston seals diameter decreased from 64.58 mm to 63.99 mm during 44408 cycles of wet sliding condition in the presence of water. While the diameter of uncoated NBR piston seal decreased from 64.50mm to 63.21mm during 19008 cycles of dry sliding condition.

Higher wear of the uncoated NBR piston seals diameter was found during dry sliding conditions with the effect of 0.5 kg mass added to pump rod mass. The diameter decreased from 64.19mm to 63.01mm during 19008 cycle. This resulted in the piston seal diameter becoming equal to the cylinder diameter after 19008 cycles. Leakage across the seal would result following this level of wear

A relationship was found between the contact area and travel distance (X) of the lip of uncoated NBR piston seal after compression. The relationship indicates that the contact area increases when the travel distance increases.

2- The presence of the water during wet sliding reduced the friction of the uncoated NBR piston seal and also caused rolling of the edge of the piston seal. The friction of the uncoated NBR piston seal during dry sliding was higher resulting in the formation of parallel line on the piston seal contact surface and higher wear of the lip.

The friction during dry sliding increases with the increasing mass of the pump rod.

A linear relationship exists between the friction force and the travel distance (X) at the tip of the uncoated NBR piston seals after compression.

3- Higher removal of material of uncoated NBR piston seal occurs during operation under dry sliding conditions, and lower removal of material occurs during wet sliding in the presence of water.

4- Uncoated NBR piston seal in dry sliding condition (with addition 0.5 kg mass added to the pump rod mass) failed after 19008 cycles. During wet sliding in the presence of water the uncoated NBR piston seal had not failed over 44408 cycles.

5- In wet sliding condition and in presence of the water the wear rate decreases after each test. In dry sliding condition the wear rate increases after each test.

A relationship exists between the wear rate and the length of the contact surface(Y) of the uncoated NBR piston seal. The volume of remove material increases when Y is large, and decreases as Y is decreasing due to wear.

6- A good agreement was found between the results obtained from experiments and FEA of the NBR piston seal over the time for both wet and dry sliding conditions,

6.2 Future Work

1-Further development of the pump rig system can be carried out to analysis the wear of NBR coated and uncoated piston seals.

2- Testing and analysis of wear of NBR coated piston seal using experimental methods with a short piston stroke.

3-Test and analysis of wear of NBR coated and uncoated piston seal using experimental methods with long and short piston strokes.

4-Analysis of the wear of NBR coated piston seal using finite element analysis (F.E.A) methods.

5-Validation of finite element analysis (F.E.A) methods by comparing with experimental results for NBR coated and uncoated piston seals.

References

[1] I kin, D., and Baumann, E., 2001. Setting up viable Supply Chains Vietnam, summary of an appraisal and impact assessment of the Government of Vietnam-IDE Hand pump promotion program, funded by ICCO, publisher RWSN, institution Skat. SDC.

[2] Jenna Martin, USF Civil & Environmental Engineering, Hand pumps for Rural Water Supply. Available from [Online], www.usfmi.weebly.com (Accessed 3 July 2013).

[3]. Smout, I.K., Technical Brief No. 27: Discharge measurements and estimates, Waterlines, Vol. 9, No.3, IT Publications, London, 1991

[4] Harvey, P.A, and Skinner. B.H, 2002, Sustainable Hand pumps projects in Africa: Report on fieldwork in Zambia, WEDC, and Loughborough University, UK. 2002.

[5] Elson B and Francey S, 1992. Technical brief No 33/ Maintaining Hand pumps, Water lines, Vol 11 (1), pp. 15-18.

[6] G. Thompson, Improving Maintainability and Reliability through Design, Professional Engineering Publishing, London and Bury, St Edwards, UK, 1999.

[7] S. Arlosoroff, G. Tschannerl, D. Grey, W. Journey, A. Karp, O. Langenegger, R. Roche, and Community Water Supply: The Hand pump Option, The World Bank, Washington D.C., 1987.

[8] P. A. Harvey, 2003, Sustainable Hand pump projects in Africa: Report on fieldwork in Uganda, WEDC, and Loughborough University.

[9] Pumps, available from www.ex-pect.com/equipment-types/pumps.html, access on 4/12/2013.

[10] Michael Lubwama, 2011, Characterization of DLC and Si-DLC with and without SiC-

Forming interlayer deposited on commercial nitrile rubber for piston seals. Dublin City University, Ireland.

[11] Mohammad Reza Mofidi and Braham Prakash, 2008. Tribology of elastomeric seal materials, Luleå University of Technology. Sewden.

[12] Sandor Bisztray, 1999. Tribology of elastomeric and composite reciprocating hydraulic seals, Periodica Polytechnica SER Mech.Eng , Vol 43 No 1, p.p 63-80, Budapest, Hungary.

[13]T.A.Stolarski (Phd, Dsc, Dic, CEng, MIMeche), 2000, Tribology in machine design, Vol C1990, part 2, Oxford, England.

[14] Nikas, G.K. 2003, ASME, J.Tribology, Nova science publishers, INC, New York, Vol 125, p.p 60-65.

[15] Nikas G. K., Hasegawa T.'Research on the tribology of hydraulic reciprocating seals' Tribology research trends (New York, USA: Nova Science Publishers2008), pp. 11-56 ch. 1.

[16] WHITE, C. M – DENNY, D. F.: The Sealing Mechanism of Flexible Packings, Ministry of Supply. Scientific and Technical Memorandum, No 3/47, 1947 (Reprinted by BHRA, 1972).

[17] Bisztray-Balku S. Design Development and tribology of reciprocating hydraulic seals, Periodica Politechnika Mechanical Engineering, Vol 47 (2004) No 1.

[18] Nikas G. K., Burridge G., Sayles R. S. Modelling and optimization of rotary vaneseals' Proc. IMechE, Part J: J. Engineering Tribology 221 J6 (2007): 699-715

[19] M. Kaneta, T. Takeshima, S. Togami, H. Nishikawa, and Y. Kanzaki. Stribeck curve in reciprocating seals.18th International Conference of Fluid Sealing, Antwerp, Belgium, 2005. BHR Group Limited.

[20] Sealing elastomers, physics of rubber available from online http://www.allsealsinc.com/allseals/Orings/or13.htm, access on 6/12/2013.

[21] J. R. Barber, M. Ciavarella, 2000. Contact of Mechanics, university of Oxford, International journal of solids and structures 37 (2000) 29-43.

[22] Hydraulic fluid seals, available from online, www.dkirubbr.com, , access on 7/12/2013.

[23] M.Y.Meyers, K.K.Chawla, 2008, Mechanical behaviour of materials, Cambridge University press, New York.

[24] Bharat Bhusham, 2000, Modern tribology Hand Book, Vol 1, p.p.273-299, Wear mechanisms.

[25] Alfred Zmitrowicz, 2006, Wear patterns and laws of wear a review, Journal of Theoretical and Applied Mechanics 44, 2, pp 219-253, Warsaw.

[26] H. M. Ayala, D. P. Hart, O. Yeh, M. C. Boyce, 1998, Wear of elastomeric seals in abrasive slurries, Cambridge, Wear, 220 (1998), pp 9-24.

[27] D.W. Borland, S. Bain, 1997. Unlubricated sliding wear of steels towards an alternative wear equation. Wear, Vol 209, issues 1-2, pp 171-178.

[28] Challen, J.M. and Oxley, P.L.B. (1979). An explanation of the different regimes of friction and wear using asperity deformation models, Wear 53, pp 229-243.

[29] Yang Limin, Hals Gorgen, Moan Torgeir. 2010. Analysis of dynamic effects relevant for the wear damage in hydraulic machines for wave energy conversion, article in journal in Ocean Engineering (Issn 0029-8018, EISSN 1873-5258), Vol 37, pp 1089-1102.

[30] Peter Andersson, J.Tamminen and C.Erik, 2002, piston seal tribology. Aliterature survey, Espoo 2002. VTT Tiedotteitea-Research notes 2173. 105 P.

[31] D. F. Moore,1972. The Friction and Lubrication and lubrication of Elastomers, Pergamon Press, Oxford. A complete account but no mention of recent work on fatigue and schallamch wave. Wear, 30 (1974) 25.

[32] D. Shen, R. F. Salant, Elastohydrodynamic analysis of the effect of shaft surface finish on lip seal behaviour, Tribol. Trans. 46 (2003) 391-396.

[33] S. Bisztray- Balku, Design development and Tribology of reciprocating hydraulic seals, Periodica Polytechnica Mechanical Engineering 47 (1) (2004) 163–178.

[34] A. Karaszkiewicz, Hydrodynamics of rubber seals for reciprocating motion, lubricating film thickness, and outleakage of O-seals, Ind. Eng. Chem. Res. 26(11) (1987) 2180–2185.

[35] B. J. Brisco, S. K. Sinha, Wear of polymers, Proc. Inst. Mech. Eng. Part J.-J. Eng. Tribol. 216- 6 (2002).

[36] Hugnell A.B.-J., Bj • orklund S., Andersson S., 1996, Simulation of the mild wear in a cam-follower contact with follower rotation, Wear, 199, 202-210

[37] Stromberg N., 1997, Thermo mechanical modelling of tribological systems, Linkoping Studies in Science and Technology. Dissertations, No. 497, Linkoping University, 1-136.

[38] Szefer G., 1998, Contact problems in terms of large deformations, Zeitschrift fur Angewandte Mathematik und Mechanik, 78, 8, 523-533

[39] Alfred Zmitrowicz. Wear pattern and laws of wear. Journal of theorytical and applied mechanics, Vol 44, pp. 219-253, 2006..

[40] Franklin F.J., Widiyarta I., Kapoor A., 2001, Computer simulation of wear and rolling contact fatigue, Wear, 250-251, Part 2, 949-955.

[41] Kato K., 2002, Classi_cation of wear mechanisms/models, Proceedings of the Institution of Mechanical Engineers Part J, Journal of Engineering Tribology, 216, J6, 349-355.

[42] Shillor M., Sofonea M., Telega J.J., 2003, Analysis of viscoelastic contact with normal compliance, friction and wear di_usion, Comptes Rendus Mecanique, 331, 6, 395-400.

[43] McColl I.R., Ding J., Leen S.B., 2004, Finite element simulation and experimental validation of freeting wear, Wear, 256, 11/12, 1114-1127

[44] Kim N.H.,Won D., Burris D., Holtkamp B., Gessel G.R., Swanson P., Sawyer W.G., 2005, Finite element analysis and experiments of metal/metal wear in oscillating contacts, Wear, 258, 11-12, 1787-1793

[45] Agelet de Saracibar C., 1998, On the numerical modelling of frictional wear phenomena & thermomechanical frictional contact problem. Computer Methods in Applied Mechanics and Engineering. Volume 5, Issue 3, pp 243-301.

[46] Bhushan, B, Surface roughness analysis and measurement techniques. In modern tribology Hand Book Bhushan, BED: CRC Press: Boca Raton, Florida, 2001, 49-114.

[47] K.A. Grosch. 1963. The relationship between the friction and viscoelastic properties of rubber. Doi: 10.1098/rspa. 1963.0112. Proc. R. soc. Lond A25. Vol 274 No 1356. pp 21-39.

[48] Roberts, A. D. and Jackson, S. A. Sliding friction of rubber, Natur, Vol 275, 1975. PP 118-120.

[49] M. E. Dan, 2009. Dry rolling friction and wear of elastomer systems and their finite element modelling, Doctoral- Ing, Xu aus Liaoning, China.

[50] B.N.J. Persson. On theory of rubber friction. Surface science 401 (1998) 445-454

[51] G. Heinrich. Rubber Chem. Technol, 70, 1 (1997).

[52]M Mofidi, B Prakash, Persson, B.N.J and Albohr. Rubber friction on smooth surface. Journal of physics condensed matter. 20 (2008) 085223 (8 pp).

[53] Nándor B. Wear simulation of a reciprocating seal by global remeshing. Periodica Polytechnic, Mech-Eng 54-2 (2010) 71-75.

[54] M. Baxquins, Mater, Sci. Engng. 73, (1985) 45.

[55] A. E. Filippov, J. Klafter, and M. Urbakh. Friction through dynamical formation and rupture of molecular bonds. Physical Review Letters, 92:135503, 2004

[56] B.N.J. Persson, 2001, Elastic instabilities at a sliding interface. Phys. Rev. B63. 104101.

[57] B.N.J. Persson, 2000, Sliding friction, physical principles and application. ISSN. 3-540-67192, 2nd Eddition Springer-Verlag Berlin Heidelberg New York.

[58] Persson, Albohr O, Mancousu F, Peveri V, Samoilov V N and Siveback I M, 2003. Wear 254.

[59] Carbon G and Mangilardi. Analysis of adhesive contact of confined layers by using a Green's function approach. Journal of the Mechanics and physics of solid. Vol. 56. Pp 684-706, 2008.

[60] B.N.J. Persson, Ke Zhao, A I Volokitin, V N Samoilov. On the origin of Amontons friction law. Journal of physics: condensed matter 20 (39). 395006, (2008).

[61] Bisztray-Balku,S.: Tribology of the reciprocating hydraulic seals. VIIIth International Conference of Seals and Sealing Technology, 1998, Wroclaw

[62] Mofidi, M., Prakash, B., "The influence of lubrication on two body abrasive wear of sealing elastomer, Journal of Elastomers and Plastics, 2011, 43 (1): 19-31.

[63] M. R. Mofidi, 2009. Doctoral thesis. Tribology of elastomeric seal materials, ISSN: 1402-1544, ISBN: 978-91-86233-26-6, Lulea University of Technology. Sweden.

[64] AL.Ghathiam, Faisal. M and Muafaq.S. Friction Forces in O-ring sealing, American journal of applied sciences (2/3), 626-632. 2005. ISSN: 1546-9239.

[65] M. Mofidi, B. Prakash. 2007. Frictional behaviour of some sealing elastomers in lubricating sliding conditions. Lulea University of Technology. Lulea SE-971 87 Sweden.

[66] Brain E. Suisse, 2005. Dynamic seal friction modelling in linear motion hydraulic piston application, University of Texas.

[67] Persson, B.N.J., Volokitin, A.I., & Tosatti, E. Role of the external pressure on the dewetting of soft interfaces. Eur. Phys. J. E 11, 409–413 (2003).

[68] B.N.J. Persson, O. Albohr, Contact area between a viscoelastic solid and a hard, randomly rough, substrate, J. Chem, Phys, 120-8770, 2004..

[69] Cyril M. Harris.2002. Shock and Vibration hand book, Mechanical properties of rubber, Ch 33, Columbia University, New York.

[70] M. Kaneta, S. Togami, H. Nishkawa, Y. Kanzaki. Friction behaviour of seals, AITC-AIT 2006. International conference on tribology,Para, Italy

[71] H.C. Meng, Wear modes and predictive equations: their form and content. Wear 181-182 (1995) 443-457.

[72] F.T. Barwell. Wear of metals, Wear, 1 (1957-1958) 317-332.

[73] S. K, Rhee. Wear equation for polymers sliding against metal surface.Wear, Vol 16, ISSU 6 (1970), pp 431-445.

[74] Archard J. F. Contact and rubbing of flat surface. Journal of applied physics (08-1953), Vol 24, p. 981-988, DOI 10.1063/1.171448.

[75] Nam. P. Suh, et al. The delamination theory of wear, Wear,Vol. 25 (1973), pp.111-124.

[76] On the numerical modeling of frictional wear phenomena C. Agelet de Saracibar, M. Chiumenti Computer Methods in Applied Mechanics and Engineering Vol 177, Issues 3-4, 1999, P. 401-426.

[77] Barwell, F.T. Report on wear presented at the institution of mechanical engineers conference. Wear, Vol 1, ISSU 5 (1958), p. 418-445.

[78] Koji. K, Koshi. A. Wear of advance ceramics, Wear, Vol 253 (2002), p. 1097-1104.

[79] F. P. Bowden and D. Tabor. The area of contact between stationary and between moving surfaces. Proc. R.Soc. Lond. A1939 -169, DOI: 10: 1098/rspa 1939. 0005.

[80] K.C. Ludema. Mechanism-based modelling of friction and wear. Wear, Vol 200 (1996), p. 1-7.

[81] Villaggio. P, 2001, Wear of an elastic block. TIB Journal, German national library of science and technology, Meccanica. Milano (2001) 36: 243-249.

[82] Fillot, N., I. Iordanoff, and Y. Berthier, Wear modeling and the third body concept. Wear, 2007. 262(7-8): p. 949-957

[83] Claudio R, Avvila da Silva jr, Gisuseppe Pintauda. Uncertainty analysis on wear coefficient of Archard model, Tribology international, Vol 41, ISSU 6 (2008), P. 473-481.

[84] Tasho Hasegawa. 2008. Tribology research trends, Nova science published, Inc New York. ISBN 978-1-6086-331-3.

[85] C Caluent, M Tirovie and T Stolanski. Design and development of an elastomer based pneumatic seal using F.E.A. mechanical engineering, part J. journal of engineering, Tribology (2002), Vol 216, p. 127-138.

[86] O-ring and seals problem solving product, Inc, available from online, www.pspglobal.com/finite-element-analysis-html, access on 2/8/2013.

[87] Y.B. Fu, R.W.Odgen, 2001. Nonlinear elasticity theory and applications, Cambridge University Press. ISBN: 9780 -52179. 6958

[88] Bryan Mac Donald, 2007, Practical stress analysis with finite elements. Dublin City University, Ireland.

[89] Hyperplastic material behaviour, 2011 Autodesk, available online, www.autodisc.com, access on 5/11/2013.

[90] Claus, R. G. Development of a High Performance, Heavy Duty Piston Seal, Proc. 49th National Conference on Fluid Power, NFPA, pp. 383-389 (2002).

[91] Nicholas B. Maser, 2006, Numerical model of a reciprocating rod seal, including surface roughness and mixed lubrication. Georgia Institute of Technology.

[92] Arthur Bullock, 2010. Fundamental concernts associated with hydraulic seals for higfh bandwidth actuation. Doctoral these, University of Bath.

[93] Zhichao.W, Don. D, Tom. H, 2006, Radial lip seal simulation using analysis non-standard procedures.

[94]. Nanndor B, 2011. Booklet of theses of Friction and wear of elastomers and sliding seals, Budapest University of Technology.

[95] E. M. Arruda and M. C. Boyce. A three dimensional constitutive model for the large stretch behaviour of rubber elastic materials, Journal of the mechanics and physics of solids, Vol 41, p. 389-412, 1993.

[96] Rivlin. R.S. large elastic deformations of isotropic materials. IV. Further developments of the general theory, Philosophical transactions of the Royal society of London. Vol 241, ISSU 835, pp. 379-397, 1948.

[97] Roland Jakel, 2010. Analysis of hyperelastic materials with mechanical theory and application examples. PTC presentation, Technische Universitat, Chemnitz.

Table of Contents

Chapter 1 introduction

Chapter 2 literature

Chapter 3 Theory

Chapter 4 Experimental set up

Chapter 5 Results and Discussions

Chapter 6 Conclusion and Future works.

Chapter 1

Introduction

Chapter 2

Literature

Chapter 3

Theory

Chapter 4

Experimental set up

Chapter 5

Results and Discussion

Chapter 6

Conclusion

Wear Testing & Finite Element Analysis of Nitrile Rubber (NBR) Hand Pump Seals

Fadel ALkadhimi

2014

School of

Mechanical and Manufacturing

Engineering

Wear Testing and Finite Element Analysis of Nitrile Rubber (NBR) Hand Pump Seals

Fadel ALkadhimi

St. No: 57211506

Supervisor: Dr. Brian Corcoran

2014

Abstract

The use of Nitrile Butadiene Rubber NBR as seal in machines has increased in recent years. NBR is considered as the standard material for sealing and NBR owes its many applications to a range of special mechanical properties. However, the non-linear mechanical properties and incompressible behaviour of NBR make the analysis of NBR very difficult. The literature review highlighted the fact that the most common technical cause of hand pump failures was the wear of the piston seals. The contact surface of the piston seals with the bore surface (Brass) of the cylinder and the piston seal contact area are the key to calculating and determining seal friction force and seal wear rate.

Several researchers carried out modelling of friction and wear processes, though little of these focused on the wear of NBR seals, and very limited research has been conducted on the wear of piston seals in the presence of water, and a very few has been reported regarding how to determined and calculating the wear rate of removal material of piston seals used in water hand pump.

In the major part of this research I have studied the friction and wear processes of NBR piston seals – Brass sliding pairs by experimental and numerical methods. Also, in the present study, the focus was on developing relationships as a practical and convenient option for computing: piston seals contact area and piston seals friction force and piston seals wear rate. The developed relationships were applied for a different diameters of the NBR piston seals in wet and dry sliding conditions, by investigating the obtained results from the experiments.

Carried out experimental tests at Dublin City University, DCU (Mechanical and Manufacturing Engineering School), Dublin, Ireland, and using pump rigs system, which operates similar to the water hand pumps, which used in developing countries. The rig was used from a previous master's project, use of the system for different cases the previous

pump rig was develop to: two similar pump rigs operating in the same time with same stroke and used pneumatic cylinder with two metalwork reed switches for each rig to move the pump rod up and down. The results obtained from the experiments show (i) the effect of wet and dry sliding conditions and (ii) the effect of time operation on the seal contact area and (iii) how the wear increase over the time.

The distribution of the stress in the contact area of NBR piston seal over the time of sliding is very complex. By using experiment method it is impossible to analysis the seal contact stress along the distance of the seal contact surface. Due to this reason and to analyse the contact stress and the wear of the NBR piston seal over the time of dry and wet sliding used finite element analysis (F.E.A) method in this research.

The literature review highlighted that there was no study to date about using F.E.A method to analyse: the contact stress, friction behaviour and wear of NBR piston seals under wet and dry sliding conditions. And to date no study exists using F.E.A method to analyse the effect of fluctuating loads of the water acting on the NBR piston seals during the extension and retraction of the strokes of the piston.

In this study, a good agreement has been observed through the comparison between the obtained results from experimental and F.E.A methods of the NBR piston seal over the time under wet and dry sliding conditions.

Acknowledgement

I would like to thank (special thanks) my supervisor Dr Brian Corcoran. His excellent guidance throughout the research ensured that I kept my focus and was able to complete my research.

Many thanks to Mr Michael May for assisting me with every query and providing much needed expertise at a moment's notice.

Also, I would like to thank Mr Laim Domican for assisting me.

I would like to thank my friend Dr Micheal Lubwama.

Finally, I would like thank my wife and my sons, who helped and supported me throughout what has been some very long years

Declaration:

I hereby certify that this material, which I now submit for assessment on the programme of study leading to the award of MEng master by research is entirely my own work, and that I have exercised reasonable care to ensure that the work original, and does not to the best of my knowledge breach any law of copyright, and has not been taken from the work of others save and to the extent that such work has been cited and acknowledged within the text of my work

Fadel ALkadhimi

Student No: 57211506

Tables of Figures

Fig.72: Length of the contact surface of the uncoated NBR piston seal over the cycles of wet and dry sliding conditions; also display the wear of the uncoated NBR piston seal over the cycles of wet and dry sliding.

Tables of Tables

: